Investigation of porcine immune response against *Actinobacillus pleuropneumoniae*

PhD thesis submitted to fulfil the requirements for the academic degree of

Doctor of Philosophy (PhD)

from the University of Veterinary Medicine, Vienna

submitted by

Elena Lucia Sassu, DVM

University Clinic for Swine, Department for Farm Animals and Veterinary Public Health

and

Institute of Immunology, Department of Pathobiology

University of Veterinary Medicine, Vienna

Vienna, April 2017

PhD committee

First supervisor

Prof. Dr. Isabel Hennig-Pauka
University Clinic for Swine
Department for Farm Animals and Veterinary Public Health
Vetmeduni Vienna
Veterinaerplatz 1
1210 Vienna, Austria
Isabel.Hennig-Pauka@vetmeduni.ac.at

Second supervisor

Prof. Dr. Monika Ehling-Schulz
Functional Microbiology
Department of Pathobiology
Vetmeduni Vienna
Veterinaerplatz 1
1210 Vienna, Austria
Monika.Ehling-Schulz@vetmeduni.ac.at

List of publications

Sassu, E. L.*, J. Frombling*, J. C. Duvigneau, I. Miller, A. Mullebner, A. M. Gutierrez, T. Grunert, M. Patzl, A. Saalmuller, A. Von Altrock, A. Menzel, M. Ganter, J. Spergser, M. Hewicker-Trautwein, J. Verspohl, M. Ehling-Schulz* and I. Hennig-Pauka*, 2017: **"Host-pathogen interplay at primary infection sites in pigs challenged with *Actinobacillus pleuropneumoniae*".** *BMC Veterinary Research*, 13, 64.

* Equal contribution

Impact factor: 2.371

Sassu, E.L., A. Ladinig, S. C. Talker, M. Stadler, C. Knecht, H. Stein, J. Frombling, B. Richter, J. Spergser, M. Ehling-Schulz, R. Graage, I. Hennig-Pauka* and W. Gerner*. (2017): **"Frequency of Th17 cells correlates with the presence of lung lesions in pigs chronically infected with *Actinobacillus pleuropneumoniae*".** *Veterinary Research,* 48, 4.

* Equal contribution

Impact factor: 3.765

TABLE OF CONTENTS

1. ACKNOWLEDGMENTS

First of all, I want to thank Prof. Isabel Hennig-Pauka for giving me the opportunity to perform my PhD project at the University Clinic for Swine and allowing me to collaborate with several institutes at the Vetmeduni. Consequently, I want to thank Prof. Monika Ehling-Schulz and Prof. Catharina Duvigneau for welcoming me in their labs and introducing me to their facilities. Especially, I´d like to thank Prof. Armin Saalmüller for giving me the possibility to complete the second part of my PhD project and finalize the PhD thesis at the Institute of Immunology.

Secondly, I am particularly thankful to Dr. Wilhelm Gerner for his scientific input, his notable support, and, most of all, for believing in me. He is to me an example not only of good scientific practice but also of excellent supervision.

I am deeply thankful to Dr. Andrea Ladinig for guiding me throughout my PhD and fighting on my side against numerous impairments that came along during the development of this project. With her strength, passion and dedication, she taught me that there is no giving up, neither in science nor in life.

Next, I am very grateful to Maria Stadler, Michaela Koch, Lisa Reiter and Stephanie Talker for their skilful technical support in the lab. Without Maria´s energy and expertise the amount of work in the lab would not have been manageable. Thanks, Stephanie, for the exchange of knowledge and great support during the nights spent in front of the Canto!

Very special thanks go to the whole team of the University Clinic for Swine. Thousand pizzas would not be enough to express my gratitude for their great help in the trial. Particularly, I´d like to thank Christian Knecht for making me laugh and giving me strength in hard times. Very important thanks go to Hanna Koinig for simply being a wonderful colleague and friend. Thanks for helping me with any kind of issues and making me feel like home in Vienna.

Moreover, I´d like to acknowledge the scientific support of Ingrid Miller, Andrea Müllebner and Kerstin Mair, who mentored me in parallel projects and created a friendly atmosphere in the lab.

Last but not least, I thank and, more important, I apologize to all friends, relatives and strangers with whom I shared the least bright sides of my PhD. I bet that, after these three years of PhD, there are more people in the world wondering about the importance of *Actinobacillus pleuropneumoniae* maybe not in regard to porcine health, but certainly to my mental stability.

Finally, this PhD project turned to be a fruitful challenge both for my professional and my personal growth. I am surely grateful for having had the chance to thrive on a hard but, eventually, fertile soil. Therefore, I thank with deep affection the special people who encouraged me to sow the first grain.

2. AUTHORS´ CONTRIBUTION

Sassu, E.L.*, J. Frömbling*, J.C. Duvigneau, I. Miller, A. Müllebner, A.M. Gutiérrez, T. Grunert, M. Patzl, A. Saalmüller, A. von Altrock, A. Menzel, M. Ganter, J. Spergser, M. Hewicker-Trautwein, J. Verspohl, M. Ehling-Schulz* and I. Hennig-Pauka* (2017): **"Host-pathogen interplay at primary infection sites in pigs challenged with Actinobacillus pleuropneumoniae".** *BMC Vet Res*, 13, 64.

*Equal contribution

EL Sassu	carried out animal experiment, ELISA assays and analysis of gene expression in tissues, and wrote the manuscript.
J Frömbling	carried out microbiological analysis, FTIR and chemometric analysis, and wrote the manuscript.
JC Duvigneau	conceived and designed the experiments.
I Miller	conceived and designed the experiments.
A Müllebner	carried out analysis of gene expression in tissues.
AM Gutiérrez	performed acute phase protein quantification in body fluids.
T Grunert	helped in carrying out FTIR and chemometric analysis.
M Patzl	assisted in interpretation of data obtained from ELISA.
A Saalmüller	assisted in designing experiments.
A von Altrock	carried out animal experiment.
A Menzel	carried out animal experiment.
M Ganter	performed laboratory diagnostic investigations.
J Spergser	assisted in carrying out microbiological analysis.
M Hewicker-Trautwein	performed histological examination.
J Verspohl	prepared the inoculum.
M Ehling-Schulz	conceived, designed the experiments and assisted in the preparation of the manuscript.
I Hennig-Pauka	conceived, designed and performed the animal experiment, and assisted in the preparation of the manuscript.

Sassu, E.L., A. Ladinig, S. C. Talker, M. Stadler, C. Knecht, H. Stein, J. Frombling, B. Richter, J. Spergser, M. Ehling-Schulz, R. Graage, I. Hennig-Pauka* and W. Gerner*. (2017): **"Frequency of Th17 cells correlates with the presence of lung lesions in pigs chronically infected with *Actinobacillus pleuropneumoniae*".** *Vet Res,* 48, 4.

*Equal contribution

EL Sassu	conceived and performed the experiments, produced the stimulus, carried out intracellular cytokine staining and FCM measurements, analysed and interpreted the results and wrote the manuscript.
A Ladinig	designed and performed the animal experiment, and assisted in the preparation of the manuscript and interpretation of the data.
SC Talker	established the protocol for intracellular cytokine staining and helped with laboratory work.
M Stadler	helped to set up the in vitro assay, isolated the lymphocytes from the organs and applied the stimulus.
C Knecht	helped to carry out animal experiment.
H Stein	helped to carry out animal experiment.
J Frömbling	carried out microbiological analysis.
B Richter	performed histopathological analyses.
J Spergser	prepared the inoculum.
M Ehling-Schulz	contributed to the organization of the experiments and edited the manuscript.
R Graage	helped with performing necropsies.
I Hennig-Pauka	planned the experiments and edited the manuscript.
W Gerner	conceived, designed the experiments and assisted in the interpretation of the data and preparation of the manuscript.

All authors read and approved the manuscripts.

4. ABSTRACT

Actinobacillus pleuropneumoniae (App), the causative agent of porcine contagious pleuropneumonia, still remains one of the major causes of respiratory diseases and subsequent economic losses in the pig industry worldwide. This PhD project aimed at investigating the porcine immune response against App both at early and late stages of the infection. To address this question, two separated experiments were conducted.

During the first experiment, six pigs were intratracheally infected with App and humanely euthanized eight hours after infection. The messenger RNA expression of inflammatory cytokines (IL-6, IL-1 and TNF-α) and acute phase proteins (haptoglobin, serum amyloid A and C-reactive protein) was studied in lung, liver, tonsil and salivary gland. The same markers were measured by quantitative immunoassays in serum, saliva and bronchoalveolar lavage fluid. In parallel, metabolic adaptations of App to primary sites of colonisation, namely lung and tonsils, were assessed by Fourier-Transform Infrared (FTIR-) spectroscopy. Next to the important reaction of the lung, a significant increase in acute phase protein expression was found in the salivary gland, which might be considered as a key-role in early oral immunity against App infection. Moreover, App metabolic adaptations to pig upper respiratory tract, where no immune response was detectable, were observed already at this early stage of infection. This finding might support the assumption that App can change its phenotype to escape immune mechanisms and persist in the host.

In the second experiment, our purpose was to characterise the T-cell immune response against an App crude capsular extract (App-CCE). Therefore, pigs were intranasally infected with App and euthanized at two different time points: 6-10 days post infection (dpi), defined as acute phase, and 27-31 dpi, defined as chronic phase. Functional and phenotypic analyses were conducted on T cells present in lymphocyte preparations from blood, tonsils, lung and tracheobronchial lymph nodes after in vitro App-specific stimulation. A subset of App-CCE

specific $CD4^{+}CD8^{dim}$ IL-17A-producing T cells, putative Th17 cells, was present in blood and lung tissue of most infected animals, independently of their disease stage. Importantly, the frequency of these cells in blood and lung of chronically infected animals was found to positively correlate with lung lesion scores and antibody titres. This suggests a potential role of Th17 cells in the pathogenesis of App infection. Further studies are needed to define whether the involvement of these cells in lung immunity is related to pathology or protection.

Overall, our results provide a detailed analysis of porcine immune response against App infection at different stages. This work highlights the relevance of host-pathogen study and T-cell analysis to gain novel insights on strategies that App might adopt to evade host immune mechanisms.

5. GENERAL INTRODUCTION

Actinobacillus pleuropneumoniae (App) is the causative agent of porcine contagious pleuropneumonia, a respiratory disease that affects the swine industry worldwide. Due to its economic importance, research, with the purpose of finding new strategies to protect susceptible animals and to reduce pathogen transmission, has been extensively conducted in the past. Vaccination and use of antibiotics are considered useful tools to reduce mortality and severity of symptoms, but they are not effective in protecting pigs from becoming asymptomatic carriers of the pathogen. Therefore, to pave the way to new approaches, a better understanding of porcine immune response to App infection at early and late stages of the disease is required.

5.1. Actinobacillus pleuropneumoniae

App is a small gram-negative bacterium belonging to the *Pasteurellaceae* family that induces porcine pleuropneumonia, a highly contagious respiratory disease in the swine herds worldwide (Gottschalk, 2012).

Strains of APP can be classified by biovar, serovar and expression of APX toxins.

On the basis of their NAD requirement to grow, App isolates can be assigned to two different categories: biovar I (NAD dependent) and biovar II (NAD independent). App strains can be further classified in a recently updated number of 16 serovars (Sarkozi et al., 2015), which differ in their capsular polysaccharide and cell wall lipopolysaccharide composition. Several bacterial virulence factors have been described. Of major importance are the four Apx toxins that present different degrees of cytotoxicity, haemolytic activity and distribution among serotypes (Schaller et al., 2000, Sarkozi et al., 2015, Frey, 1995). Apx I is strongly cytotoxic, strongly haemolytic and is produced by serotypes 1, 5a, 5b, 9, 10, 11, 14 and 16. Apx II is moderately cytotoxic and weakly haemolytic and expressed by all serotypes except for 10 and 14. Apx III is strongly cytotoxic, non-haemolytic and occurs in serotypes 2, 3, 4, 6, 8 and 15.

Importantly, a fourth toxin, ApxIV, is produced by all serotypes in vivo and is therefore extensively used for diagnostics (Dreyfus et al., 2004).

Prevalence of App strains varies between different countries (Gottschalk, 2012). On the European territory the most predominant strain is App serotype 2, which shows traits of high virulence in Europe but is almost not virulent in North America. Here, differently from Europe, serotypes 5 and 7 were recently pointed as the most dominant (Gottschalk, 2015).

The outcome of App infection can be diverse. It can occur as a peracute, acute or chronic disease. Pigs affected by the peracute form of App infection can present apathy, a body temperature of up to 41.5°C and anorexia; but most commonly dead animals, with typical foamy blood running out of the nose, are found in the pens before the detection of any premonitory sign. In acute outbreaks the mortality can range from 1 to 10% with morbidity exceeding 50% (Fenwick and Henry, 1994). Acutely affected pigs have increased body temperatures from 40.5-41 °C, sudden loss of appetite, respiratory symptoms like dyspnoea, cough and, in severe cases, sitting posture with open mouth breathing. Pneumonia can be monolateral or bilateral, diffuse or multifocal and can involve every lung lobe. Classically, the lung is altered by the presence of necro-haemorrhagic areas of consolidation and the pleural space is crossed by layers of fibrin. Blood-tinged fluid can be found in the thoracic cavity. If pigs overcome the acute phase of infection, they frequently fail in solving the infection and enter a status of chronic disease. This is mostly characterised by mild symptoms like little or absent fever, intermittent cough and reduced feed intake. Studies trying to address if this condition affects the average daily weight gain reported conflicting results (Andreasen et al., 2001, Straw et al., 1989). Acute haemorrhagic lesions often resolve in necrotic foci demarked by granulation tissue with an abscess-like structure. Accumulation of fibrin between the parietal and visceral pleural layers results in fibro-adhesive pleurisy, which is detected at the slaughterhouse when parts of the lung adhere to the thoracic wall.

Pigs of all ages can be affected, but 12-week-old fattening pigs are more likely to develop clinical disease since in this period the maternally derived immunity is not present anymore (Chiers et al., 2002). Other than age, there are several factors that can influence susceptibility to App infection such as co-infections with *Mycoplasma hyopneumoniae* (Marois et al., 2009) or PRRSV (van Dixhoorn et al., 2016); genetics (Hoeltig et al., 2009); virulence of serotypes (Rosendal et al., 1985); the purchase of carrier gilts and poor biosecurity (Maes et al., 2001) and the environmental enrichment of the housing system (van Dixhoorn et al., 2016).

Recently an increased occurrence of clinical App outbreaks and chronic lung lesions recorded at the abattoir have been reported in Europe, especially in Sweden (Sjolund and Wallgren, 2010). This could be a consequence of Swedish implementation of the Council Directive 2008/120/EC, which has the purpose of laying down minimum standards for the protection of pigs. Following the regulation, no piglets shall be weaned from the sow at less than 28 days of age and this is applied in Sweden even in a stricter manner by weaning piglets from 4 to 6 weeks of age. Considering that App is known to act as a late colonizer, this procedure could dramatically increase the risk of App transmission from the dam to the offspring (Gottschalk, 2012). Consequently this higher prevalence of clinical disease can lead to a higher usage of antibiotics, which should be avoided in view of a reported antimicrobial resistance of App isolates (Vanni et al., 2012, Yoo et al., 2014, Archambault et al., 2012, Gutierrez-Martin et al., 2006). Prevention by implementing biosecurity, enrichment of the housing system and disinfection should be, at least in theory, a straight-forward strategy to contain the disease.

Nevertheless, when App outbreaks are recurrent in a farm, one tool that can be used to contain the amount of required antimicrobials, is vaccination. This has been widely studied in the past (Ramjeet et al., 2008). Two main categories of commercially available vaccines are in use: bacterins (killed bacteria) and subunit toxin-based vaccines. Even though bacterins showed to be inefficient in inducing protection against challenge with heterologous serotypes, they are

still most widely used in the practice (Gottschalk, 2012). Subunit vaccines containing Apx toxins can confer better cross-protection, but still the limitation relies on the fact that they are based on non-replicating antigen. To enhance the local immunogenicity of non-replicating antigen, recombinant DNA technology has been developed. An example of this can be a *Saccharomyces cerevisiae* expressing Apx II, used for oral immunization in pigs, which induced protective immune response but couldn´t act directly on the respiratory tract (Shin et al., 2013). In fact, the ideal vaccine candidate should induce both systemic and mucosal protective immunity (Ramjeet et al., 2008). Recently, an M-cell targeting ligand conjugated with ApxII toxin proved to induce protective immune response after nasal immunization in a murine model by enhancing IL-17-producing cells in both systemic and mucosal compartments (Park et al., 2015). A pig model to evaluate the efficiency of this vaccine candidate in the target species would be beneficial. Furthermore, the role of Th17 cells in vaccine-induced immunity in pigs has not been elucidated so far. Later in this thesis, an attempt at shedding the light on the role of Th17 cells in the pathogenesis of App infection will be presented.

Vaccination can reduce mortality and the severity of symptoms, but cannot prevent pigs from becoming subclinical carriers. Persistence of the bacteria in the upper respiratory tract of pigs results into a constant source of spreading to naïve subpopulations and thus represents a predisposing factor for re-occurrence of outbreaks.

5.2. Innate immune responses against App infection (acute phase proteins, interleukins, neutrophils and macrophages)

5.2.1. Acute–phase proteins and inflammatory cytokines in App infection

Acute-phase proteins are glycoproteins mainly synthetized in the liver upon induction by pro-inflammatory cytokines and then released into the blood (Murata et al., 2004, Petersen et al., 2004). Major acute-phase proteins in the pig are haptoglobin (Hp), serum amyloid A (SAA), C-reactive protein (CRP) and Pig major acute phase protein (Pig-MAP).

Their detection in saliva, serum and meat juice and their possible use as biomarkers to evaluate porcine health status has been widely studied (Gomez-Laguna et al., 2010, Heegaard et al., 2011). A relationship between Hp serum concentration and severity of lung lesion in pigs has been demonstrated (Pallares et al., 2008). SAA, CRP and/or Hp serum concentration increases from 1 day after App infection (Skovgaard et al., 2009, Gomez-Laguna et al., 2014).

Cytokines, which are known to increase during acute App infection, are IL-1β, TNF-α (Huang et al., 1999), IL-6 (Johansson et al., 2001), IL-8 (Baarsch et al., 2000), representing a pro-inflammatory response, but also IL-10 (Cho et al., 2005) which has anti-inflammatory functions. Recently, the expression of IL-17 mRNA in App lung lesions has also been observed by high-throughput RT-qPCR (Brogaard et al., 2015). While IL-1β and TNF-α serum concentrations show to be subjected to high variation, IL-6 seems to be a putative biomarker both for monitoring bacterial infections in pigs (Fossum et al., 1998) and, even though to a lesser extent than CRP, for evaluation of efficacy of antimicrobial treatment (Lauritzen et al., 2003). In a recent experiment, IL-1β, TNF-α and IL-6 serum concentration was measured every two hours for 18 hours post App infection and mean peak concentration of TNF-α and IL-6 appeared at 12 and 10 hours post infection, respectively (Wyns et al., 2015).

5.2.2. Neutrophils and macrophages in App infection

Phagocytic cells like macrophages, monocytes, granulocytes and dendritic cells represent one major branch of the innate immune system. In the lung, the first cells to encounter most pathogens are pulmonary alveolar macrophages (PAMs). After recognition and phagocytosis of App, PAMs excrete inflammatory mediators to attract neutrophils to the site of infection. The ability of PAMs to produce IL-1β, TNF-α and induce chemotaxis of neutrophils via IL-8 production after App stimulation was already described 20 years ago (Huang et al., 1999). A recent study showed that Ahd, a protein mediating App adhesion to host cells, is responsible for inducing PAMs apoptosis in a time-related manner, stimulating the release of pro-inflammatory cytokines (IL-1β, TNF-α and IL-8) and inhibiting the secretion of anti-inflammatory cytokines like IL-10 (Wang et al., 2016). While App can survive in alveolar macrophages up to 90 min, neutrophils have the capability to kill App intracellularly (T. L. Cruijsen et al., 1992). However, App and its cytolysins can stimulate neutrophil-production of oxygen radicals at low concentrations, but can also kill neutrophils at high concentrations; thus resulting in a respiratory burst that can damage the lung tissue (Dom et al., 1992). During acute infections, total WBC count can remain unchanged as the amount of mature neutrophils migrating to the lung is immediately replaced by band neutrophils released by the bone marrow (Baarsch et al., 2000). Lung lesions are the result of both a direct effect of the bacterium and its toxins on lung epithelial cells, and an indirect effect of an exaggerate cytokine release in loco (Huang et al., 1999).

5.3. T-cell mediated immune responses against App

The main effectors of the adaptive immune response are B and T cells. After encountering App, activated antigen-specific B cells induce production of antibodies to combat extracellular bacteria. Humoral immunity is indeed effective in attenuating the severity of the symptoms (Devenish et al., 1990): antibodies can enhance bacterial phagocytosis via opsonisation and act against circulating toxins by neutralizing them (Cruijsen et al., 1995). Nevertheless, App seems to evade these mechanisms and persist in host niches as chronic lung lesions and/or tonsils (Vigre et al., 2002). To acquire more insights into App pathogenesis and persistence, a closer look into T-cell mediated immune responses is also relevant. So far, only few studies addressed this point. An indication that T cells might be of relevance in this disease was stated already in 1997, when Furesz et al. reported that the intensity of delayed-type hypersensitivity was associated with protection (Furesz et al., 1997). Additionally, an increase in CD4:CD8 ratio in peripheral blood of low-dose App immunized pigs, subsequently challenged with high-dose of App, appeared to be beneficial for protection (Appleyard et al., 2002). More insights about the lymphocyte subpopulations involved in the response against App infection were given by Faldyna et al., who described an increase of $CD8^-$ γδ T cells in bronchoalveolar lavage fluid (BALF) and tracheobronchial lymph nodes of pigs challenged with App (Faldyna et al., 2005). Recently, IL-17, a cytokine that can be produced both by $CD4^+$ and γδ T cells in swine (Stepanova et al., 2012), has been reported to be highly expressed, on a transcriptional level, in lungs affected by App (Brogaard et al., 2015). IL-17 producing $CD4^+$ T cells, named Th17, are known to be involved in autoimmune diseases and in the fight against extracellular pathogens by recruiting neutrophils and macrophages to the lung (McGeachy, 2013). These cells together with other IL-17 producing cells, as $CD8^+$ T_C17 cells and innate lymphoid cells type 3 (ILC3s), are effector cells belonging to so called type-3 immunity (Annunziato et al., 2015). Depending on various co-

factors, IL-17 can have protective or pathologic roles in lung disease (Way et al., 2013). During bovine pneumonia induced by *Mannheimia haemolytica*, which like App belongs to the *Pasteurellaceae* family and induces neutrophilic lung infiltration, IL-17 producing γδ T cells were found to be increased (McGill et al., 2016). Therefore, IL-17 could possibly also contribute to App pathogenesis.

Another possibility of immune evasion by App might be the induction of an immunosuppressive status in the host. Regulatory T cells (T_{reg}) can be triggered by the pathogen, so that bacterial clearance is hampered which paves the way to chronic infection (Boer et al., 2015). Differentiated T_{reg} secrete TGF-β and IL-10, which inhibit the inflammatory response, but can also support the survival of specific microorganisms such as *Mycobacterium tuberculosis* (Redford et al., 2011).

Unbeaten paths in the direction of unravelling the mechanisms of App immune evasion as well as pathogenesis and persistence are still numerous. The work presented in this thesis aims at paving the way to explore some of them.

6. AIMS AND HYPOTHESES OF THE STUDY

Considering the economic impact, the recent re-emergence of App outbreaks and the increasing antibiotic resistance of some App isolates, research on porcine immune response against App is of high relevance. A detailed analysis of host-pathogen interactions at primary sites of App infection combined with the acquisition of new insights into both, porcine innate and cellular immune response, may foster the investigation of novel strategies in combating App infection.

The following major points are addressed in this thesis:

I) Evaluation of early porcine immune response against App and parallel identification of an App metabolic adaptation to the host.

Hypotheses:

- Porcine immune response can trigger different App adaptation strategies depending on the body compartment of colonization.
- Investigation of cytokine and acute phase protein expression in a broad range of organs will help to gain more insight about local inflammation during App infection.

II) Characterization of porcine T-cell response against App infection

Hypotheses:

- App-specific antibodies are not efficient in clearance of bacteria. Cell-mediated immune responses play a role in persistence.
- Neutrophilic infiltration in lung lesions is caused by a type-3 immune response.

7. PUBLICATIONS

"Host-pathogen interplay at primary infection sites in pigs challenged with *Actinobacillus pleuropneumoniae*"

"Frequency of Th17 cells correlates with the presence of lung lesions in pigs chronically infected with *Actinobacillus pleuropneumoniae*"

Sassu et al. BMC Veterinary Research (2017) 13:64
DOI 10.1186/s12917-017-0979-6

BMC Veterinary Research

RESEARCH ARTICLE Open Access

Host-pathogen interplay at primary infection sites in pigs challenged with *Actinobacillus pleuropneumoniae*

Elena L. Sassu[1†], Janna Frömbling[2†], J. Catharina Duvigneau[3], Ingrid Miller[3], Andrea Müllebner[3], Ana M. Gutiérrez[4], Tom Grunert[2], Martina Patzl[5], Armin Saalmüller[5], Alexandra von Altrock[6], Anne Menzel[6], Martin Ganter[6], Joachim Spergser[2], Marion Hewicker-Trautwein[7], Jutta Verspohl[8], Monika Ehling-Schulz[2†] and Isabel Hennig-Pauka[1*†]

Abstract

Background: *Actinobacillus (A.) pleuropneumoniae* is the causative agent of porcine pleuropneumonia and causes significant losses in the pig industry worldwide. Early host immune response is crucial for further progression of the disease. *A. pleuropneumoniae* is either rapidly eliminated by the immune system or switches to a long-term persistent form. To gain insight into the host-pathogen interaction during the early stages of infection, pigs were inoculated intratracheally with *A. pleuropneumoniae* serotype 2 and humanely euthanized eight hours after infection. Gene expression studies of inflammatory cytokines and the acute phase proteins haptoglobin, serum amyloid A and C-reactive protein were carried out by RT-qPCR from the lung, liver, tonsils and salivary gland. In addition, the concentration of cytokines and acute phase proteins were measured by quantitative immunoassays in bronchoalveolar lavage fluid, serum and saliva. In parallel to the analyses of host response, the impact of the host on the bacterial pathogen was assessed on a metabolic level. For the latter, Fourier-Transform Infrared (FTIR-) spectroscopy was employed.

Results: Significant cytokine and acute phase protein gene expression was detected in the lung and the salivary gland however this was not observed in the tonsils. In parallel to the analyses of host response, the impact of the host on the bacterial pathogen was assessed on a metabolic level. For the latter investigations, Fourier-Transform Infrared (FTIR-) spectroscopy was employed. The bacteria isolated from the upper and lower respiratory tract showed distinct IR spectral patterns reflecting the organ-specific acute phase response of the host.

Conclusions: In summary, this study implies a metabolic adaptation of *A. pleuropneumoniae* to the porcine upper respiratory tract already during early infection, which might indicate a first step towards the persistence of *A. pleuropneumoniae*. Not only in lung, but also in the salivary gland an increased inflammatory gene expression was detectable during the acute stage of infection.

Keywords: FTIR, Salivary gland, Acute phase proteins, Early immune response, Gene expression

* Correspondence: isabel.hennig-pauka@vetmeduni.ac.at
†Equal contributors
[1]University Clinic for Swine, Department of Farm Animals and Veterinary Public Health, University of Veterinary Medicine Vienna, Vienna, Austria
Full list of author information is available at the end of the article

Background

Actinobacillus (A.) pleuropneumoniae is the etiological agent of porcine contagious pleuropneumonia, which results in increased mortality throughout swine production worldwide [1]. The outcome of infection ranges from colonisation of the upper respiratory tract without any clinical signs to severe lung infection with peracute death. The severity has been ascribed to variation in serotype-related virulence, influenced by biotic and abiotic factors in the pig environment [1]. If the pig overcomes the acute phase of the disease, it can harbour the bacterium in chronic lung lesions, tonsillar crypts and nasal cavities. Thus, infected pigs become persistent carriers of the infectious agent [2]. The Waldeyer's ring is the first immunological and mechanical barrier faced by inhaled pathogens [3, 4]. Its failure allows persistence of *A. pleuropneumoniae* at this site or may lead to reoccurrence of acute outbreaks. Early innate immune response to respiratory disease is not restricted to the lung as the primary site of infection, but additionally involves peripheral lymphoid tissues, the liver [5] and the salivary gland [6]. The acute immune response is characterised by the self-sustaining production of acute phase proteins and inflammatory cytokines. Particularly for *A. pleuropneumoniae* the synergic action of endotoxins and the pore forming exotoxins Apx I to IV, in enhancing the production of inflammatory cytokines, such as IL-6, TNF-α and IL-1 is well known [5, 7–9]. Thus, these bacterial virulence factors can cause tissue damage, directly by Apx cytotoxic effect and indirectly by mounting an exacerbated inflammatory response.

To gain insight into the early stages of host-pathogen interaction, we experimentally challenged pigs with *A. pleuropneumoniae* using the endotracheal infection route and studied in parallel the host and the pathogen during the first few hours of infection. We investigated the mRNA expression of inflammatory cytokines and acute phase proteins in the lung, liver, salivary gland and tonsils as well as the protein levels of these markers in bronchoalveolar lavage fluid (BALF), serum and saliva samples. For studying the influence of the host milieu on the bacterial pathogen, Fourier-Transform Infrared (FTIR) spectroscopy, was employed. FTIR spectroscopy is a well-established vibrational spectroscopic technique that can be used for the generation of spectral fingerprints from a broad range of biological materials [10, 11]. Recently, chemometric assisted FTIR spectroscopy was shown to be a valuable tool for studying metabolic adaptation of bacterial pathogens to host environments. For instance, FTIR spectroscopy was successfully applied for the examination of host genotype-specific imprints on the metabolism of *Listeria monocytogenes* re-isolated from mice with different genotypes [12]. In another study, FTIR spectroscopic analysis of *Streptococcus uberis* re-isolated during the progression of the uterine clearance process of post-partum cows revealed specific *S. uberis* biotypes, which could be linked to the uterine health status [13]. This renders FTIR spectroscopy a suitable technique to investigate bacterial host adaptation on a macromolecular and metabolic level not only for human but also for animal pathogens. In our current study, we showed that already in the early stages of porcine infection *A. pleuropneumoniae* undergoes organ specific metabolic changes that mirror those detected in the host.

Methods

Animals

Ten 6–8 week-old healthy pigs (German Landrace) were used in this study. Animals were derived from a closed breeding herd of a high health status that is routinely tested negative for *A. pleuropneumoniae*, Porcine Reproductive and Respiratory Syndrome Virus (PRRSV), toxigenic *Pasteurella multocida*, endo- and ectoparasites. After arrival, all pigs tested negative for *A. pleuropneumoniae* using an Apx-II Enzyme-linked immunosorbent assay (ELISA) [14]. At arrival, animals were individually marked with ear tags and randomly assigned to a control ($n = 4$) or infection ($n = 6$) group. Within a one-week adaptation period pigs became familiar to the housing conditions. Twice a day commercial feed was supplied. Pigs were housed under specific pathogen-free conditions according to FELASA guidelines and were continuously observed during the whole experiment. A humane intervention point (HIP) checklist, which has been developed and approved previously for infection experiments with *A. pleuroneumoniae*, was used during monitoring the animals continuously for clinical signs by trained staff (participants of FELASA B training course) [15, 16]. HIP was conducted by injection of 60 mg pentobarbital/kg body weight intravenously in deep anaesthesia of the animals as soon as behavioural changes or a significant increase in body temperature reflected the development of early respiratory disease.

Experimental infection protocol

The experiment was part of a comprehensive study to characterise the early stages of inflammatory lung alterations by imaging techniques such as infrared thermography (data not published).

Pigs were not fed on the day of infection to decrease the risk of pulmonary aspiration of stomach content under anaesthesia. An acute infection trial lasting 8–10 h was carried out and included anaesthesia, surgical implantation of the central catheter into the *Vena cava cranialis*, intratracheal infection, clinical examination and collection of blood and saliva samples till scheduled euthanasia. Pigs were anaesthetized intramuscularly with

15 mg ketamine (Ursotamin®, Serumwerk-Bernburg AG, Bernburg, Germany) per kg body weight (bw) and 2 mg azaperon (Stresnil®, Janssen-Cilag GmbH, Baar, Switzerland) per kg bw. Intratracheal infection was performed under visible control using a flexible fiberoptic bronchoscope (IT3; Olympus, Hamburg, Germany) as previously described [15]. Briefly, the tip of the bronchoscope was placed cranial the *Bifurcatio tracheae* and 5 ml of inoculum was instilled gently into the main bronchi. *A. pleuropneumoniae* biotype 1-serotype 2 strain (no. C3656/0271/11, isolated from a fattening pig with respiratory symptoms during an acute outbreak of porcine pleuropneumonia in northern Germany and stored at the Institute of Microbiology, University of Veterinary Medicine, Hannover, Germany [17]) was cultivated in fresh pleuropneumonia-like organism (PPLO) liquid medium to reach an optical density of approximately 0.45 at 600 nm for infection as described elsewhere [18]. This culture was subsequently diluted 1:1000 with 154 mM sterile NaCl solution, resulting in a challenge dose of approximately $1.6x10^6$ CFU per pig determined retrospectively by serial dilution and overnight culture. Control pigs were treated with 154 mM sterile NaCl (sham control). Blood and saliva samples were taken at 2 h prior to and 2, 5 and 8 h post infection and clinical scores were recorded simultaneously.

Blood samples were collected by means of the central catheter into vacutainer tubes with either EDTA for haematological examination or sodium heparin for biochemical examination as anticoagulants.

Saliva samples were obtained by allowing pigs to chew a cotton wool swab (Salivette®, Numbrecht, Germany). The cotton wool swabs were replaced in the original tube, centrifuged at 3000 × g for 10 min and the supernatants stored at−20 °C. Rectal body temperature was measured every hour. At the end of the experiment all pigs were euthanized by intravenous application of 60 mg pentobarbital (Euthadorm®, CP-Pharma, Burgdorf, Germany)/kg bw at eight to ten hours after infection and necropsy was performed immediately.

Clinical evaluation

Clinical examinations were carried out before infection and at 2, 5 and 8 h post infection (hpi) and a total clinical score was calculated for each animal at each time point. This total clinical score was obtained by summing up the single scores for six clinical parameters, as dyspnoea (heavy breathing = 1; open-mouth breathing = 2), coughing (=1), posture (sitting = 1; lying = 2), body temperature (38.0–39.5 °C = 0; >39.5 °C = 1; <38.0 °C = 2), vomiting (=1) and sudden death (=2 extra), so that an individual maximal clinical score of 10 was possible. Scores recorded at 8 hpi were statistically compared between the groups.

Post-mortem examinations

After euthanasia lungs were removed immediately from the carcasses. The severity of lung alterations was assessed using the lung lesion score (LLS) proposed by Hannan et al. [19] and as recommended by the European Pharmacopoeia for the control of vaccine efficacy (3rd edition, EDQM, Council of Europe, Strasbourg, France). Briefly, using a schematic map of the porcine lung as a guide, the organ was virtually subdivided into 74 triangles (7 triangles for cranial and middle lobes, 19 triangles for caudal lobes and 8 triangles for the accessory lobe). Then, the number of triangles with pathological lung alterations were expressed as a fraction and multiplied by five for each lobe, so that each lobe could reach a maximum score of 5, resulting in a maximum LLS of 35 when the entire lung was affected.

One main bronchus was separated from the lung by a surgical clamp. Lung tissue samples were taken from the clamped lung lobe, while the other lung lobe was lavaged with 100 ml of 154 mM sterile NaCl solution. Lung lavage fluid was collected by gently pouring in a glass container moistened inside with concentrated heparin solution. Tissue samples from the clamped main lung lobes were fixed in 10% formalin containing 2% calcium acetate for the preparation of paraffin sections. Routine histology sections were stained with hematoxylin-eosin (HE, hemalaun after Delafield). For mRNA extraction, approximately 500 mg tissue samples from liver, tonsils, salivary gland and lung were snap frozen in liquid nitrogen and then stored at −80 °C.

Blood and lung lavage fluid analyses

Leucocyte cell counts and differential blood counts were determined (Haemotology analyser, Celltag alpha, Nihon Kohden, Kleinmachnow, Germany) immediately after blood collection. Serum haptoglobin (Hp) concentrations were analysed with a colorimetric method (Tridelta Phase Haptoglobin Assay, Tridelta Development Limited, Maynooth, Ireland), while serum C-reactive protein (CRP) was determined by ELISA (Phase Porcine CRP Assay, Tridelta Development Limited).

Total leukocyte counts were determined in the undiluted lavage fluid in a Neubauer-counting chamber prior to centrifugation of the fluid (10 min, 200 × g, 4 °C). The sediment was used for further cytological examination. Cytospots were prepared for differential cell determination of the bronchoalveolar lavage fluid (BALF) by centrifugation of small amounts of resuspended sediments in a cytocentrifuge (Multifuge KR®, Heraeus, Thermo, Osterode, Germany) at 200 × g for 10 min. Cells were stained with a Pappenheim staining solution (Merck, Darmstadt, Germany) and 400 cells were differentiated at 1000 × magnification. The cell-free supernatant of lung lavage fluid was stored at −80 °C.

Analysis of gene expression in tissues

RNA was extracted and reverse transcribed as described previously [20]. The primer sequences and hybridization probes used for the detection of porcine cytokine mRNAs (IL-2, IL-4, IL-10, IL-6, INF-γ and IL-1) as well as the internal references (GAPDH, cyclophilin A and β-actin) were reported by Duvigneau et al. (2005) [21]. The primer sequences and hybridization probes for the detection of porcine stress gene mRNAs (iNOS/HO1/TNF-α) were detailed in a previous work [20]. The primer sequences used for the specific amplification of porcine CRP and Hp were described by Skovgaard et al. (2009) [5], and the primer sequence for amplification of porcine SAA was characterised by Soler et al. (2011a, b) [22, 23]. Primers used for the detection of IL-8 expression were designed for this study as follows: forward: AACAGCCCGTGTCAACATGA and reverse: TGCACT GGCATCGAAGTTCT. The suitability of the newly designed primers was verified in separate experiments by performing a dilution series using the PCR products as well as a dilution series of the cDNA pool, generated by collecting equal aliquots of all investigated cDNA samples. The dilution series, in conjunction with the melting characteristics of the PCR product, were used to optimise the assays regarding the primer concentration as well as the annealing and extension times for the PCR. Further details about the validation of the qPCR assays are provided (see Additional file 1). All primers (Invitrogen, Carlsbad, CA, USA) and probes (Eurofins MWG Operon, Ebersberg, Germany) were synthesised commercially. Specificity of the generated PCR products was verified using melt curve analysis and by randomly verifying correct fragment sizes using gel electrophoresis.

PCR assays were performed as described in [21, 24]. All samples were measured in duplicate. Each plate contained corresponding randomly assigned RT-minus controls of about 15% of all samples, the non-template controls (NTC) as well as the internal standard (IS), which was generated by pooling aliquots of all samples investigated in this study. Data were analysed as described previously [23] and normalised against cyclophilin A and β-actin. The obtained ΔΔCq values of the replicates were averaged and expressed as fold change relative to the IS.

Quantitative ELISA of serum and BALF

Serum and BALF samples were analysed for IL-6, TNF-α and IL-1 expression by means of commercially available sandwich ELISA assay (Duoset DY686, DY690B, DY681, R&D Systems, Biomedical medical products GmbH and Co KG, Vienna, Austria) according to the manufacturer's instructions with minor modifications. For the preparation of standard curves, the recombinant cytokines were diluted in the same body fluid as the samples. Therefore, serum samples from four or BALF from two healthy age-matched pigs were pooled to decrease the risk of individual variation in the matrix. For serum samples, in order to increase signal intensity, the working concentrations of capture and detection antibodies and of the streptavidin-HRP conjugate were doubled. The respective recombinant protein was diluted serially (1:2) in the serum pool. Sera were analysed undiluted and all samples, controls and standard concentrations were run in duplicate. For BALF samples, the working concentrations of antibodies and HPR-conjugates were used as recommended. The BALF pool to create the standard curves was used in the same dilution as the samples. BALF was used undiluted for TNF-α and diluted 1:4 for IL-1 and IL-6 detection. The detection limits of the assays were 150 pg/ml for IL-6, 200 pg/ml for TNF-α and 70 pg/ml for IL-1, respectively. Tetramethylbenzidine (TMB) was used for colour development and 1 M sulphuric acid as stopping solution according to the manufacturer's instructions. Optical density was measured at 450 nm and at 690 nm as the reference with an ELISA reader (Tecan, Sunrise, Grödig, Austria) and concentrations were calculated with Magellan software (Tecan) using the standard curves as allocation base.

Time-resolved fluorometry immunoassay of saliva and BALF

The concentrations of Hp and CRP in saliva and BALF samples were quantified using previously developed and validated one-step non-competitive sandwich type immunoassays based on time-resolved fluorometry technology [25, 26]. The assays used for Hp and CRP measurements comprise calibration curves with seven standards with concentrations between 10 and 1500 ng/ml approximately. This wide dynamic range allows the quantification of samples with highly varying protein concentrations. For saliva, the optimal sample dilution was 1:10 and 1:2 for Hp and CRP measurements respectively, as reported previously. However, described assays had not been evaluated for BALF samples so far, so that the procedures were modified by using optimised dilutions of 1:100 and 1:10 for Hp and CRP quantifications respectively.

Bacterial isolation and cultivation

Lung and tonsillar tissue samples, as well as nasal swabs of four control (C1-4) and six infected (I1-6) animals were examined for the presence of *A. pleuropneumoniae*. For bacterial isolation swabs from organ tissue and nostrils were streaked on Columbia sheep blood agar (Oxoid, Wien, Austria). *Staphylococcus aureus* was used as nurse to facilitate the isolation of *A. pleuropneumoniae* from organs carrying a high bacterial background microbiota, such as tonsils and nostrils [1]. Subsequent cultivation of bacteria was performed in PPLO broth (Difco™, Becton, Dickinson and Company, Franklin Lakes, USA)

supplemented with 10 mg/l NAD (AppliChem GmbH, Darmstadt, Germany) for molecular analyses or grown as solid cultures supplemented with 14 g/l bacteriological agar (Oxoid) for FTIR spectroscopy (see below). All bacterial cultivations were carried out at 37 °C and 5% CO_2.

Serotype 2 specific PCR

Serotype 2 specific PCR using primers for the capsular biosynthesis genes *cps2AB* was performed to confirm the identity of *A. pleuropneumoniae* re-isolated from infected host tissue [27]. Briefly, pelleted bacteria from 2–4 ml liquid culture were re-suspended in 100 μl ddH_2O and lysed at 100 °C for 10 min. Cell debris was removed by 3 min centrifugation at 13.000 × g. 2 μl supernatant containing 50 ng/μl genomic DNA served as a template for a 25 μl PCR reaction mixture containing 5 μl 5× Green GoTaq® Flexi buffer (Promega, Madison, USA), 2.5 μl 25 mM $MgCl_2$, 0.5 μl 20 mM dNTP, 0.25 μl APPcps2F and APPcpsR Primer each (50 pmol), 0.125 μl GoTaq® Flexi DNA Polymerase (5 U/μl; Promega, Madison, USA) and 14.38 μl ddH_2O. DNA was amplified for 35 cycles with the following parameters: 30 s denaturation at 94 °C, 30 s annealing at 58 °C and 30 s elongation at 72 °C. PCR products were analysed on a 1.5% agarose gel.

DNA fingerprinting of bacteria

Genetic stability of bacteria was confirmed by M13 - PCR typing of re-isolated *A. pleuropneumoniae* and the original challenge strain grown *in vitro* as previously described by Henderson et al. [28]. Genomic DNA was isolated with the MasterPure™ DNA Purification Kit (Epicentre, Madison, USA) following the manufacturer's instructions. 2 μl genomic DNA (50 ng/μl) was used as a template for a 25 μl PCR reaction mixture containing 5 μl 5 × Green GoTaq® Flexi buffer (Promega, Madison, USA), 2.5 μl 25 mM $MgCl_2$, 0.5 μl 20 mM dNTP, 0.5 μl Primer M13 (50 pmol/μl; 5'-GAGGGTGGCGGCTCT-3'), 0.15 μl GoTaq® Flexi DNA Polymerase (5 U/μl; Promega, Madison, USA) and 14.35 μl ddH_2O. The amplification was performed using the following parameters: 35 cycles of 35 s of denaturation at 95 °C, 1 min annealing at 40 °C and 2 min of extension at 72 °C. PCR products were analysed on a 2% agarose gel.

Preparation of crude capsular extract

Crude capsule extracts (CEs) were prepared from *A. pleuropneumoniae* isolates derived from lung and tonsils of the infected pigs by mild water-phenol extraction. In brief, fresh 50 ml liquid cultures of *A. pleuropneumoniae* isolates were grown to an OD_{600} of 0.2 and bacteria were harvested by centrifugation at 6530 × g for 5 min. Per gram of bacterial mass 18 ml 1% phenol were added and capsules were extracted by shaking for 5 min at 37 °C followed by an incubation step at 4 °C for 30 min. Bacterial debris was pelleted by centrifugation at 27000 × g for 30 min at 4 °C. Supernatant was sterile filtrated with a syringe sterile filter (pore size 22 μm) to remove remaining cellular debris. The phenol solution was removed by vacuum centrifugation and CE was re-suspended in ddH_2O and immediately analysed by FTIR spectroscopy.

FTIR spectroscopy and spectral data analyses

FTIR spectroscopy was employed to investigate the impact of the host on the metabolism of *A. pleuropneumoniae* re-isolated from organs and tissues of infected pigs. Infrared spectra reflect the biochemical composition of living cells by mirroring the stretching and bending vibrations of proteins, nucleic acids, polysaccharides and fatty acids within different frequency areas [11], which makes FTIR spectroscopy a powerful and highly discriminatory tool for the generation of bacterial metabolic fingerprints and to study host-pathogen interactions [12]. For the generation of a metabolic fingerprint, a loop full of a bacterial mass of the different isolates was cultivated as a lawn on PPLO agar at 37 °C for 24 h and samples were prepared for FTIR spectroscopy as described previously [29, 30]. In brief, one loop-full of bacteria was suspended in 100 μl sterile distilled water. Subsequently, an aliquot of 30 μl cell suspension was transferred to a zinc selenide (ZnSe) optical plate (BrukerOptics GmbH, Ettlingen, Germany) and dried for 40 min at 40 °C. Infrared absorption spectra were recorded in transmission mode in the range of 4000 to 500 cm^{-1}, with a resolution of 6 cm^{-1}, zero-filling factor 4 and Blackmann-Harris 3-term apodization by the aid of a HTS-XT microplate adapter coupled to a Tensor 27 FTIR spectrometer (BrukerOptics GmbH). An average spectrum of 32 scanned interferograms was calculated with background subtraction for each spectrum. Spectral data were processed and analysed and subsequent chemometric analysis was performed using OPUS software (Version 7.2; BrukerOptics GmbH). The frequency range 1150–1100 cm^{-1} in the polysaccharide region (1200–900 cm^{-1}) provided the maximum discriminatory information to assess the tissue-related bacterial metabolic fingerprints by hierarchical cluster analysis (HCA). Most characteristic frequency areas to assess differences specifically related to the bacterial capsule were the polysaccharide region (1200–900 cm^{-1}) and the protein region (1800–1500 cm^{-1}) [11]. Dendrograms of 2^{nd}-derivative spectra (9-point Savitzky-Golay filter) were generated using the Ward's algorithm with normalisation to repro level 30. Measurements of CE were performed with minor alterations as previously described [31].

Statistical analysis

Statistical data analysis was performed for protein and mRNA level and for the clinical score by using the SPSS

software (2011, IBM, SPSS Statistics for Windows, Version 20.0, Armonk, NY, IBM Corp.). Since data were not normally distributed, non-parametrical tests were performed. For statistical evaluation of group differences between infected and sham control pigs the Wilcoxon rank sum test was used. Parameters in paired samples prior to and after infection within one group were compared by the Wilcoxon Signed-Rank test.

Results

Clinical and post-mortem findings

Four hours after infection all pigs experimentally infected with *A. pleuropneumoniae* showed signs of respiratory disease such as dyspnoea, open mouth breathing and coughing. Rare episodes of vomiting were observed in both, infected and control animals, most likely due to a side effect of anaesthesia. Control animals did not display any sign of respiratory disease (Table 1). Successful experimental infection was additionally confirmed by macroscopic and microscopic pathological lung alterations. In the lungs of all infected animals red foci of consolidation and multifocal haemorrhagic lesions associated with interlobular oedema were found (Fig. 1a). In one animal scattered layers of fibrin on the *Pleura visceralis* indicated an incipient pleurisy. Lung lesion scores of infected animals were significantly higher than those of controls as shown in Table 1 ($p \leq 0.01$). Microscopic lung tissue alterations in infected pigs were dominated by a severe neutrophilic infiltration as well as fibrin exudation into the alveolar spaces and interalveolar septa leading to an obstruction of bronchioli (Fig. 1b). The histological diagnosis was a fibrinopurulent, necrotizing and haemorrhagic pleuropneumonia (Table 1). Control pigs showed no histological signs of pleuropneumonia.

Cytological findings in blood

At no time point after infection did the total number of neutrophils in the blood differ between the two groups. Nevertheless, differences were detectable when considering singularly granulocyte fractions. As shown in Fig. 2, eight hours after infection segmented neutrophils in infected animals decreased to a significantly lower level than in control pigs, while a significant increase in immature granulocytes, both band cells and metamyelocytes, was observed in infected pigs in comparison to the sampling prior to infection. Already five hours after infection band neutrophils rose in infected pigs (Fig. 2).

BALF was harvested eight to ten hours after infection from the isolated lungs. Significantly ($p \leq 0.01$) higher total leukocyte cell counts, as well as a trend ($p = 0.057$) in lymphocytes and alveolar macrophages, were observed in infected pigs (Table 2).

Gene expression in host tissue

Gene expression of inflammatory cytokines (IL-6, IL-1 and TNF-α), chemokine IL-8, and the anti-inflammatory cytokine IL-10 was evaluated in liver, lung, salivary gland and tonsils (Fig. 3). Gene expression of iNOS, HO1, IL-2, IL-4 and IFN-γ was below the detection limit and for this reason is not mentioned further in this study (data not shown). In infected animals, IL-6 expression was significantly up-regulated in the liver ($p \leq 0.05$), lung and salivary gland (both $p \leq 0.01$) in comparison to control pigs, but in the tonsils, only a tendency was detected ($p = 0.06$). In the lung tissue of infected animals, all pro-inflammatory cytokines and IL-8 were significantly ($p \leq 0.05$) up-regulated. In addition, IL-1 expression was significantly increased ($p \leq 0.05$) in the salivary gland of infected pigs. No significant differences were found for IL-10 expression in any tissue. In the tonsils none of the investigated parameters were changed (Fig. 3A). The mRNA expression of acute phase proteins (CRP, Hp and SAA) was also assessed in the same tissues (Fig. 3B). Serum amyloid A (SAA) expression was found to be significantly up-regulated ($p \leq 0.01$) in all tissues apart from tonsils. In the salivary gland, the expression of all acute phase proteins was significantly up-regulated ($p \leq 0.01$), while in the tonsils no difference in gene expression in comparison to the control group was found.

Protein expression in serum, BALF and saliva

Concentrations of pro-inflammatory cytokines (IL-6, IL-1, TNF-α) were determined in serum and BALF and acute phase proteins (CRP and Hp) were quantified in serum, BALF and saliva. In sera of infected animals, no significant changes in inflammatory cytokines were detected (data not shown).

Interestingly, TNF-α was not detected in BALF after infection. In contrast, the median concentrations of IL-6 and IL-1 were increased in infected animals while remaining below the detection limit in control pigs. Acute phase proteins behaved similarly in serum and BALF. While Hp concentrations remained unchanged throughout the study, CRP increased significantly at eight hours after infection (Table 2.).

Table 1 Clinical score (CS), lung lesion score (LLS) and histological evaluation of lung lesions in control and infected animals

Group	Clinical score	Lung lesion score	Histological evaluation
Control ($n = 4$)	0 (0–0.75)	0 (0–0.6)	Moderate infiltrates of neutrophils and macrophages in interalveolar septa
Infected ($n = 6$)	**4** (2.75–5.5)**	**7.39** (3.1–16.56)**	Fibrinopurulent, necrotizing, hemorrhagic pleuropneumonia

**$p \leq 0.01$; Wilcoxon rank sum test

CS prior to death (8 hpi) and LLS at the time of the necropsy are expressed as median (interquartile range). Significant values are marked in bold

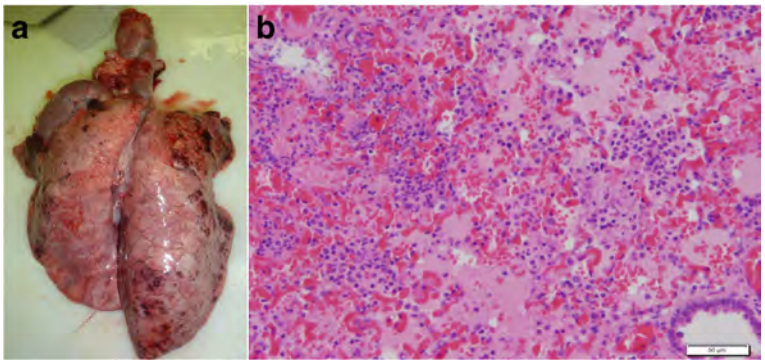

Fig. 1 Pathological lung tissue alterations in a pig 8 hpi with *A. pleuropneumoniae* serotype 2. **a** Macroscopic lung alterations are characterised by multifocal and disseminated haemorrhagic lung tissue consolidations; **b** Histopathological findings are dominated by fibrinous exudates in alveolar spaces and interlobular septa (H&E stain; bar = 50 μm)

The concentrations of CRP and Hp analysed in saliva showed increased levels in the infected animals. Specifically, at the last time point, Hp increased significantly ($p \leq 0.05$) whereas CRP showed only a trend ($p = 0.07$). In control animals no changes were detected.

Metabolic fingerprinting of *A. pleuropneumoniae* re-isolated from host tissues

A. pleuropneumoniae was isolated from the lung of all six, the tonsils of two and the nostrils of three infected animals (Table 3). Serotype 2 specific PCR (APPcps2 PCR) was used to confirm that the isolated *A. pleuropneumoniae* colonies are indeed derived from the *A. pleuropneumoniae* serotype 2 strain used for infection, [27]. The clonality and genetic stability of the isolates were checked by DNA fingerprinting via M13-PCR [28]. All isolates showed the same band pattern via M13-PCR indicating that all isolates are indeed progenitors of the strain used for infection (data not shown). FTIR spectra of all *A. pleuropneumoniae* isolates from the host tissues were recorded and subjected to chemometric analysis. Hierarchical cluster analysis (HCA) of the normalised and pre-processed spectral data revealed a distinct organ-specific clustering of the isolates, indicating organ-specific impacts on the metabolism of host passaged *A. pleuropneumoniae*. From the recorded IR spectra, the spectral window of 1150 to 1100 cm^{-1}, representing a part of the polysaccharide region, showed the highest discriminatory power, resulting in 4 major clusters (Fig. 4). While cluster A covers all isolates from the lung and the inoculation strain, isolates of the upper respiratory tract (tonsillar and nostril isolates) cluster apart from cluster A in the three clusters B-D (Fig. 4). Further passaging showed that the bacterial metabolic adaptation remained stable for the first passages. Consecutive cultivation under laboratory conditions revealed that these metabolic changes are reversible. HCA of FTIR spectral data from bacteria passed 5 times under laboratory conditions showed that isolates from the upper and lower respiratory tract are clustering together (see Additional file 2). The latter results indicate that the observed adaptation is indeed a metabolic adaptation triggered by the organ-specific environment, which is lost over time due to consecutive cultivation under laboratory conditions.

Analysis of *A. pleuropneumoniae* CEs

The metabolic fingerprints of the *A. pleuropneumoniae* lung and upper respiratory tract (nostrils and tonsils) isolates obtained by FTIR spectroscopy showed remarkable differences in the polysaccharide and the protein region. Since the capsule, which is an important virulence factor of *A. pleuropneumoniae* [32], mainly consists of polysaccharides, CE from the re-isolated bacteria were prepared. In order to retain CE associated proteins, a mild aqueous phenol capsule extraction method without further purification was used for the latter. The extracted CE was subjected to FTIR spectroscopy and subsequent chemometric analysis. HCA of the FTIR spectral date of the CEs, using the frequency areas 1800–1500 cm^{-1} (protein region) and 1200–900 cm^{-1} (polysaccharide region), revealed two major clusters: one cluster comprising of the CE spectra from the strain used for infection and its isolates derived from the lung of the infected pigs I1-4 and I6, and one cluster comprising the CE spectra from the tonsil isolates of the infected pig I4 (Fig. 5). Differential FTIR spectral analysis was carried out to search for host site-specific imprints in the CE from the re-isolated bacteria. Therefore, subtraction of a second derivate, vector-normalised, average FTIR spectrum of the CE from *A. pleuropneumoniae* lung isolates from the average spectrum of tonsillar isolates was performed (Fig. 6). The comparison between the CE of isolates revealed significant alterations within the protein (1800–1500 cm^{-1}) and carbohydrate (1200–900 cm^{-1}) regions. Higher amounts of substances absorbing at 1637 cm^{-1} were recorded in CE of lung isolates. This band can be assigned to amide I of β-pleated

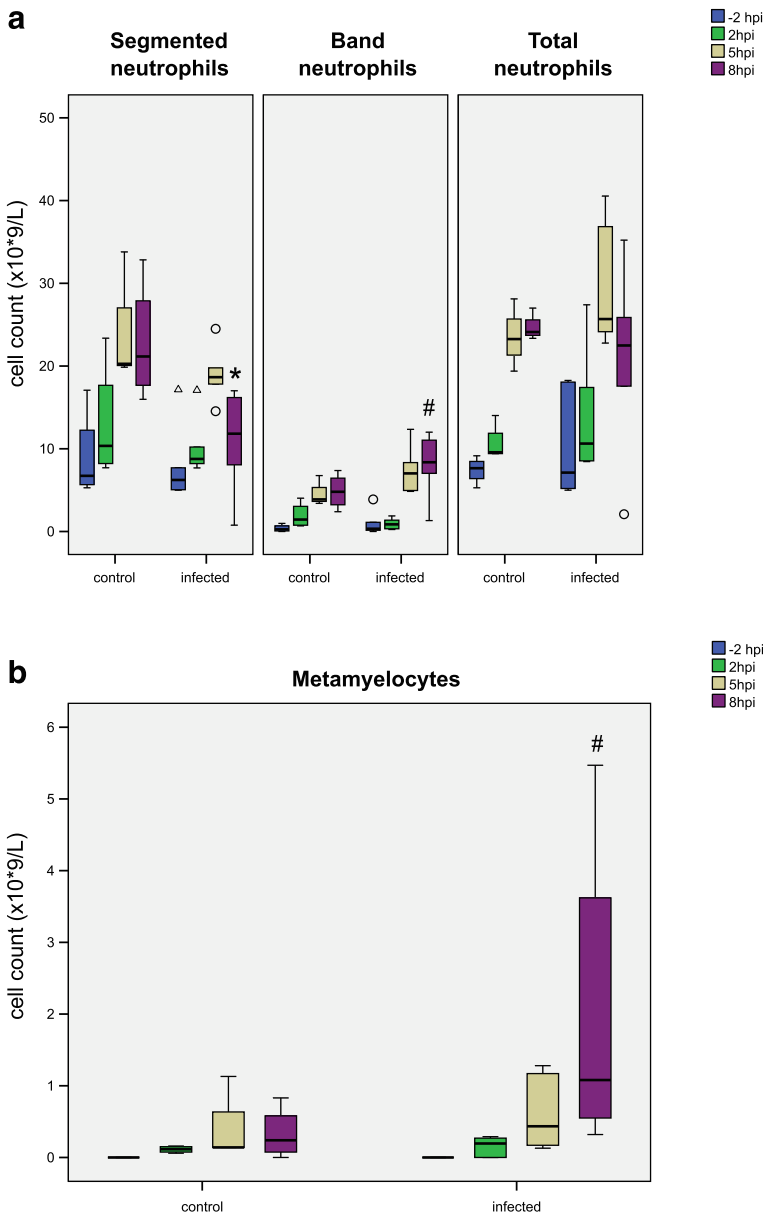

Fig. 2 Cytological findings in the blood during the course of infection. The absolute numbers of mature and immature neutrophils (**a**: total, segmented, band neutrophils, **b**: metamyelocytes) prior to and at 2, 5 and 8 hpi of control ($n = 4$) and infected ($n = 6$) animals are shown. Box-plots show median (line within the box), 25th and the 75th percentiles (box), 1.5 times the interquartile range (whiskers) and outliers (circles and triangles). *$p \leq 0.05$ Wilcoxon rank sum test in comparison to control, # $p \leq 0.05$ Wilcoxon signed-rank test in comparison to sampling prior to infection within the same group

sheet structures [33]. Another significant difference could be detected in the tonsillar CE at 984 cm^{-1} compared to the CE of the lung. Being part of the carbohydrate region this band falls into the spectral range in which O–C, C–O structures dominated by ring vibrations of carbohydrates C–O–P and P–O–P absorb [34].

Discussion

Early induced immune response is the first line of defence against many common microorganisms, including *A. pleuropneumoniae*. Its failure in eliminating the pathogen can result in the development of a chronic and persistent infection status [2, 35]; for this reason, the acute stage of porcine pleuropneumonia, where early immune response usually takes place, was investigated in this study. To induce an acute stage of infection an intratracheal infection route was applied. The experimental model used in this study resulted in diffuse bilateral pneumonia in all infected pigs and the LLS mirrored clinical signs, thus confirming the reproducibility of infection.

Table 2 Concentrations of cytokines (IL-6, IL-1 and TNF-α), acute phase proteins (CRP, Haptoglobin) and cells in different bodily fluids from control and infected animals

	Control ($n = 4$)[a]	Infected ($n = 6$, [c]$n = 3$)
BALF Cytokines:		
IL-6 (pg/ml)	ND	434.2 (ND-2491.5)
IL-1β (pg/ml)	ND	1166.8 (ND-2808.1)
TNF-α (pg/ml)	129.5 (ND-410.4)	ND
BALF acute phase proteins:		
CRP (ng/ml)	89.7 (39.5–189.6)	389.7 (192.6–554.4)
Hp (μg/ml)	6.7 (5.2–9.1)	6.2 (5.1–7.5)
BALF Cells:		
Leukocytes ($\times 10^9$/l)	2.9 (1.8–5.1)	**11.4** (7.8–16.9)**
Lymphocytes ($\times 10^9$/l)	0.1 (0–0.3)	[c]2.5 (0.8–6.1)
Alveolar Macrophage ($\times 10^9$/l)	1.7 (1.5–2.3)	[c]6.2 (4.5–10.6)
	Infected (pre-infection)[b]	Infected (8 hpi)
Serum acute phase proteins:		
CRP (μg/ml)	49.7 (18.4–71.5)	**202.2** (93.9–309)*
Hp (mg/ml)	0.7 (0.2–1.1)	0.7 (0.5–1.3)
Saliva acute phase proteins:		
CRP (ng/ml)	3 (1.3–7.4)	27.9 (8.4–37.6)
Hp (μg/ml)	0.4 (0.2–1)	**1.9** (1.3–3.6)*

Results are expressed as median values (interquartile range). [a]Differences between control and infected group in the BALF immediately after death. *$p \leq 0.05$
**$p \leq 0.01$ Wilcoxon rank test. [b]Differences within the infected group between the last time point of sampling (8 hpi) and prior to infection. *$p \leq 0.05$ Wilcoxon signed ranks test. [c]Lymphocytes and alveolar macrophages were not detectable in the BALF of three animals out of the infection group
ND = not detectable because below detection limit
Significant values are marked in bold

These results are in line with previous studies using other *A. pleuropneumoniae* serotypes for experimental infection [16]. The intratracheal infection model used ensures equally distributed lesions and partially overcomes the limitation of the small sample size in this study by a reduction in the variability commonly associated with other routes of infection [16].

After eight hours of infection, the drop in segmented neutrophils in combination with a rise in band cells and metamyelocytes reveals the kinetics of the cellular innate immune response associated with a fast migration of immature band cells from the bone marrow to the blood as well as a migration of mature neutrophils from the blood stream to the site of infection. Rapid neutrophilic infiltration and high levels of IL-8 expression in lung tissue of infected pigs confirm the key role of this neutrophil-chemokine interaction in the pathogenesis of the disease [8, 16].

In serum, no changes in IL-1 concentrations and only slight increases in IL-6 and TNF-α were recorded within the first eight hours after infection, which is in accordance with results of previous studies [8, 36]. Fossum et al. (1998) reported an increase in IL-6, as the earliest detectable pro-inflammatory cytokine, at 20 hpi with *A. pleuropneumoniae* serotype 2 [36]. Recently, a study from Wyns et al. (2015) showed that all three cytokines increased after the experimental infection and the mean peak concentrations of TNF-α and IL-6 in serum were registered at 12 and 10 hpi respectively [37]. In contrast to these findings for pro-inflammatory cytokines, serum CRP concentration raised eight hours after infection. Serum Hp concentration was not affected during the infection trial.

Our findings of a 4-fold increase in serum CRP is in line with the previously described range of a 2- to 9-fold increase after infection. The normal CRP concentrations in the plasma of healthy pigs vary from 11–77 μg/ml with a high individual variation [38, 39], which is also in accordance with our findings. In contrast to CRP, the slow reacting acute phase protein Hp remained at a physiological level (0.19–0.52 mg/ml) [5, 40] in the serum from both groups. In contrast to serum data, IL-6 and IL-1 were increased in BALF from infected animals; leading to the idea that acute bacterial respiratory tract infection might induce localised rather than systemic cytokine responses. However, TNF-α protein was not detectable in infected pigs, even though its mRNA was found to be highly expressed in the lung. The same outcome was observed in a former study [8]. A study in mice showed the ability of surfactant protein A to enhance the production of secretory leukoprotease inhibitor (SLPI), which is known to induce down-regulation of TNF-α production by inhibiting LPS-induced NF-kB activation [41]. Thus, it is tempting to speculate that LPS-induced NF-kB activation might also be involved in the down-regulation of TNF-α detected in BALF of infected pigs compared to control. Nevertheless, further studies are necessary to test the latter hypothesis.

Although the Waldeyer's ring was bypassed by the intratracheal inoculation route the examined innate immune responses were not confined to the lung, but rather disseminated to organs of the upper respiratory tract. While pro-inflammatory cytokines were primarily induced in the lung tissue of all infected animals, the salivary gland was the main site of expression of acute phase proteins, IL-6 and IL-1. The latter finding was unexpected, because it is in contrast to the lack of immune reaction in tonsillar tissue, although both organs might have had pathogen contact at the same time but later than the lung.

Despite their common localisation, the salivary gland and tonsils showed a completely different pattern in the host immune response. Neither acute phase protein nor pro-inflammatory cytokine mRNAs were differentially

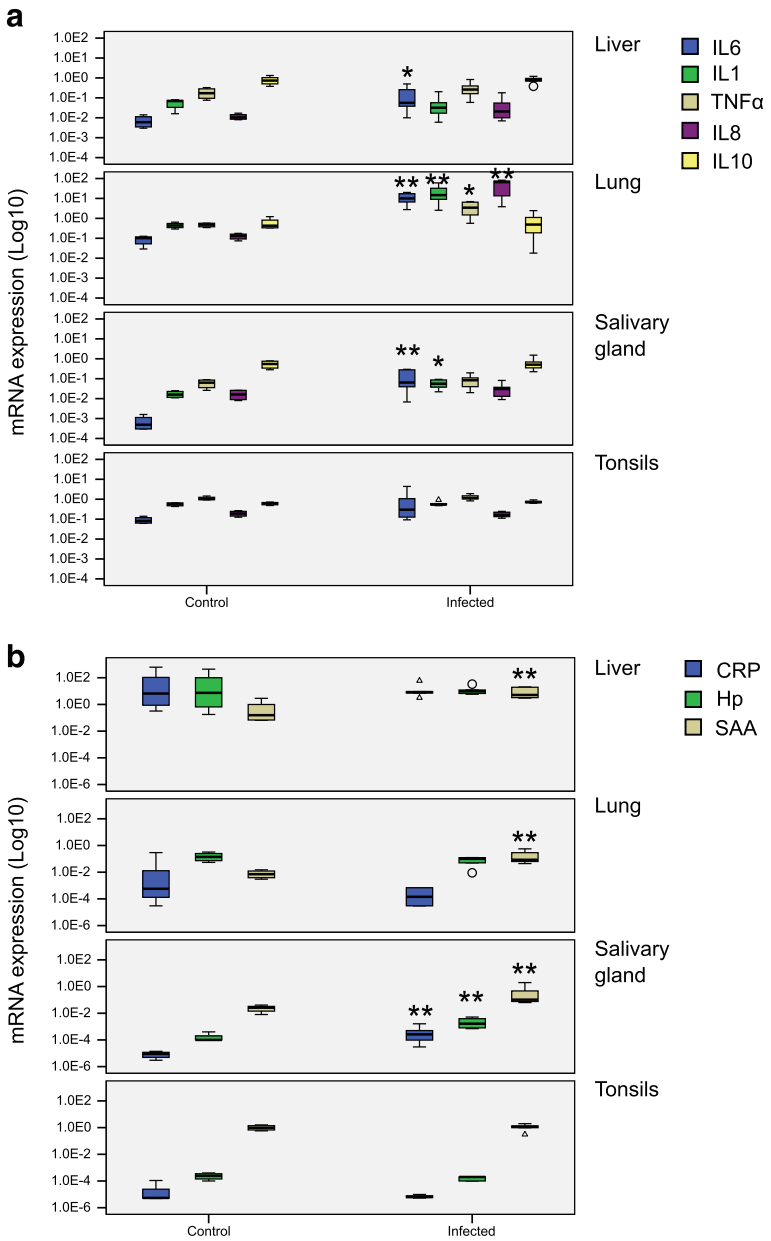

Fig. 3 Cytokine and acute phase protein mRNA analyses. mRNA expression of (**a**) cytokines IL-6, IL-1, TNF-α, IL-8, IL-10 and (**b**) acute phase proteins CRP, C-Reactive Protein; Hp, Haptoglobin and SAA, Serum Amyloid A in different tissues of control ($n = 4$) and infected ($n = 6$) animals. Box-plots show median (line within the box), 25th and the 75th percentiles (box), 1.5 times the interquartile range (whiskers) and outliers (circles and triangles). The results were normalised to reference genes (Actin and Cyclophilin A) and to the internal standard. *$p \leq 0.05$, **$p \leq 0.01$

Table 3 *A. pleuropneumoniae* re-isolated from different tissues of acutely infected animals

		Animal					
Tissue		I1	I2	I3	I4	I5	I6
Lung		x	x	x	x	x	x
Nostril	Left	-	x	-	x	-	-
	Right	-	x	-	-	x	-
Tonsil	Left	-	x	-	x	-	-
	Right	-	-	-	x	-	-

expressed in tonsillar tissue. Acute phase protein extra hepatic production in peripheral lymphoid tissue was previously described during acute *A. pleuropneumoniae* infection [5]. However, the impact of the salivary gland in extra hepatic production of acute phase proteins is largely unknown. Immuno-histochemical findings by Gutierrez et al. (2012) revealed localisation of Hp in the glandular acini and duct epithelial cells of the salivary gland [6]. In our study, not only Hp and SAA, but also CRP was significantly increased in pigs infected with *A.*

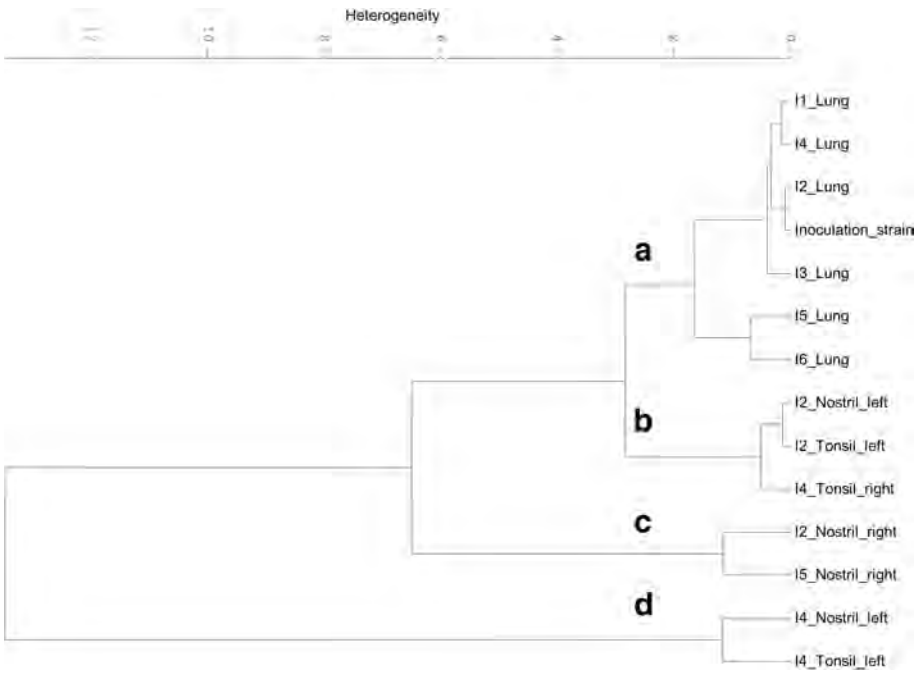

Fig. 4 Hierarchical cluster analysis of FTIR spectra recorded from *A. pleuropneumoniae* serotype 2 re-isolated from different organs of infected pigs. Isolates from different organs of the infected pigs 1–6 (I1-I6) and the strain used for infection were grown for 24 h on PPLO at 37 °C and 5% CO_2, subsequently subjected to FTIR spectroscopy and hierarchical cluster analysis was performed. For calculation of the dendrogram the FTIR spectral regions of 1150 to 1100 cm^{-1} and the Ward's algorithm were used *A. pleuropneumoniae* re-isolated from the lung of all six animals (I1-6) group and the inoculation strain group together in cluster (**a**), while the bacteria isolated from the tonsils and the nostrils group in cluster (**b**–**d**)

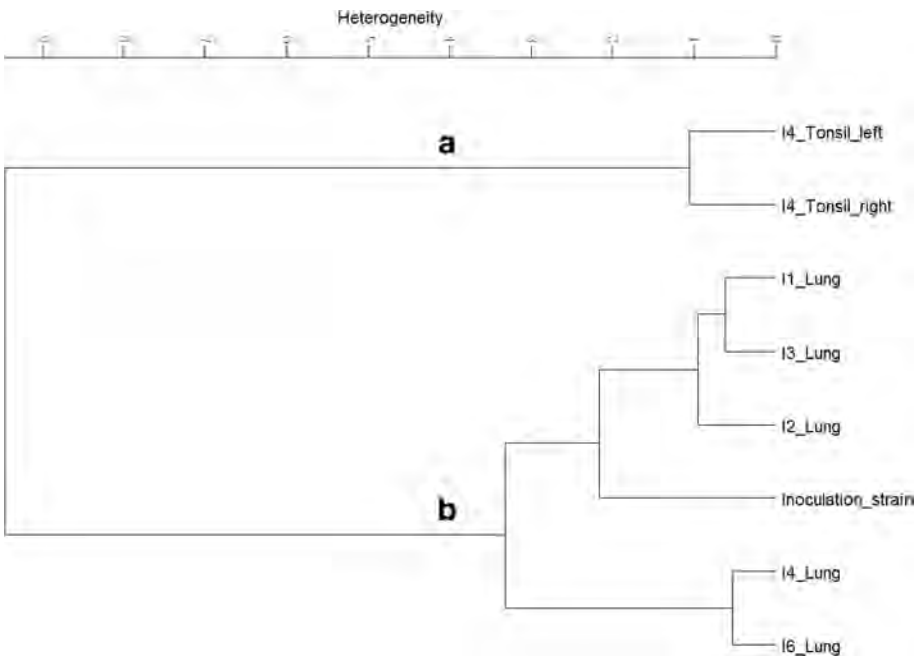

Fig. 5 Hierarchical cluster analyses of FTIR spectroscopic data from CEs of the *A. pleuropneumoniae* serotype 2. Hierarchical cluster analysis was performed using recorded FTIR spectra from the CEs of the infection strain grown *in vitro* and after re-isolation from different organs of the infected pigs 1–4 and 6 (I1-4 and I6): isolates from the lung of I1-4 and 6 as well as the inoculation strain (Cluster **b**), isolates from the left and right tonsil of I4 (Cluster **a**). For calculation of the dendrogram the Ward's algorithm and the FTIR spectral regions of 1200–900 cm^{-1} and 1800–1500 cm^{-1} were used

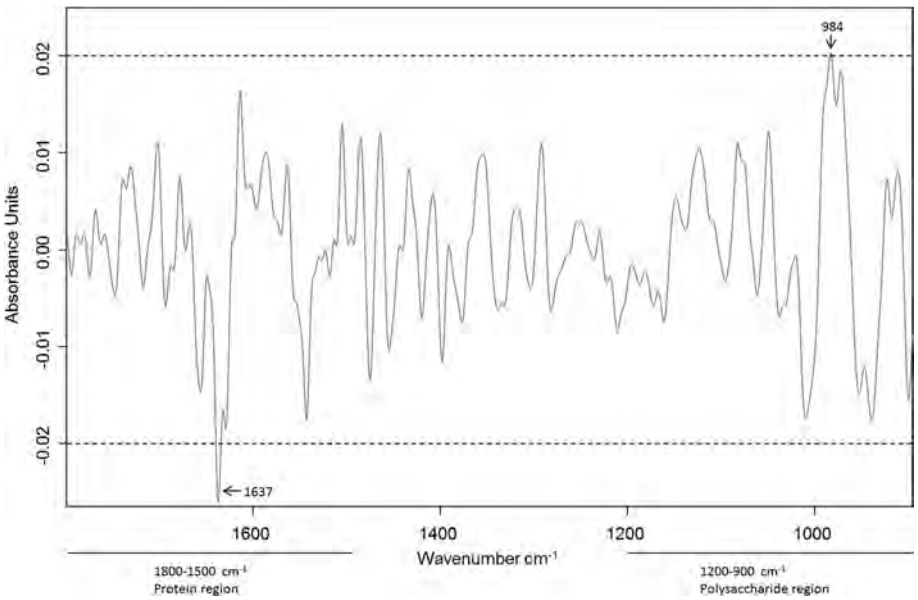

Fig. 6 Differential FTIR spectral analyses. The second derivate, vector-normalised average spectra were calculated from CE of re-isolated *A. pleuropneumoniae* Serotype 2 from the left and right tonsil of the infected pig 4 (I4) and the lung of the infected pigs 1–4 und 6 (I1-4 and I6), respectively. The average spectrum of the lung of I1-4 and 6 was subtracted from the average spectrum of the tonsils of I4. Most pronounced differences could be detected in the frequency area of 1800–900 cm^{-1} and can be related to the protein region (1800–1500 cm^{-1}) and the carbohydrate region (1200–900 cm^{-1})

pleuropneumoniae. This expression was evident both, at a transcriptional level and at the level of the protein, since Hp and CRP reached higher values also in saliva from infected animals. Whether this prominent implication of the salivary gland during acute bacterial infection is linked to the direct presence of *A. pleuropneumoniae* in this site is hitherto unknown. Nonetheless, the detection of the bacterium in the tonsils sited in anatomical proximity, and the reported susceptibility of the salivary gland to *A. pleuropneumoniae* colonisation [42], is a hint that the bacteria could invade this organ. Interestingly, bacteria could be re-isolated from tonsillar tissue, as a consequence of coughing or transport by the mucocillary escalator. However, a host immune response in tonsillar tissue, which would have been indicated by an increase in cytokine or acute phase protein expression, was not detected (Fig. 3).

During the last two decades, FTIR spectroscopy has become a well-established technique for identification of microorganism on the species and subspecies level [11]. Due to its high discriminatory power, FTIR spectroscopy is increasingly employed not only for bacterial identification but also for studying environmental impacts, such as abiotic stress or host genotypes, on the metabolic fingerprints of bacteria [12, 43]. Thus, FTIR spectroscopy represents a suitable tool for exploring the host impacts on *A. pleuropneumoniae* in parallel to the analyses of host reactions in response to the bacterial infection.

In the first step, *A. pleuropneumoniae* re-isolated from different host tissues was subjected to molecular analysis to confirm its genotypic identity with the strain used for inoculation. All isolates were positive in the *A. pleuropneumoniae* serotype 2 specific PCR and showed the same M13-PCR profiles. In contrast to the results from the molecular typing, FTIR spectral analysis revealed a distinct clustering of the isolates. The isolates clustered according to the tissue of re-isolation (Fig 4), reflecting the physiological metabolic adaptation due to their movement from the lower to the upper respiratory tract (Fig. 4–5). This might be indicative for different adaptation strategies, depending on the body compartment of colonisation or infection. Notably, the inoculation strain forms one cluster with the lung isolates while the isolates from the upper respiratory tract formed a separate cluster. This observation fosters out hypothesis that the bacteria are indeed rapidly adapting to the upper respiratory tract, which is reflected in their metabolic fingerprints that are distinct from the ones of the lung isolates and the inoculation strain. Furthermore, our results revealed that the laboratory culture medium (PPLO) and culture conditions used for growth of the inoculation strain mimick the host environment that bacteria are facing during acute infections in the lung (Fig. 4). As shown previously, growth conditions can significantly impact the metabolism and the expression of virulence factors of bacterial pathogens [12] and must be considered when inoculation samples for infection

studies are prepared. The observed phenotypical metabolic adaptation of *A. pleuropneumoniae* was reversible, which is in line with recent findings on the loss of host environmentally triggered memory effects over time reported from other bacteria [12, 44, 45]. Since isolation of *A. pleuropneumoniae* from tonsils and nostrils of swine not showing any clinical signs is common, the pathogen is considered to persist at these sites of infection [46]. Thus, when colonizing various host organs, differences in metabolic adaptations may have facilitated a persistence of *A. pleuropneumoniae*. Indeed, the HCA revealed a unique cluster for the lung isolates, while the isolates of the upper respiratory tract were more diverse (Fig. 4). The diversity observed among the latter isolates might reflect the individual appearance of acute disease symptoms, such as coughing.

The most pronounced influence on the metabolic fingerprint during bacterial host organ-specific adaptation was attributed to the spectral range of 1150–1100 cm^{-1}. This frequency area is part of the polysaccharide region (1200–800 cm^{-1}), which is dominated by a complex sequence of peaks associated to stretching ring vibrations of carbohydrates (C—O—C, C—O—P) [47]. Since a comparison of FTIR spectra of the CEs from *A. pleuropneumoniae* from the tonsils with the FTIR spectra recorded from the lung isolates revealed significant differences within their protein and carbohydrate compositions (Fig. 6), it is tempting to speculate that the capsule of the bacteria has an influence on the specific metabolic adaptation of the bacterium to the different host organs. The stronger appearance of β-sheet structures in the CEs from lung isolates indicates a shift towards a higher expression of β-sheet carrying proteins. To decipher the bacterial molecules and mechanisms involved in observed host tissue specific adaptation of *A. pleuropneumoniae* detailed quantitative and qualitative carbohydrate and protein analyses of the capsule are needed, which are clearly beyond the scope of our current work. Preliminary results from an ongoing study also point towards a reduced production of capsule material in the tonsil isolates (Frömbling et al., unpublished) and for *S. aureus* it has already been reported that the loss of capsule expression is advantageous to establish and maintain a chronic infection in humans as well as in animals (e.g. chronic osteomyelitis, bovine mastitis) [48]. Based on our results, it is tempting to speculate that the capsule formation is important for bacterial adaptation to the porcine tonsils as one step towards deciphering persistence of *A. pleuropneumoniae* in infected pig herds.

Conclusions

Altogether, our results indicate an important role of the salivary gland in oral immunity, already eight hours after infection. Contrarily to the lung, *A. pleuropneumoniae* was not able to provoke any immune response in the tonsils. Thus, the specific changes observed in the metabolic fingerprints of *A. pleuropneumoniae* are presumably crucial for bacterial adaptation to porcine tonsils. Further studies will be necessary to decipher the exact role and contribution of the tonsils as a reservoir of host adapted *A. pleuropneumoniae* for the development and establishment of chronic infections.

Additional files

Additional file 1: Information about IL8 primers and optimised qPCR assays. More details about the optimisation and validation of qPCR assays for target gene-specific primers in the pig are included. Particularly in the figure is shown that the suitability of the newly designed primers was verified in separate experiments by performing of a cDNA pool. In melt curve and amplification plots samples are shown in green while controls (no reverse transcription control (NRT) and no template control (NTC)) are shown in yellow and orange respectively. Additionally, an agarose gel electrophoresis of the PCR products of undiluted cDNA pool and controls was performed. (DOCX 349 kb)

Additional file 2: Hierarchical cluster analysis of FTIR spectroscopic data recorded from A. pleuropneumoniae serotype 2 after 2 and 5 passages under laboratory conditions. After re-isolation from different organs of the infected pigs 1–6 (I1-I6) recorded FTIR spectroscopic data of 2 and 5 passages on laboratory medium were subjected to hierarchical cluster analyses. After two passages nostril and tonsil isolates (upper respiratory tract isolates) cluster apart from all lung isolates, while passaging for five times leads to two intermingled clusters of lung and upper respiratory tract isolates as well as to a decrease in heterogeneity between the samples. For calculation of the dendrogram, the FTIR spectral regions of 900 to 1200 cm^{-1} and 1500 to 1800 cm^{-1} and Ward's algorithm were used. (PPTX 63 kb)

Acknowledgments
The authors thank K.-H. Waldmann for housing the animals and providing technical equipment.

Funding
Anne Menzel, the design and performance of the animal trial and the animal data collection were supported by the German Research Community (DFG, HE 6419/1-1). Elena L. Sassu and Janna Frömbling as well as all laboratory work, materials, analysis and interpretation of data were supported by the Graduate School for Pig and Poultry Medicine of the University of Veterinary Medicine Vienna, Austria. Elena L. Sassu and Janna Frömbling were supported by the Graduate School for Pig and Poultry Medicine of the University of Veterinary Medicine Vienna.

Availability of data and materials
The datasets used and analysed during the current study are available from the corresponding author on reasonable request.

Authors' contributions
IHP, MES, AS, CD and IM conceived and designed the experiments. AA, IHP, ES and AMe performed infection and clinical examination. MG performed laboratory diagnostic examination. JV produced and verified bacterial inocula. JF and JS performed microbiological analysis of samples. MHT performed histological examination. ES and MP performed cytokine measurements in body fluids. AMG performed acute phase protein quantification in BALF and saliva. AM, ES, CD, and IM carried out analysis of gene expression in tissues. JF and TG performed FTIR and chemometric analysis. ES, JF, MES and IHP wrote the paper. All authors read and critically revised and approved the final manuscript.

Competing interests
The authors declare that they have no competing interests.

Consent for publication
Not applicable.

Ethics approval
All animal experiments were approved by the Ethics and Animal Welfare Committee of the University of Veterinary Medicine Hannover and in accordance with the requirements of the German national animal welfare law. The study has been approved by the local permitting authorities in the Lower Saxony State Office for Consumer Protection and Food Safety (approval number: 33.9- 445 42502-12/0835) according to the guidelines of FELASA and ARRIVE.

Author details
[1]University Clinic for Swine, Department of Farm Animals and Veterinary Public Health, University of Veterinary Medicine Vienna, Vienna, Austria. [2]Department of Pathobiology, Functional Microbiology, Institute of Microbiology, University of Veterinary Medicine Vienna, Vienna, Austria. [3]Department of Biomedical Sciences, Institute for Medical Biochemistry, University of Veterinary Medicine Vienna, Vienna, Austria. [4]Department of Animal Medicine and Surgery, University of Murcia, Murcia, Spain. [5]Department of Pathobiology, Institute of Immunology, University of Veterinary Medicine Vienna, Vienna, Austria. [6]Forensic Medicine and Ambulatory Services, Clinic for Swine and Small Ruminants, University of Veterinary Medicine Hannover, Hannover, Germany. [7]Department of Pathology, University of Veterinary Medicine Hannover, Hannover, Germany. [8]Institute for Microbiology, University of Veterinary Medicine Hannover, Hannover, Germany.

Received: 13 February 2016 Accepted: 16 February 2017
Published online: 28 February 2017

References

1. Gottschalk M. Actinobacillosis. In: Zimmerman JJ, Karriker LA, Ramirez A, Schwartz KJ, Stevenson GW, editors. Diseases of Swine. Ames, Iowa, USA: Wiley-Blackwell; 2012. p. 653–69.
2. Chiers K, De Waele T, Pasmans F, Ducatelle R, Haesebrouck F. Virulence factors of Actinobacillus pleuropneumoniae involved in colonization, persistence and induction of lesions in its porcine host. Vet Res. 2010; 41:65.
3. Hellings P, Jorissen M, Ceuppens JL. The Waldeyer's ring. Acta Otorhinolaryngol Belg. 2000;54:237–41.
4. Liebler-Tenorio EM, Pabst R. MALT structure and function in farm animals. Vet Res. 2006;37:257–80.
5. Skovgaard K, Mortensen S, Boye M, Poulsen KT, Campbell FM, et al. Rapid and widely disseminated acute phase protein response after experimental bacterial infection of pigs. Vet Res. 2009;40:23.
6. Gutierrez AM, Yelamos J, Pallares FJ, Gomez-Laguna J, Ceron JJ. Local identification of porcine haptoglobin in salivary gland and diaphragmatic muscle tissues. Histol Histopathol. 2012;27:187–96.
7. Fenwick BW, Osburn BI. Immune responses to the lipopolysaccharides and capsular polysaccharides of Haemophilus pleuropneumoniae in convalescent and immunized pigs. Infect Immun. 1986;54:575–82.
8. Baarsch MJ, Scamurra RW, Burger K, Foss DL, Maheswaran SK, et al. Inflammatory cytokine expression in swine experimentally infected with Actinobacillus pleuropneumoniae. Infect Immun. 1995;63:3587–94.
9. Chen ZW, Chien MS, Chang NY, Chen TH, Wu CM, et al. Mechanisms underlying Actinobacillus pleuropneumoniae exotoxin ApxI induced expression of IL-1beta, IL-8 and TNF-alpha in porcine alveolar macrophages. Vet Res. 2011;42:25.
10. Wenning M SS, Naumann D. Infrared Spectroscopy in the Identification of Microorganisms. In: M Diem PG, JM Chalmers, editor. Handbook of Vibrational Spectroscopy for Medical Diagnosis. Hoboken: John Wiley & Sons; 2008. p. 71–96.
11. Naumann D, Helm D, Labischinski H. Microbiological characterizations by FT-IR spectroscopy. Nature. 1991;351:81–2.
12. Grunert T, Monahan A, Lassnig C, Vogl C, Muller M, et al. Deciphering host genotype-specific impacts on the metabolic fingerprint of Listeria monocytogenes by FTIR spectroscopy. PLoS One. 2014;9:e115959.
13. Wagener K, Grunert T, Prunner I, Ehling-Schulz M, Drillich M. Dynamics of uterine infections with Escherichia coli, Streptococcus uberis and Trueperella pyogenes in post-partum dairy cows and their association with clinical endometritis. Vet J. 2014;202:527–32.
14. Leiner G, Franz B, Strutzberg K, Gerlach GF. A novel enzyme-linked immunosorbent assay using the recombinant Actinobacillus pleuropneumoniae ApxII antigen for diagnosis of pleuropneumonia in pig herds. Clin Diagn Lab Immunol. 1999;6:630–2.
15. Hennig I, Teutenberg-Riedel B, Gerlach GF. Downregulation of a protective Actinobacillus pleuropneumoniae antigen during the course of infection. Microb Pathog. 1999;26:53–63.
16. Baarsch MJ, Foss DL, Murtaugh MP. Pathophysiologic correlates of acute porcine pleuropneumonia. Am J Vet Res. 2000;61:684–90.
17. Hennig-Pauka I, Baltes N, Jacobsen I, Stratmann-Selke J, Gerlach GF, et al. Study of the virulence of Actinobacillus pleuropneumoniae in finishing pigs as a basis for vaccination development. Berl Munch Tierarztl Wochenschr. 2008;121:189–97.
18. Brauer C, Hennig-Pauka I, Hoeltig D, Buettner FF, Beyerbach M, et al. Experimental Actinobacillus pleuropneumoniae challenge in swine: comparison of computed tomographic and radiographic findings during disease. BMC Vet Res. 2012;8:47.
19. Hannan PC, Bhogal BS, Fish JP. Tylosin tartrate and tiamutilin effects on experimental piglet pneumonia induced with pneumonic pig lung homogenate containing mycoplasmas, bacteria and viruses. Res Vet Sci. 1982;33:76–88.
20. Kozlov AV, van Griensven M, Haindl S, Kehrer I, Duvigneau JC, et al. Peritoneal inflammation in pigs is associated with early mitochondrial dysfunction in liver and kidney. Inflammation. 2010;33:295–305.
21. Duvigneau JC, Hartl RT, Groiss S, Gemeiner M. Quantitative simultaneous multiplex real-time PCR for the detection of porcine cytokines. J Immunol Methods. 2005;306:16–27.
22. Soler L, Gutierrez A, Martinez-Subiela S, Ceron JJ. Fast measurement of serum amyloid A in different specimens from swine by using a new one-step time-resolved fluorescent immunoassay. J Vet Diagn Invest. 2011;23:902–8.
23. Soler L, Luyten T, Stinckens A, Buys N, Ceron JJ, et al. Serum amyloid A3 (SAA3), not SAA1 appears to be the major acute phase SAA isoform in the pig. Vet Immunol Immunopathol. 2011;141:109–15.
24. Soler L, Gutierrez A, Mullebner A, Ceron JJ, Duvigneau JC. Towards a better understanding of salivary and meat juice acute phase proteins determination in pigs: an expression study. Vet Immunol Immunopathol. 2013; 156:91–8.
25. Gutierrez AM, Martinez-Subiela S, Ceron JJ. Evaluation of an immunoassay for determination of haptoglobin concentration in various biological specimens from swine. Am J Vet Res. 2009;70:691–6.
26. Gutierrez AM, Escribano D, Fuentes M, Ceron JJ. Circadian pattern of acute phase proteins in the saliva of growing pigs. Vet J. 2013;196:167–70.
27. Hussy D, Schlatter Y, Miserez R, Inzana T, Frey J. PCR-based identification of serotype 2 isolates of Actinobacillus pleuropneumoniae biovars I and II. Vet Microbiol. 2004;99:307–10.
28. Henderson I, Duggleby CJ, Turnbull PC. Differentiation of Bacillus anthracis from other Bacillus cereus group bacteria with the PCR. Int J Syst Bacteriol. 1994;44:99–105.
29. Oberreuter H, Seiler H, Scherer S. Identification of coryneform bacteria and related taxa by Fourier-transform infrared (FT-IR) spectroscopy. Int J Syst Evol Microbiol. 2002;52:91–100.
30. Schabauer L, Wenning M, Huber I, Ehling-Schulz M. Novel physico-chemical diagnostic tools for high throughput identification of bovine mastitis associated gram-positive, catalase-negative cocci. BMC Vet Res. 2014;10:156.
31. Grunert T, Wenning M, Barbagelata MS, Fricker M, Sordelli DO, et al. Rapid and reliable identification of Staphylococcus aureus capsular serotypes by means of artificial neural network-assisted Fourier transform infrared spectroscopy. J Clin Microbiol. 2013;51:2261–6.
32. Dubreuil JD, Jacques M, Mittal KR, Gottschalk M. Actinobacillus pleuropneumoniae surface polysaccharides: their role in diagnosis and immunogenicity. Anim Health Res Rev. 2000;1:73–93.
33. Naumann D. Infrared Spectroscopy in Microbiology. In: Meyers RA, editor. Encyclopedia of Analytical Chemistry 102–131 ed. John Wiley & sons: Chichester; 2000.
34. Beekes M, Lasch P, Naumann D. Analytical applications of Fourier transform-infrared (FT-IR) spectroscopy in microbiology and prion research. Vet Microbiol. 2007;123:305–19.
35. Hoeltig D, Hennig-Pauka I, Thies K, Rehm T, Beyerbach M, et al. A novel Respiratory Health Score (RHS) supports a role of acute lung damage and pig breed in the course of an Actinobacillus pleuropneumoniae infection. BMC Vet Res. 2009;5:14.
36. Fossum C, Wattrang E, Fuxler L, Jensen KT, Wallgren P. Evaluation of various cytokines (IL-6, IFN-alpha, IFN-gamma, TNF-alpha) as markers for acute bacterial infection in swine–a possible role for serum interleukin-6. Vet Immunol Immunopathol. 1998;64:161–72.

37. Wyns H, Croubels S, Vandekerckhove M, Demeyere K, De Backer P, et al. Multiplex analysis of pro-inflammatory cytokines in serum of Actinobacillus pleuropneumoniae-infected pigs. Res Vet Sci. 2015;102:45–8.
38. Lauritzen B, Lykkesfeldt J, Skaanild MT, Angen O, Nielsen JP, et al. Putative biomarkers for evaluating antibiotic treatment: an experimental model of porcine Actinobacillus pleuropneumoniae infection. Res Vet Sci. 2003;74: 261–70.
39. Heegaard PM, Klausen J, Nielsen JP, Gonzalez-Ramon N, Pineiro M, et al. The porcine acute phase response to infection with Actinobacillus pleuropneumoniae. Haptoglobin, C-reactive protein, major acute phase protein and serum amyloid A protein are sensitive indicators of infection. Comp Biochem Physiol B Biochem Mol Biol. 1998;119:365–73.
40. Sorensen NS, Tegtmeier C, Andresen LO, Pineiro M, Toussaint MJ, et al. The porcine acute phase protein response to acute clinical and subclinical experimental infection with Streptococcus suis. Vet Immunol Immunopathol. 2006;113:157–68.
41. Ramadas RA, Wu L, LeVine AM. Surfactant protein A enhances production of secretory leukoprotease inhibitor and protects it from cleavage by matrix metalloproteinases. J Immunol. 2009;182:1560–7.
42. Chiers K, Haesebrouck F, van Overbeke I, Charlier G, Ducatelle R. Early in vivo interactions of Actinobacillus pleuropneumoniae with tonsils of pigs. Vet Microbiol. 1999;68:301–6.
43. Alvarez-Ordonez A, Mouwen DJ, Lopez M, Prieto M. Fourier transform infrared spectroscopy as a tool to characterize molecular composition and stress response in foodborne pathogenic bacteria. J Microbiol Methods. 2011;84:369–78.
44. Afroz T, Biliouris K, Kaznessis Y, Beisel CL. Bacterial sugar utilization gives rise to distinct single-cell behaviours. Mol Microbiol. 2014;93:1093–103.
45. Kotula JW, Kerns SJ, Shaket LA, Siraj L, Collins JJ, et al. Programmable bacteria detect and record an environmental signal in the mammalian gut. Proc Natl Acad Sci U S A. 2014;111:4838–43.
46. Sidibe M, Messier S, Lariviere S, Gottschalk M, Mittal KR. Detection of Actinobacillus pleuropneumoniae in the porcine upper respiratory tract as a complement to serological tests. Can J Vet Res. 1993;57:204–8.
47. Yu C, Irudayaraj J. Spectroscopic characterization of microorganisms by Fourier transform infrared microspectroscopy. Biopolymers. 2005;77:368–77.
48. Tuchscherr L, Loffler B, Buzzola FR, Sordelli DO. Staphylococcus aureus adaptation to the host and persistence: role of loss of capsular polysaccharide expression. Future Microbiol. 2010;5:1823–32.

Additional file 1: Optimisation and validation of qPCR assays for target gene-specific primers in the pig.

Table : Information about Intron-spanning primers.

Target	Accession number	Sequence	Position. on plus-strand	Product-length (bp)	Exon junctions in	Intron size (bp)
IL8	NM_213867.1	AACAGCCCGTGTCAACATGA	68	125	product	~1000
		TGCACTGGCATCGAAGTTCT	192			

Table: Optimised protocol and validation studies using cDNA pool dilution series.

Target	Annealing temp (°C)/time (sec)	Extension temp (°C)/time (sec)	ΔCt (RT+ to RT-)	slope	Correlation Coefficient (Pearson) R^2	Verified dynamic range
IL8	62/30	72/40	n.d.	-3.545	0.998	10^6

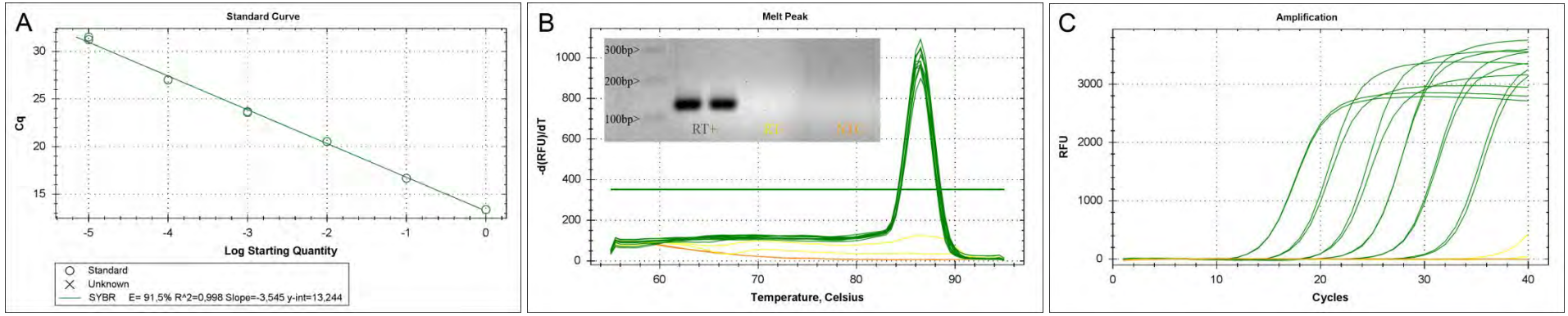

Figure The suitability of the newly designed primers was verified in separate experiments by performing of a cDNA pool (**A**). In melt curve (**B**) and amplification plots (**C**) samples are shown in green while controls (no reverse transcription control (NRT) and no template control (NTC)) are shown in yellow and orange respectively. In the inlet in B shows an agarose gel electrophoresis of the PCR products of undiluted cDNA pool and controls.

Additional file 2

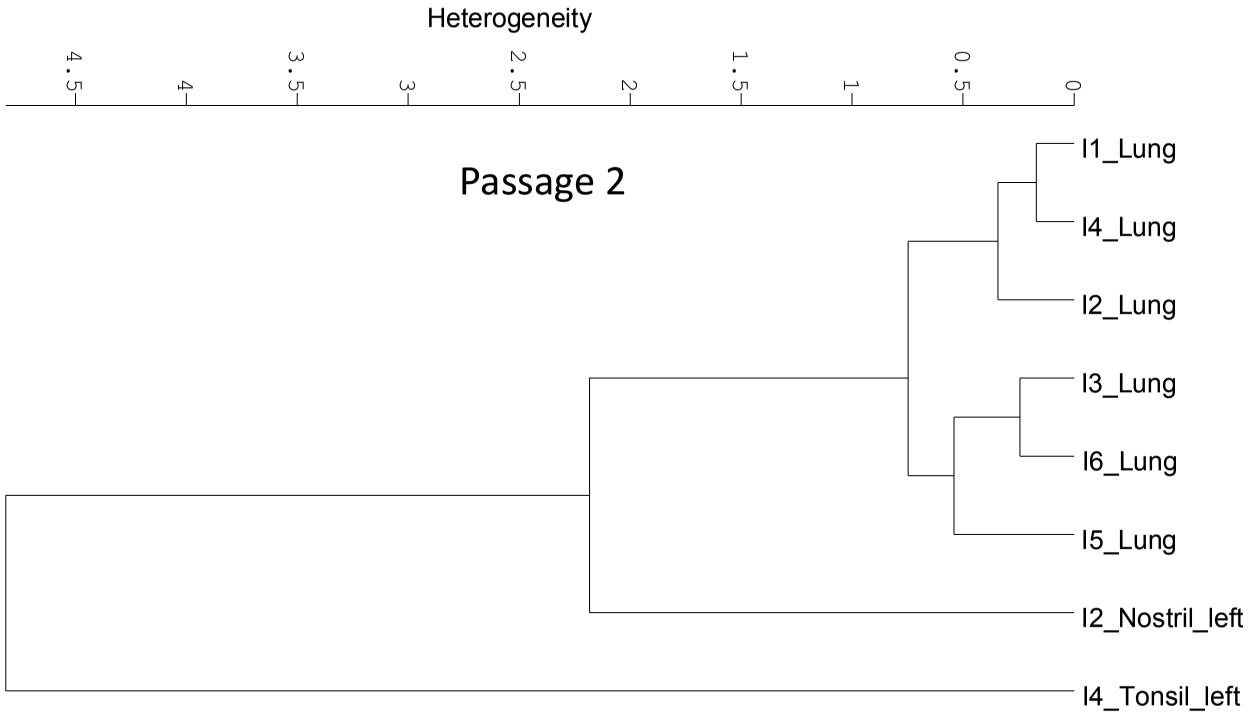

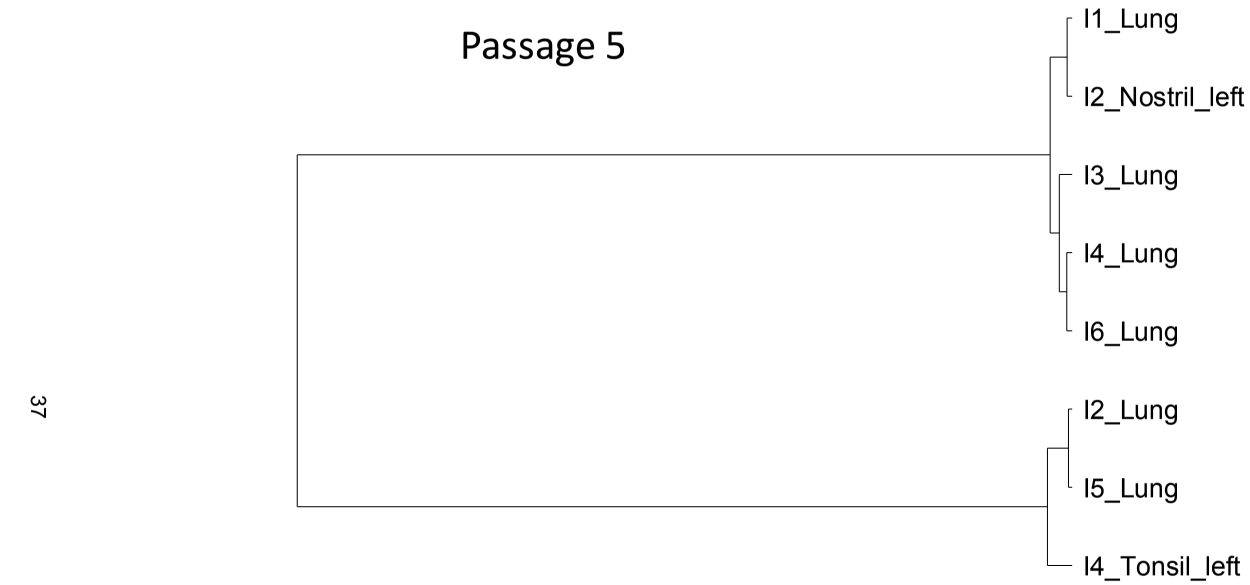

Sassu *et al. Vet Res (2017) 48:4*
DOI 10.1186/s13567-017-0411-z

VETERINARY RESEARCH

RESEARCH ARTICLE Open Access

Frequency of Th17 cells correlates with the presence of lung lesions in pigs chronically infected with *Actinobacillus pleuropneumoniae*

Elena L. Sassu[1], Andrea Ladinig[1], Stephanie C. Talker[2], Maria Stadler[2], Christian Knecht[1], Heiko Stein[1], Janna Frömbling[3], Barbara Richter[4], Joachim Spergser[3], Monika Ehling-Schulz[3], Robert Graage[5], Isabel Hennig-Pauka[1†] and Wilhelm Gerner[2*†]

Abstract

Porcine contagious pleuropneumonia caused by *Actinobacillus pleuropneumoniae* (APP) remains one of the major causes of poor growth performance and respiratory disease in pig herds. While the role of antibodies against APP has been intensely studied, the porcine T cell response remains poorly characterized. To address this, pigs were intranasally infected with APP serotype 2 and euthanized during the acute phase [6–10 days post-infection (dpi)] or the chronic phase of APP infection (27–31 dpi). Lymphocytes isolated from blood, tonsils, lung tissue and tracheobronchial lymph nodes were analyzed by intracellular cytokine staining (ICS) for IL-17A, IL-10 and TNF-α production after in vitro stimulation with crude capsular extract (CCE) of the APP inoculation strain. This was combined with cell surface staining for the expression of CD4, CD8α and TCR-γδ. Clinical records, microbiological investigations and pathological findings confirmed the induction of a subclinical APP infection. ICS-assays revealed the presence of APP-CCE specific $CD4^+CD8\alpha^{dim}$ IL-17A-producing T cells in blood and lung tissue in most infected animals during the acute and chronic phase of infection and a minor fraction of these cells co-produced TNF-α. APP-CCE specific IL-17A-producing γδ T cells could not be found and APP-CCE specific IL-10-producing $CD4^+$ T cells were present in various organs but only in a few infected animals. The frequency of identified putative Th17 cells ($CD4^+CD8\alpha^{dim}IL\text{-}17A^+$) in lung and blood correlated positively with lung lesion scores and APP-specific antibody titers during the chronic phase. These results suggest a potential role of Th17 cells in the immune pathogenesis of APP infection.

Introduction

Actinobacillus pleuropneumoniae (APP) is a gram negative bacterium, belonging to the *Pasteurellaceae* family that causes porcine respiratory disease worldwide. The outcome of the infection can vary from sudden death with bloody nasal discharge to an acute disease with fever and coughing that frequently results in chronic infections [1]. Vaccination and antibiotic based therapies can help to reduce the severity of the symptoms and decrease the mortality rates, but are not effective in clearing the bacteria [2]. In fact, pigs overcoming the acute phase can become subclinically infected and persistent carriers, harboring APP in tonsils and chronic lung lesions [3]. Since 1957, when APP was first reported, most research activities were focused on the elucidation of the humoral immune response [4–6]. Thereby it also became clear that APP developed several strategies to avoid humoral host defense mechanisms. For example, in vitro experiments indicated that APP can survive in alveolar macrophages [7], has the capacity for enhanced biofilm formation in anaerobic conditions [8], and changes the polysaccharide composition of the capsule [3]; all possibly contributing

*Correspondence: Wilhelm.Gerner@vetmeduni.ac.at
†Isabel Hennig-Pauka and Wilhelm Gerner contributed equally to this work
[2] Institute of Immunology, Department of Pathobiology, University of Veterinary Medicine Vienna, Vienna, Austria
Full list of author information is available at the end of the article

to an escape from humoral immunity and to the establishment of chronic infection in lung tissue and tonsils.

For a more thorough understanding of APP pathogenesis and persistence, cell-mediated immune mechanisms also need to be taken into focus. In particular, T-cell responses may equip the host with additional means to combat APP infections, but could also be involved in dysfunctional immune responses [9] or could support immune escape mechanisms [10]. Hitherto, the T-cell mediated immune response to APP has been poorly characterized in swine. Early studies indicated the potential relevance of T cells, because the intensity of a T-cell dependent delayed-type hypersensitivity reaction was associated with protection against an APP challenge infection [11]. In addition, a change in the CD4:CD8 ratio in peripheral blood following low-dose APP immunization and high-dose APP challenge has been reported, but the phenotype of involved cells was not further studied [12]. Furthermore, Faldyna et al. [13] described an increase of $CD8\alpha^-$ γδ T cells in bronchoalveolar lavage fluid (BALF) as well as B-cells in tracheobronchial lymph nodes of pigs challenged with APP suggesting a role of γδ T cells in this infection. More recently, IL-17 was shown to be induced on the transcriptional level in lungs of pigs affected by APP [14] and it has been demonstrated that $CD4^+$ and γδ T cells are capable to produce IL-17 in swine [15–17]. From studies in mice and humans it is known that IL-17-producing $CD4^+$ T (Th17) cells are involved in the clearance of extracellular pathogens in peripheral organs by attraction and stimulation of neutrophils [18]. There is also some evidence that Th17 cells can be involved in chronic airway inflammation [19]. Moreover, in vivo and in vitro studies with *Mannheimia haemolytica*, which like APP belongs to the *Pasteurellaceae* family and induces neutrophilic infiltration in the lung, suggested an IL-17 production by bovine γδ T cells [20]. Thus we hypothesized that IL-17 production by Th17 but also γδ T cells might be involved in the porcine immune response to APP. Since the anti-inflammatory cytokine IL-10 may support the survival of microorganisms in the host via inhibiting their cell-mediated immune response [21–23], we investigated in parallel its role in persistence of APP.

To address these issues we developed an APP infection model and an in vitro stimulation assay making use of an APP crude capsular extract (APP-CCE). Cytokine production by $CD4^+$ and γδ T cells was investigated by intracellular cytokine staining (ICS) of lymphocytes isolated from different host compartments during the acute and chronic phase of APP infection. We found that the majority of pigs infected with APP harbor APP-CCE specific IL-$17A^+$ $CD4^+$ T cells in the lung and in the blood during the acute and the chronic phase of APP infection. In chronically infected animals, the frequency of these cells in lung and peripheral blood was found to correlate positively with lung lesions and APP-specific antibody titers.

Materials and methods

Experimental APP infection model

Thirty 5-week-old male castrated pigs (German Landrace), routinely tested to be negative for APP, porcine reproductive and respiratory syndrome virus (PRRSV), toxigenic *Pasteurella multocida*, endo- and ectoparasites, were derived from a closed breeding herd of high health status in Mecklenburg-Western Pomerania, Germany. Animals were moved to Austria, following European guidelines on protecting the welfare of animals during transport, stated by Regulation (EC) No 1/2005. Upon arrival, animals entered a biosafety level 2 facility at the University of Veterinary Medicine Vienna, where they were kept for the entire duration of the experiment. Animals were weighed, individually marked with ear tags, and then, according to their body weight, divided into a control and an infected group of ten and twenty animals respectively. Control and infected group were housed in separate compartments. Within the infected group, animals were assigned to two subgroups of ten animals each, which were kept under identical conditions but euthanized either 6–10 days post-infection (dpi) (acute infected group) or 27–31 dpi (chronic infected group). At the time of arrival, the APP-free status of the pigs was confirmed by bacteriological examination of nasal and tonsillar swabs and by serological testing for antibodies against Apx-IV using the commercially available IDEXX APP-ApxIV Ab Test ELISA (IDEXX Laboratories, Westbrook, USA). After 2 weeks of adaptation, at day 0 an intranasal spray infection was performed. For the infection, an APP biotype 1 serotype 2 strain (Lab number C3656/0271/11) was used, isolated originally by the Institute of Microbiology, University of Veterinary Medicine, Hanover, Germany from a diseased fattening pig during an acute outbreak of porcine pleuropneumonia in northern Germany [24]. After initial isolation, bacteria were animal-passaged once and lab-passaged four times in PPLO medium supplemented with NAD. Pigs were infected with 2 mL (1 mL into each nostril) of bacterial culture containing 2×10^4 CFU/mL. The bacterial culture was vaporized directly into the nostrils of the pigs by using a mucosal atomization device (LMA MAD Nasal™, Teleflex Medical GmbH, Athlone, Ireland). Control pigs underwent the same procedure, but received 2 mL of 154 mM sterile NaCl instead of the bacterial culture. Daily clinical examinations were carried out and assembled in a clinical score, considering rectal temperature, presence of dyspnea and/or coughing and changes

in behavior (see Additional file 1 for details). Additionally, pig body weights were recorded weekly. To screen for presence of APP in the upper respiratory tract, nasal and tonsillar swabs were examined at 14 and 21 dpi. At the end of the experiment, after animals were euthanized, tonsillar tissues were taken instead of swabs. Blood samples were taken by puncture of the *V. cava cranialis* or *V. jugularis* on the same days. Sera were used for detection of APP 2 specific antibodies, while heparinized samples were obtained to isolate peripheral blood mononuclear cells (PBMCs). Euthanasia was performed on five consecutive days (two infected pigs and one control pig per day) in two different time frames: 6–10 dpi and 27–31 dpi for the acutely and the chronically infected group, respectively. Within these two periods, animals were randomly selected for euthanasia, which was performed by intracardial administration of T61® (T61®: Embutramid, Mebezoniumiodid, Tetracainhydrochlorid, 1 mL/10 kg BW, MSD, Whitehouse Station, NJ, USA) during anesthesia (Narketan®, Stresnil®). All animal procedures were approved by the institutional ethics committee, the Advisory Committee for Animal experiments (§12 of Law for Animal Experiments, Tierversuchsgesetz—TVG) and the Federal Ministry for Science and Research (reference number bmwfw GZ 68.205/0138-WF/V/3b/2015).

Gross necropsy and pathological examination

At necropsy, a general pathological examination of the carcass was performed, with focus on the respiratory tract. Organs of interest for the study were extracted in the following order: salivary gland (*Glandula mandibularis*, GM), tonsils, tracheobronchial lymph node (TBLN) and lung. After evaluation of the thoracic cavity, the lung was extracted from the chest while paying particular attention to the presence of pleural effusion or pleural adhesions. Then the severity of the pathological findings was determined using the lung lesion score (LLS) by Hannan et al. [25] and using the slaughterhouse pleurisy evaluation system (SPES) [26] for assessment of the pleura status. After clamping off the left main bronchus, the right lung was flushed with 100 mL of 154 mM sterile NaCl for collection of BALF, while tissue samples were taken from the dorsal portion of the left caudal lobe. If no lesions were detected in this particular area, an additional sample from another affected part of the lung was taken for histologic and bacteriological investigations. For histology, samples were fixed in 10% neutral buffered formalin, processed in 3-µm-thick paraffin-embedded sections and stained with haematoxylin and eosin.

Microbiological investigation

Nasal and tonsillar swabs from living animals and nasal swabs, salivary gland, tonsils, tracheobronchial lymph node, lung and BALF from euthanized animals were investigated for the presence of APP by streaking the samples on Columbia sheep blood agar (Oxoid, Vienna, Austria). *Staphylococcus aureus* was used as nurse to facilitate the isolation of APP from organs carrying a high bacterial background flora, such as tonsils and nose [1]. Subsequently, APP was transferred to PPLO agar supplemented with 10 mg/L NAD (AppliChem GmbH, Darmstadt, Germany). Plates were incubated overnight at 37 °C and 5% CO_2. Identification of the re-isolated bacteria was confirmed by serotype 2 specific PCR, using primers for the capsular biosynthesis genes *cps2AB* [27]. In addition, snap frozen tissue samples were examined directly by a conventional PCR based on detection of the apxIVA gene [28].

Determination of APP 2-specific antibody titers in serum

Sera obtained prior to infection (day 0), at the time of euthanasia and at 14 and 21 dpi were analyzed for antibodies against APP 2 using the commercial Swinecheck® APP 2 ELISA (Biovet, St-Hyacinthe, Canada) according to the manufacturer's instructions. Results were recorded as S/P ratio, obtained by the ratio between optical density (OD) of each sample (S) and the mean OD of the positive control (P): ODs/MODp.

Preparation of APP crude capsular extract for in vitro recall experiments

To stimulate lymphocytes in vitro, a crude capsular extract (CCE) from the APP serotype 2 strain C3656/0271/11, which has been used to infect the animals, was prepared following a modified protocol from Wittkowski et al. [29]. In detail, 300 mL liquid cultures of APP biotype 1, serotype 2, strain C3656, were grown to an OD_{600} of approximately 0.2 and harvested by centrifugation at 6530 *g* for 5 min. Aqueous phenol (1%, w/v) was added to the harvested bacteria (18 mL per gram of bacterial wet weight). Thereafter, the suspensions were shaken for 10 min at 37 °C and transferred to conical 25 mL flasks and the solution was gently stirred for 4 h at 4 °C. After centrifugation at 21 420 *g* for 30 min at 4 °C, the supernatant was filtrated (0.2 µm, Filtropur, Sarstedt, Nümbrecht, Germany), dialyzed against MilliQ-H_2O (2–4 L replaced every 4 h during the first day, then every 8 h) at 4 °C for 2 days, using 1 kDa MWCO membrane (Mini Dialysis Kit, GE Healthcare) and finally lyophilized overnight. To preserve the integrity of potential immunogenic proteins in the capsular extract, no further purification was performed. Lyophilized samples were dissolved in phosphate buffered saline (PBS) to reach a final concentration of 1 mg/mL. The stimulus was tested for potential toxicity in ConA-stimulated (3 µg/mL) PBMCs labelled with violet proliferation dye

as described elsewhere [30]. After 4 days of cultivation, PBMCs were harvested and stained with Live/Dead® Near-IR stain kit (Invitrogen, Carlsbad, CA, USA) according to manufacturer's instructions and subjected to flow cytometry (FCM). Frequencies of dead cells and proliferating cells were determined and by a dose titration of the CCE, the optimal working concentration was found to be 4 µg/mL.

Sample collection and isolation of lymphocytes

Blood samples were collected in Lithium-Heparin tubes (Primavette®, KABE Labortechnik, Nümbrecht, Germany) prior to infection (day 0), at 14 and 21 dpi and at the time of death. PBMCs were isolated by density gradient centrifugation (Pancoll human, density 1.077 g/mL, PAN Biotech, Aidenbach, Germany) as described elsewhere [31]. Tonsils and tracheobronchial lymph nodes were subjected to a procedure for isolation of lymphocytes as previously described [30].

For isolation of lymphocytes from lung tissue, a block of tissue (approx. 4 × 3 × 2 cm) from the dorsal portion of the left caudal lobe was cut into small pieces (approx. 3 × 3 × 3 mm) and lymphocytes were isolated as described elsewhere [32]. Cells from the various tissues and blood were counted and suspended in cell culture medium (RPMI1640 with stable glutamine supplemented with 10% FCS, 100 IU/mL penicillin, 100 µg/mL streptomycin, all from PAN Biotech and 90 µg/mL gentamicin, from Sigma-Aldrich, Schnelldorf, Germany) for in vitro cultivation. To standardize the isolation of lymphocytes from lung tissue, we decided to sample a defined region of the lung, independently of the presence of lesions. The dorsal portion of the left caudal lobe was selected for this purpose, since the caudal lobes have been described to be a common site for APP lesions [33] but the right lung was washed for the collection of BALF.

Histopathological analysis of lung tissue

Lung samples for histopathological analysis from acutely and chronically infected animals were fixed in neutral buffered formalin and embedded in paraffin wax. Tissue slides were routinely stained with hematoxylin and eosin and examined by a pathologist blinded to the different treatment groups. The samples were located adjacent to tissue used for lymphocyte isolation. Histopathological lesions associated with porcine pleuropneumonia, such as tissue necrosis, neutrophilic, histiocytic and lymphocytic infiltration, vascular leakage (including edema, bleeding, and fibrin in tissue or air spaces) and fibroplasia were graded (0 = not present, 1 = low grade, 2 = moderate grade, 3 = high grade).

In vitro stimulation of lymphocytes

Freshly isolated cells from lung, blood, tracheobronchial lymph nodes and tonsils were stimulated in vitro with APP-CCE (4 µg/mL) for 18 h at 37 °C in 5% CO_2. Cells were cultured in round-bottomed 96-well plates, at 5×10^5 cells per well, in a volume of 200 µL. Four hours prior to harvesting the cells, Brefeldin A (BD GolgiPlug™, BD Biosciences, San Jose, CA, USA) was added at a final concentration of 1 µg/mL. In parallel, cells incubated in cell culture medium only served as a negative control. As a positive control for cytokine production, a further set of cells was cultivated in cell culture medium overnight but stimulated with phorbol 12-myristate 13-acetate (PMA; 50 ng/mL; Sigma-Aldrich) and Ionomycin (500 ng/mL; Sigma-Aldrich) during the last 4 h of incubation.

Intracellular cytokine staining and FCM analysis

For FCM staining, cells were harvested and resuspended in PBS (without Ca^{2+}/Mg^{2+}) supplemented with 3% FCS. Monoclonal antibodies (mAbs) and secondary reagents that were used for cell surface staining and subsequent intracellular cytokine staining are listed in Table 1. Staining was performed in 96-well round-bottom plates with all incubation steps lasting for 20 min at 4 °C. For discrimination of dead cells, Live/Dead® Near-IR stain kit (Invitrogen) was used. To fix and permeabilize the cells, BD Cytofix/Cytoperm and BD Perm/Wash (BD Biosciences, CA, USA) was employed according to manufacturer's instructions.

FCM samples were analyzed on a FACSCanto™ II flow cytometer (BD Biosciences) equipped with three lasers (405, 488 and 633 nm). For automatic calculation of the compensation, single-stain samples were prepared. Between 5×10^5 and 1×10^6 lymphocytes were recorded per sample. Gating of the lymphocytes, doublet discrimination and dead-cell exclusion were performed for all samples as displayed in Additional file 2. Data were processed by FACSDiva software (Version 6.1.3 BD Biosciences) and transferred to Microsoft Excel (Office 2010; Microsoft, Redmond, WA, USA) for further calculations and preparation of graphs.

Statistical analysis

Spearman's rank correlation test was used to investigate the correlation between the frequency of Th17 cells and disease parameters in individual pigs. Spearman's rank correlation coefficients (ρ) and corresponding p values were calculated in SPSS software (2011, IBM, SPSS Statistics for Windows, Version 20.0, Armonk, NY, IBM Corp.). SPSS was also applied to produce correlation graphs. For further elaboration of graphs, Inkscape

Table 1 Antibody panels

Antigen	Clone	Isotype	Fluorochrome	Labelling strategy	Source of primary Ab
Intracellular cytokine staining for IL-17A and TNF-α					
CD4	74-12-4	IgG2b	PerCP-Cy5.5	Directly conjugated	BD Biosciences
CD8α	11/295/33	IgG2a	Pe-Cy7	Secondary antibody[a]	In house
TCR-γδ	PPT16	IgG2b	BV421	Biotin–streptavidin[b]	In house
IL-17A	SCPL1362	IgG1	Alexa647	Directly conjugated	BD Biosciences
TNF-α	MAb11	IgG1	BV605	Directly conjugated	BioLegend
Intracellular cytokine staining for IL-10					
CD4	74-12-4	IgG2b	Alexa647	Secondary antibody[c]	In house
CD8α	11/295/33	IgG2a	BV421	Biotin–streptavidin[b]	In house
IL-10	945A 4C4 37B1	IgG1	PE	Secondary antibody[d]	Invitrogen

[a] Goat Anti-Mouse IgG_{2a}-PE-Cy7, SouthernBiotech.

[b] Brilliant Violet 421™ Streptavidin, BioLegend.

[c] Goat Anti-Mouse IgG_{2b}-AlexaFluor647, Invitrogen.

[d] Goat Anti-Mouse IgG_1-PE, SouthernBiotech.

(Version 0.91; Free and Open Source Software licensed under the GPL) was used.

Results

Establishment of an infection model for APP subclinical infection

To confirm the establishment of a subclinical APP infection in the pigs of our study, bacteriological and clinical parameters were investigated (Figure 1). APP could be isolated from the nose of the majority of infected animals both from the acute (6–10 dpi) and from the chronic period (27–31 dpi) (Figure 1A). Animals belonging to the latter group were additionally tested at 14 and 21 dpi, for weekly monitoring. The nasal swabs of some of these animals were positive during weekly monitoring but not at the time of death (indicated by a § in Figure 1A). Isolation of APP from tonsils was often impaired by overgrowth of contaminating flora, but for the majority of animals from the chronic phase (8 out of 10) APP could be identified by PCR. At the early endpoint (6–10 dpi), the location from which APP was most frequently isolated was the lung, with 7 positive samples out of 10. In contrast, at the late endpoint (27–31 dpi) only 1 out of 10 samples was positive in the lung. APP was detected in BALF and TBLN of only one animal, which died suddenly at 8 dpi (#19). APP could not be detected in salivary glands (*G. mandibularis*, GM) of any animal.

Macroscopically visible lung tissue alterations were highly variable, which is partially reflected by the lung lesion and SPES scores (Figure 1B; Additional file 3 for representative animals). On average, LLS scores from animals sacrificed during the acute phase were higher than during the chronic phase. Typical histopathological findings indicating porcine pleuropneumonia were found in infected pigs varying from acute (hyperemia, edema, neutrophilic infiltration) to chronic (sequestration of necrotic areas by a mixed inflammatory infiltrate and fibroplasia) inflammatory tissue alterations (Additional file 4).

To evaluate the health status of the pigs, rectal temperature was measured daily together with other clinical parameters. Generally, infected animals developed clinical symptoms like dyspnea and coughing and were more lethargic than controls within the first 10 dpi. No significant differences in average daily weight gain were observed between infected (mean 724.7 g ± standard deviation of 92.6 g) and control (785.3 g ± standard deviation of 130.7 g) animals during the first 3 weeks post infection. Body temperature of infected animals started rising towards 40 °C immediately after the day of infection (day 0), with some animals reaching high temperature levels within 1–10 dpi (Figure 1C). Then, the rectal temperature stabilized between 39.5 and 40 °C for 2 weeks to finally align with the levels of control animals at the end of the study period (25–31 dpi). In parallel, the APP 2-specific humoral response was evaluated throughout the experiment (Figure 1D). Most of the infected animals produced antibodies against APP 2 after 14 days, i.e., antibodies were only detectable in animals that survived until the chronic phase of infection. No APP 2 antibodies were detectable in control animals at any time point.

Production of IL-17A and/or TNF-α by $CD4^+$ T cells in response to APP-CCE

For characterization of the T-cell mediated immune response, freshly isolated cells from lung, PBMCs, TBLN and tonsils were subjected to in vitro stimulation with

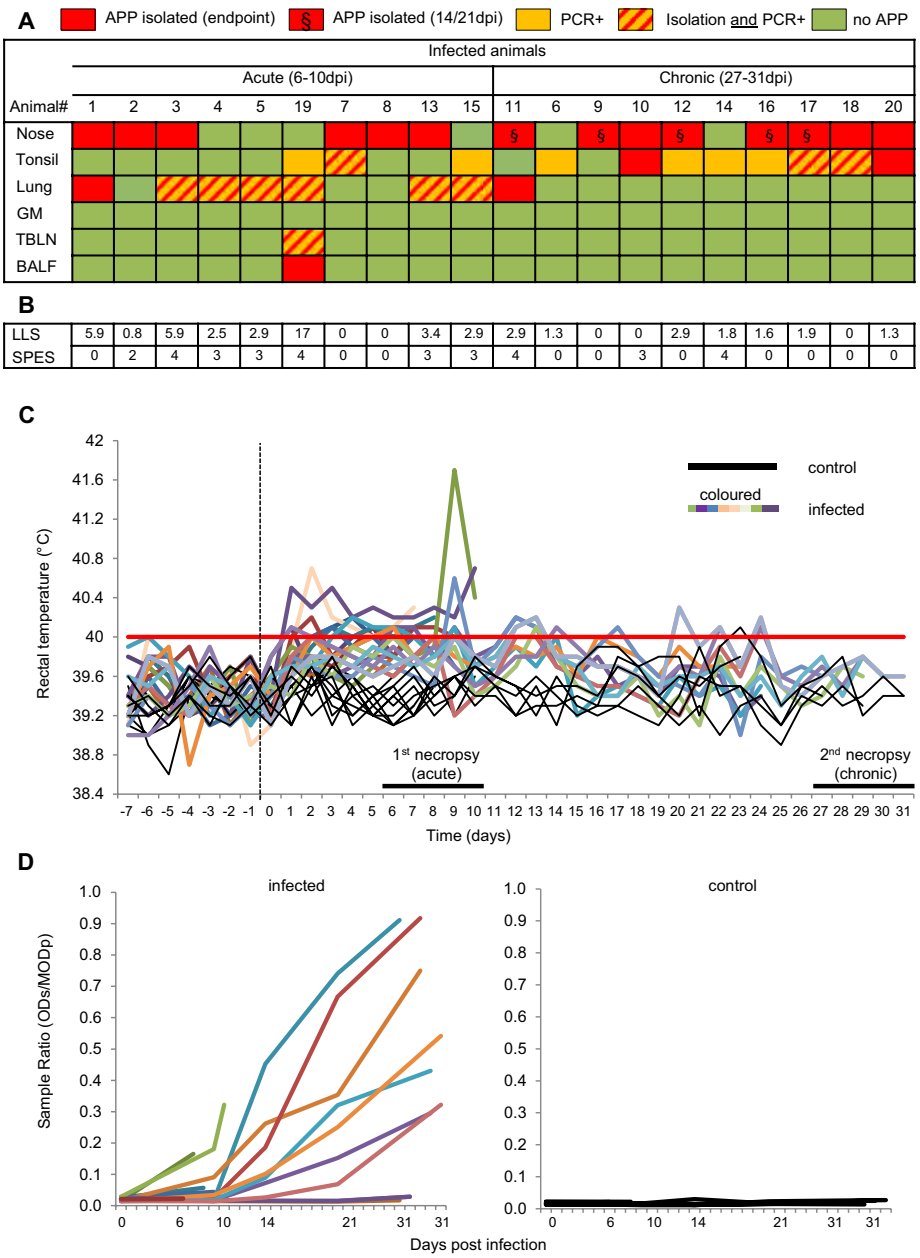

Figure 1 Microbiological investigation, lung pathology, clinical signs and antibody titers of APP-infected pigs. A The presence of APP was investigated at different host locations during necropsy (GM, *Glandula mandibularis*; TBLN, tracheobronchial lymph node; BALF, bronchoalveolar lavage fluid). Red boxes indicate APP detection by agar isolation, orange boxes indicate APP detection by PCR and orange boxes with red lines indicate positive results by both techniques. Green boxes indicate negative findings for APP. Results shown in the table refer to sampling on the day of euthanasia. The nasal swabs of animals #11, 9, 12, 16 and 17 were tested positive only on day 14 and/or 21 pi. This is indicated by red boxes with §. **B** Pathology of the lung was assessed by lung lesion score (LLS) for the lung tissue and by slaughterhouse pleurisy evaluation system (SPES) for the pleura. **C** Rectal temperatures were measured daily in both infected (colored lines) and control (black lines) animals. Body temperature of 40 °C or higher was considered as fever (red line). **D** Humoral response against APP serotype 2. Data are expressed as a ratio between optical density of the sample (ODs) and the mean of the optical density of the positive control (MODp). Colored lines in the left graph show ratios for infected animals, black lines in the right graph indicate ratios from sera of control animals.

APP-CCE of APP 2 followed by ICS for IL-17A and TNF-α. Medium- and PMA/Ionomycin-stimulated cultures served as negative and positive controls, respectively. Total living lymphocytes were gated and analyzed for CD4 expression and IL-17A production (Additional files 2A–D). A considerable variability in frequencies of

IL-17A$^+$ CD4$^+$ T cells was found between different animals and organs following APP-CCE stimulation (Figure 2). Figure 2A shows representative data of IL-17A production and CD4 expression in lung-derived lymphocytes isolated from different animals during the acute and chronic phase. For each time point, original FCM data from one animal with a high and a low frequency of APP-CCE-responsive IL-17A$^+$ CD4$^+$ T cells is shown. In addition, respective contour plots for lymphocytes from an APP-infected but apparently non-responding animal (frequency of IL-17A$^+$ CD4$^+$ T cells was higher or at the same level for medium stimulation as compared to APP-CCE stimulation) as well as an animal from the control group are presented. Following PMA/Ionomycin stimulation IL-17A production was found in a subpopulation of CD4$^+$ T cells from all animals. Similar findings were obtained in PBMC cultures, albeit frequencies of IL-17A$^+$ CD4$^+$ T cells were somewhat lower (Additional file 5). Overall, the highest number of animals with elevated frequencies of APP-CCE reactive-IL-17A$^+$ CD4$^+$ T cells was found within lung and PBMCs (Figure 2B). During the acute phase the frequencies of IL-17A$^+$ CD4$^+$ T cells in the lung were substantially higher in five out of nine animals compared to the control animals. This was similar during the chronic phase, with two animals (#11, #12) showing even increased frequencies of IL-17A$^+$ CD4$^+$ T cells. Within PBMCs the number of responding animals was similar to the lung during the acute phase but, later in the chronic phase, the median of the frequency of IL-17A$^+$ CD4$^+$ T cells dropped down to control levels. In TBLN and tonsils, CD4$^+$ T cells of only a few infected animals responded with IL-17A production to APP-CCE stimulation, regardless of the time post infection (Figure 2B).

Expression of CD8α is correlated with activation and/or memory formation of porcine CD4$^+$ T cells [34] and following PMA/Ionomycin stimulation, IL-17A producing CD4$^+$ T cells mainly have a CD8α$^+$ phenotype [17]. We therefore analyzed CD8α expression and IL-17A production in gated CD4$^+$ T cells following APP-CCE stimulation (Figure 3; Additional file 6). In the lungs of animals belonging to the acute group, the majority of IL-17A$^+$ CD4$^+$ T cells following APP-CCE and PMA/Ionomycin stimulation were CD8α^{dim}, whereas in the chronic phase CD8α expression tended to be higher and this applied equally to APP-CCE and PMA/Ionomycin stimulated cells (Figure 3). Similar results were obtained with PBMCs albeit here an up-regulation of CD8α in IL-17A-producing CD4$^+$ T cells from the acute to the chronic phase was less obvious (Additional file 6).

Next, we analyzed co-production of IL-17A and TNF-α within APP-CCE-stimulated CD4$^+$ T cells (Figure 4; Additional file 7; for gating strategy see Additional files 2E and F), since frequent co-production of TNF-α has been observed in PMA/Ionomycin-stimulated porcine IL-17A$^+$ CD4$^+$ T cells [17]. The majority of IL-17A-producing CD4$^+$ T cells isolated from lung tissue (Figure 4) or within PBMC (Additional file 7) did not co-produce TNF-α following APP-CCE stimulation (Figure 4A; Additional file 7A, indicated by arrowhead 1). In contrast, but in accordance with previously published data [17] following PMA/Ionomycin stimulation most IL-17A$^+$ CD4$^+$ T cells co-produced TNF-α (Figure 4A; Additional file 7A, arrowhead 2). Despite low frequencies for the majority of APP-infected animals, a tendency of higher frequencies of TNF-α$^+$ IL-17A$^+$ CD4$^+$ T cells was found within lymphocytes from APP-infected pigs compared to control animals following APP-CCE stimulation. This applied to cells isolated from lung tissue (Figure 4B) and blood (Additional file 7B).

APP-CCE stimulation induced production of IL-17A by a subset of lymphocytes that is neither TCR-γδ$^+$ nor CD4$^+$

After stimulation with APP-CCE, at least for some animals a considerable number of CD4$^-$ cells showed the ability to produce IL-17A in parallel to CD4$^+$ T cells (Figure 2A). This finding was more prominent in the lung, but it was detected also in PBMCs (Additional file 5). Since porcine γδ T cells were previously identified as potential IL-17A producers following PMA/Ionomycin stimulation [16], we hypothesized that these cells might also contribute to IL-17A production following APP-CCE stimulation. Hence, CD4$^-$ cells were further gated for expression of TCR-γδ and IL-17A (Additional files 2E and G). Interestingly, these IL-17A-producing cells induced by APP-CCE stimulation were TCR-γδ$^-$ (Figure 5; Additional file 8, arrowhead 1). However, they were also present in lymphocytes isolated from control animals (Figure 5; Additional file 8, last column), which seems to indicate that these cells did not require a preceding in vivo priming by APP. Their frequency was quite variable between individual animals but mostly exceeded the very low frequency of IL-17A-producing CD4$^-$ TCR-γδ$^-$ cells identified in medium stimulated cultures. Following PMA/Ionomycin stimulation, IL-17A-producing γδ T cells could be identified (Figure 5; Additional file 8, bottom panel, arrowhead 2), although IL-17A producing cells isolated from lung tissue showed a dim expression of TCR-γδ. Overall, this confirms the potential of porcine γδ T cells for IL-17A production but our data suggests that APP-CCE stimulation does not induce IL-17A production in this prominent porcine T-cell subset.

Inconsistent IL-10 production by CD4$^+$ T cells following APP-CCE stimulation

To investigate a potential induction of IL-10-producing lymphocytes in our APP-CCE in vitro stimulation assay

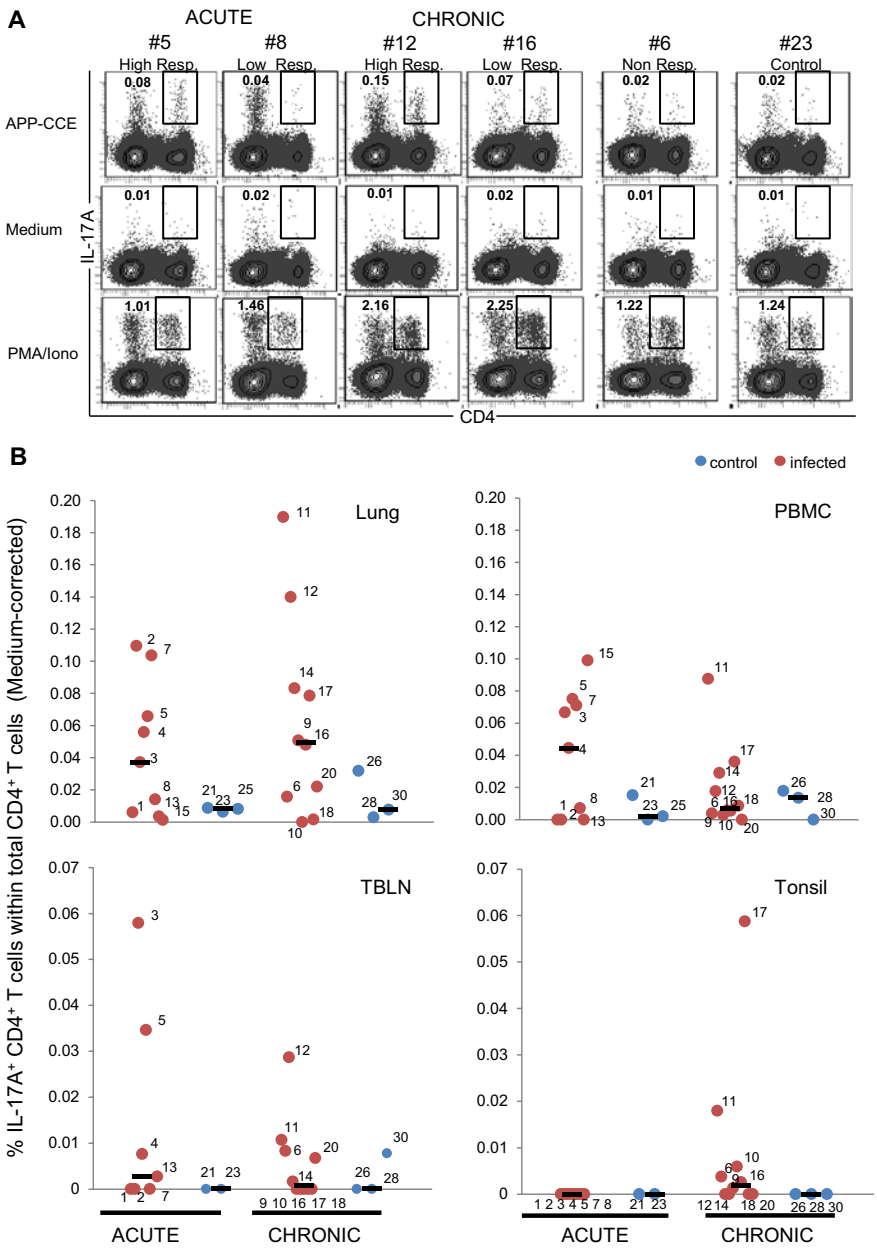

Figure 2 APP-CCE specific IL-17A-producing CD4$^+$ T cells in lung, blood, tracheobronchial lymph nodes and tonsils. Cells isolated from lung, blood (PBMC), tracheobronchial lymph nodes (TBLN) and tonsils were incubated overnight with APP crude capsular extract (APP-CCE), medium or PMA/Ionomycin. Living lymphocytes were gated (not shown; see Additional file 1) and further analyzed for the expression of IL-17A and CD4. **A** For the lung, data from representative animals from different groups are displayed: #5 and #8 for the acute phase, designated as "high responder" and "low responder" respectively; #12 and #16 for the chronic phase designated as "high responder" and "low responder" respectively; #6, designated as non-responder and control #23. Approximately 1 × 10^6 (APP and medium) and 2 × 10^5 (PMA/Ionomycin) cells are shown in the contour plots. Numbers displayed within the contour plots indicate the percentages of IL-17A$^+$ CD4$^+$ T cells within total CD4$^+$ T cells. **B** Frequency of IL-17A$^+$ CD4$^+$ T cells within total CD4$^+$ T cells in lung, blood (PBMC), tracheobronchial lymph node (TBLN) and tonsils of all infected animals (red dots) and control animals (blue dots) during acute and chronic phase. Numbers next to colored dots indicate numbers of individual animals. Median percent values are indicated by black bars. Medium-corrected percent values are presented (% of IL-17A$^+$ CD4$^+$ T cells within total CD4$^+$ T cells for APP-CCE stimulation minus % of IL-17A$^+$ CD4$^+$ T cells within total CD4$^+$ T cells for medium incubation).

the production of IL-10 was analyzed in parallel samples to that of IL-17A/TNF-α in combination with cell surface staining for CD4 and CD8α expression. Overall, with the exception of cells isolated from the APP-infected pig #17, frequencies of IL-10$^+$ CD4$^+$ T cells were low and inconsistently distributed between individual animals

during the acute and the chronic phase as well as different organs (Figure 6). However, in cells of some animals, the frequency of IL-10$^+$ CD4$^+$ T cells was at least two-fold higher following APP-CCE stimulation compared to medium and was also higher compared to that from control animals. This applied to animals #3, 5 and 7 in the lung during the acute phase and animal #18 during the chronic phase (see also Figure 6A for original FCM data). Similarly, within PBMCs, animals #7, 4, 5, 11 and 15 appeared to have APP-CCE-reactive IL-10$^+$ CD4$^+$ T cells above background levels (see also Additional file 9 for original FCM data). Isolated during the chronic phase, CD4$^+$ T cells from animal #17 showed an exceptionally high frequency of IL-10 producing cells after APP-CCE stimulation, both in lung and in tonsils (Figures 6A and B). The reasons for this are unknown. CD4$^-$ IL-10-producing cells were identified (Figure 6A; Additional file 9 and data not shown) but similar frequencies were found for APP-CCE- and medium-stimulated cultures.

Frequency of IL-17A$^+$ CD4$^+$ T cells correlates positively with disease parameters during the chronic phase of infection

We next investigated whether the variable frequency of APP-CCE-reactive IL-17A$^+$ CD4$^+$ T cells between different animals and organs correlated with parameters of APP pathogenesis and also APP-specific antibody titers. In chronically infected animals, the frequency of APP-CCE-reactive IL-17A$^+$ CD4$^+$ T cells isolated from the lung showed a positive correlation with LLS (Spearman's rho = 0.858; $p = 0.001$) and with APP 2 antibody titers (Spearman's rho = 0.632, $p = 0.05$). For IL-17A$^+$CD4$^+$ T cells within PBMCs of the same group of animals also a positive correlation with LLS and antibody titers was found (Spearman's rho of 0.679; $p = 0.031$ and 0.742, $p = 0.014$ respectively) (Figure 7). In contrast, for acutely infected animals no positive correlation of IL-17A$^+$ CD4$^+$ T cells isolated from lung or blood with the LLS was found (Additional file 10). Additionally, the frequencies of APP-CCE-reactive IL-17A$^+$ CD4$^+$ T cells isolated from the lung and blood were tested for correlation with histological scores of the lung tissue adjacent to tissue used for isolation of lymphocytes (Additional file 11). A total histological score for each sample was calculated by summing up all analyzed parameters (see Additional file 4) and was used to calculate the correlation. No significant correlation was found, which may indicate that APP-CCE-reactive IL-17A$^+$ CD4$^+$ T cells have a general capacity for lung homing.

Discussion

The main focus of the study was to characterize the cytokine response of T cells isolated from pigs undergoing either an acute or a subclinical APP infection. To address this question, we first aimed to establish an infection model that evokes typical but not lethal APP disease symptoms and induces a status of subclinical infection. Most of the experimental infections described in the literature so far focused on studying the acute phase of

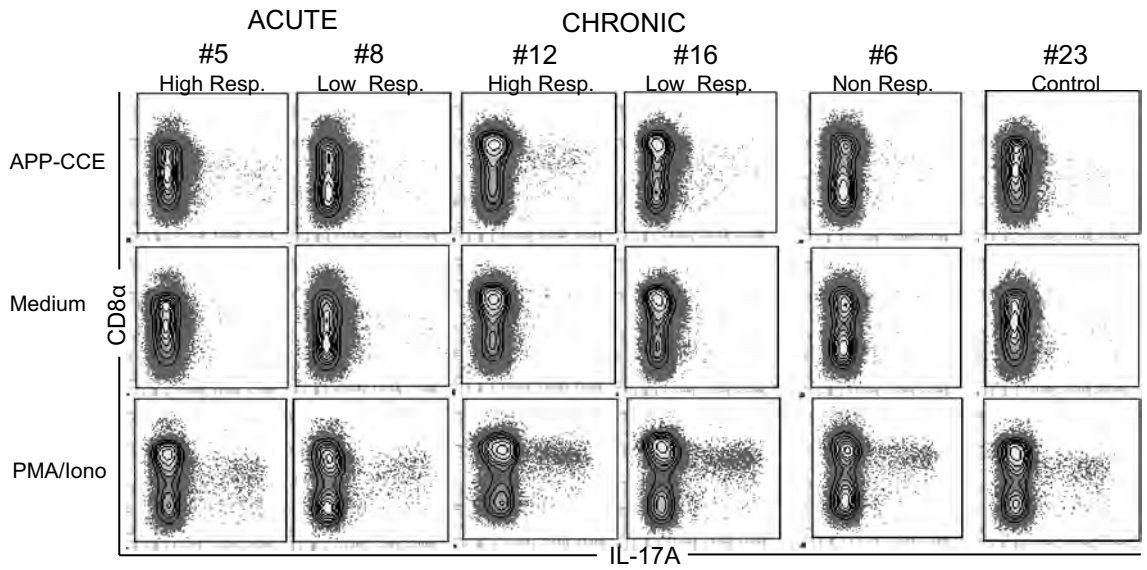

Figure 3 Expression of CD8α by IL-17A$^+$ CD4$^+$ T cells in the lung. Cells isolated from lung tissue were incubated overnight with APP crude capsular extract (APP-CCE), medium or PMA/Ionomycin and subsequently analyzed for CD4, CD8α and IL-17A expression by FCM. Living CD4$^+$ T cells were gated (not shown; see Additional file 1) and subsequently investigated for expression of CD8α and IL-17A. Data from the same animals as in Figure 2 are shown. Approximately 1 × 10^5 (APP and medium) and 5 × 10^4 (PMA/Ionomycin) CD4$^+$ T cells are shown in the contour plots.

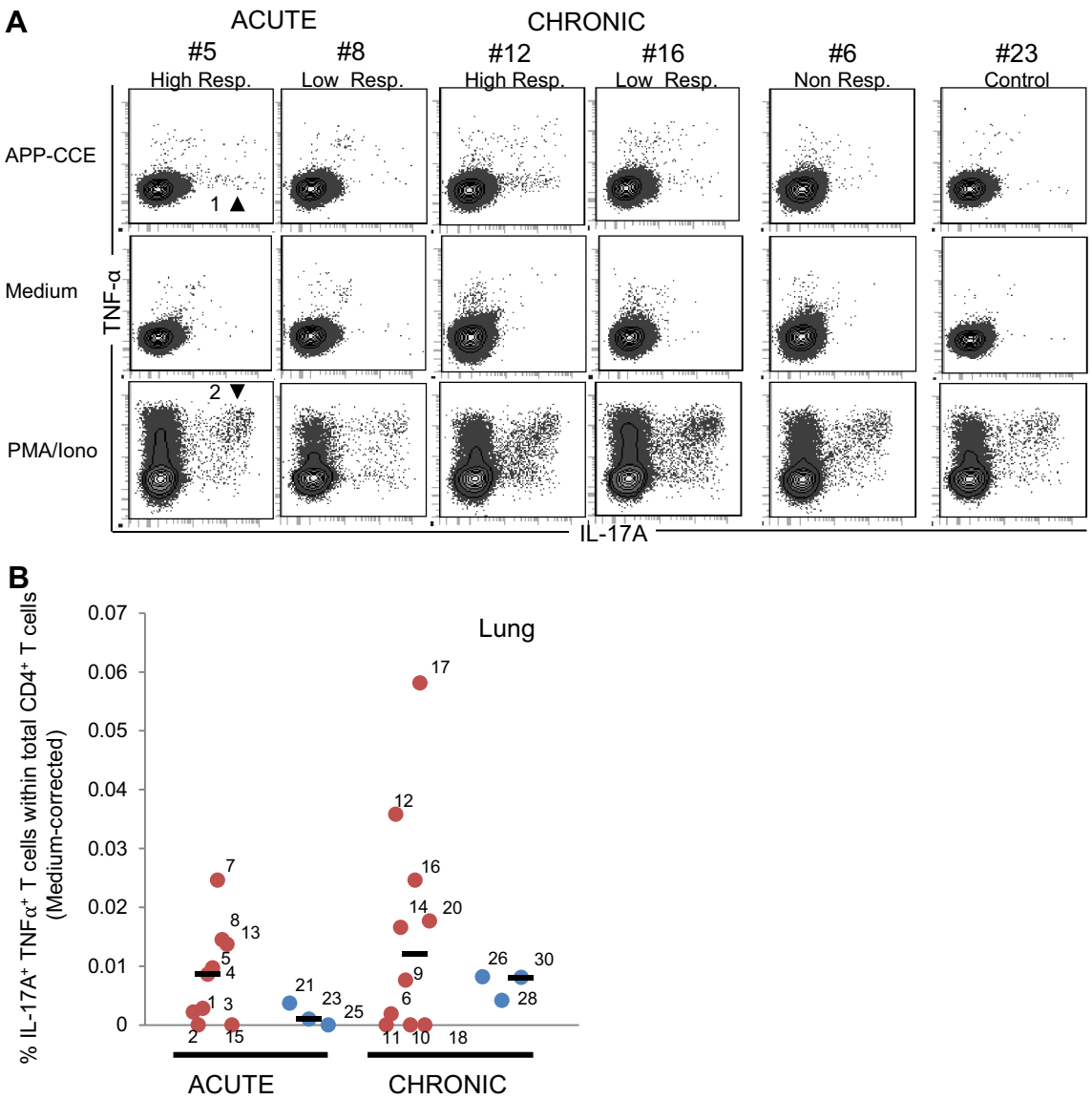

Figure 4 Co-production of TNF-α and IL-17A by CD4$^+$ T cells in the lung. Phenotyping and intracellular cytokine staining were performed on cells from lung tissue following overnight in vitro stimulation (APP-CCE, medium, PMA/Ionomycin). **A** Living CD4$^+$ T cells were gated (not shown; see Additional file 1) and further analyzed for production of TNF-α and IL-17A. Data from the same animals as in Figure 2 are shown. Approximately 1×10^5 (APP and medium) and 5×10^4 (PMA/Ionomycin) cells are shown in the contour plots. **B** Frequency of IL-17A/TNFα co-producing CD4$^+$ T cells in lung tissue of infected animals (red dots) and control animals (blue dots) during acute and chronic phase. Numbers next to colored dots indicate numbers of individual animals. Median percent values are indicated by black bars. Medium-corrected percent values are presented (% of IL-17A$^+$ TNF-α$^+$ cells within total CD4$^+$ T cells for APP-CCE stimulation minus % of IL-17A$^+$ TNF-α$^+$ cells within total CD4$^+$ T cells for medium-incubation). Arrow heads are introduced in the main text.

APP infection [35–37]. The outcome of APP infection is depending on the route of infection, the dose and the virulence of the strain [38]. Baarsch et al. [39] demonstrated that the route of infection influences the distribution of lung lesions, with the intranasal inoculation provoking mainly unilateral lesions and the endotracheal infection inducing diffuse bilateral pneumonia. To better mimic natural infection, we decided to perform an intranasal inoculation. To avoid loss of bacterial solution by swallowing or miscalculation of the actual infection dose by aerosol administration, the inoculum was sprayed directly into the nostrils rather than deposited as a liquid. Considering that vaporizing the bacterial solution into finely atomized particles increases the chance of

APP reaching the alveoli [1], the infection dose was kept to low levels to avoid the induction of a per-acute form. The endpoints where chosen to compare acute and subclinical phase of infection. We hypothesized that at days 6–10 a first activation of T cells may be measurable like previously reported for acute influenza A virus infection [40]. Additionally, the median duration of APP tonsillar colonization was reported around 7–8 weeks post-infection (pi) [41] leading to the assumption that APP would still be present at days 27–31 pi causing a subclinical infection. Pathological and clinical findings confirmed the establishment of a bi-phasic course of infection. The variety of rectal temperatures obtained during the acute phase paralleled with the variety of lung lesions observed at necropsy, with patterns ranging from severe and diffuse pneumonia with dark red–purple areas (per-acute), localized necrotizing pneumonia accompanied by fibrinous pleurisy (acute) to firm adhesive pleurisy and organized sequestra (chronic). On the opposite, during the chronic phase animals showed more uniform lesions and their body temperatures dropped down to physiological levels. These results indicate that our infection model successfully induced an acute infection that resolved into a subclinical one. Furthermore, this dichotomy could also be found by analyzing the presence of APP at different host compartments. During the acute phase, APP was mostly detected in the lung (7 out of 10), and hardly in the tonsils (3 out of 10). During the chronic phase, only one animal was positive in the lung, whereas in the tonsils 8 out of 10 tested positive. This might indicate a shift in the tropism of the bacteria from the lower to the upper respiratory tract and might be interpreted as an attempt of the bacteria to escape from the local immune response in the lung.

In frame of this study, we developed an in vitro stimulation assay using a crude capsular extract of APP. This assay was used to investigate the production of IL-17A, TNF-α and IL-10 in lymphocytes isolated from lung, peripheral blood, tracheobronchial lymph node and tonsil. Our data suggest that IL-17A-producing $CD4^+$ T cells are induced in the lung tissue and blood of most APP-infected pigs. IL-17 is a pro-inflammatory cytokine, known to play a role in pulmonary infection and neutrophil recruitment [42, 43]. Its role in veterinary animal species [44] and its up-regulation in the surroundings of APP colonies in affected lung lesions on mRNA level have been previously described [14]. Thus it is tempting to speculate that the APP-CCE-reactive IL-17A producing $CD4^+$ T cells identified in this study represent APP-specific Th17 cells. The specificity of these cells is corroborated by two findings. First, similar to PMA/Ionomycin-induced IL-$17A^+$ $CD4^+$ T cells, these putative APP-specific Th17 cells expressed low or intermediate levels of CD8α. Its expression in porcine $CD4^+$ T cells is related to activation and/or memory formation [34, 45]. Therefore, this CD8α expression can be interpreted as an indication that APP-CCE-reactive IL-17A-producing $CD4^+$ T cells performed an in vitro recall response. Secondly, APP-CCE

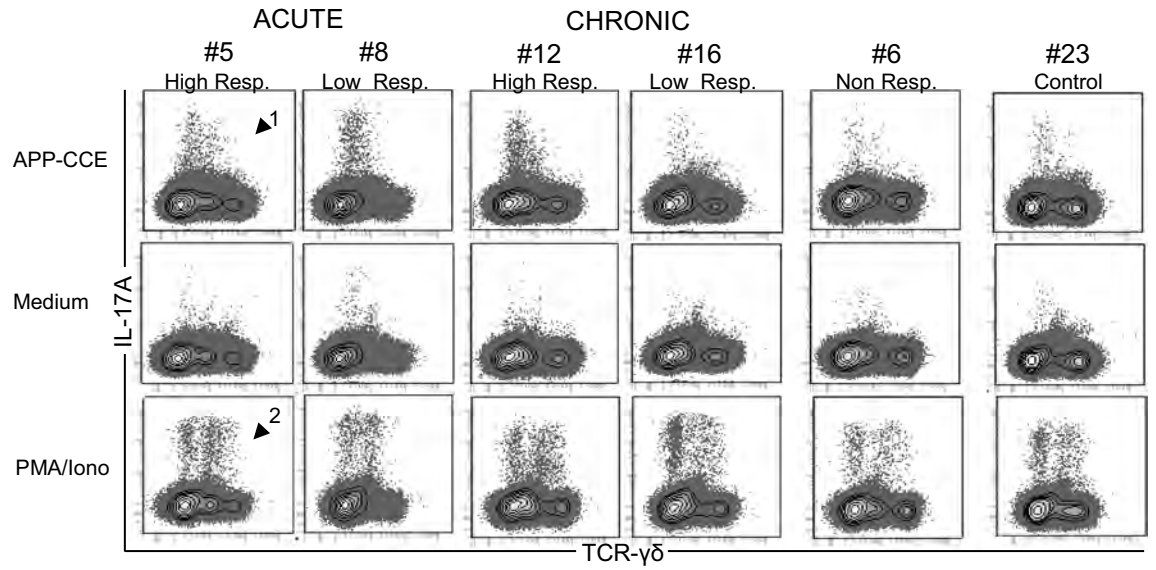

Figure 5 Production of IL-17A by non-$CD4^+$ cells and γδ T cells in the lung. Cells isolated from lung tissue were incubated overnight with APP-CCE, medium or PMA/Ionomycin and subsequently analyzed for CD4, TCR-γδ and IL-17A expression by FCM. Living lymphocytes excluding $CD4^+$ T cells (not shown; see Additional file 1) were gated and further analyzed for expression of IL-17A and TCR-γδ. Data from the same animals as in Figure 2 are shown. Approximately 1×10^6 (APP and medium) and 2×10^5 (PMA/Ionomycin) cells are shown in the contour plots. Arrow heads are introduced in the main text.

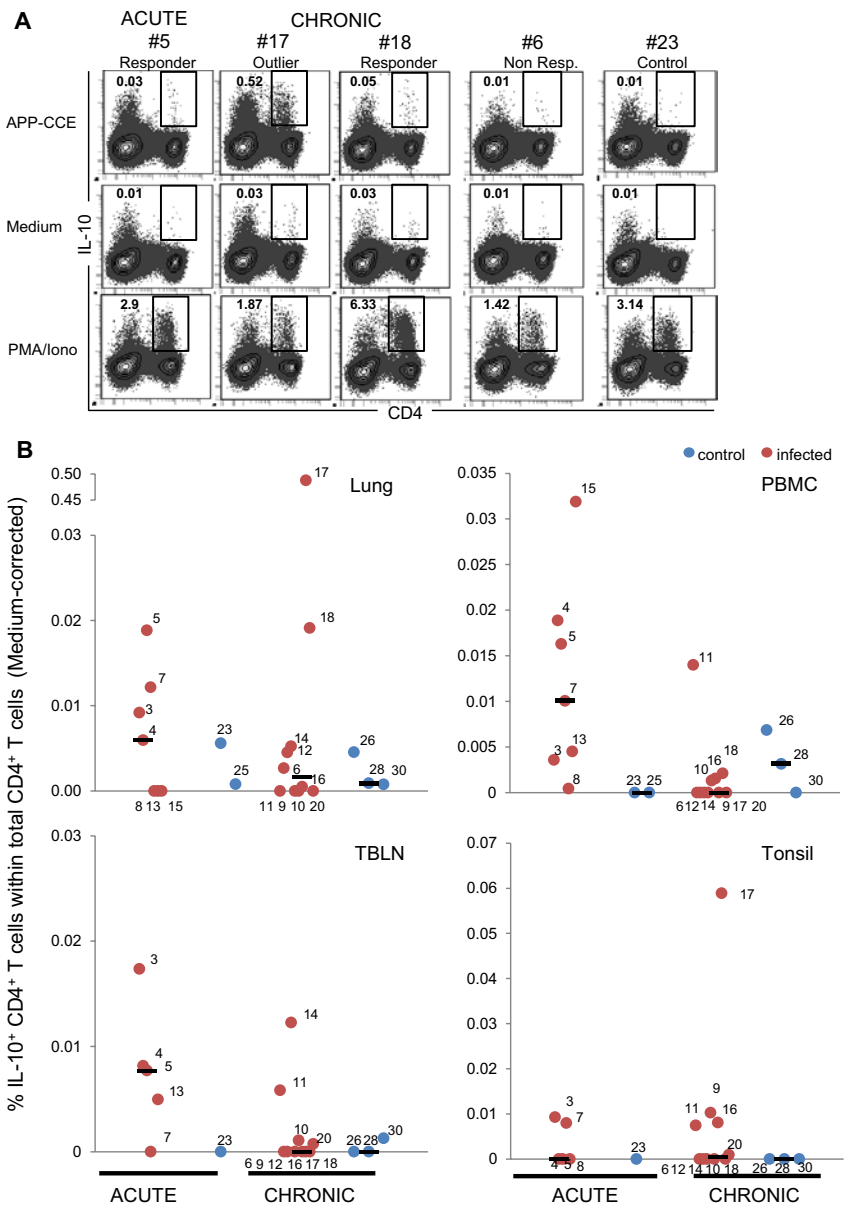

Figure 6 APP-CCE specific IL-10-producing CD4$^+$ T cells in lung, peripheral blood, tracheobronchial lymph nodes and tonsils. Cells isolated from lung, blood (PBMC), tracheobronchial lymph nodes (TBLN) and tonsils were incubated overnight with APP-CCE, medium or PMA/Ionomycin and subsequently analyzed by FCM. Living cells were gated (not shown; see Additional file 1) and further analyzed for expression of IL-10 and CD4. **A** For the lung, data from representative animals from different groups are displayed: #5 for the acute phase, designated as "responder"; #17 and #18 for the chronic phase, designated as "outlier" and "responder", respectively; #6, designated as "non-responder" and control pig #23. Approximately 5 × 10^5 (APP and medium) and 1.5 × 10^5 (PMA/Ionomycin) cells are shown in the contour plots. Numbers displayed within the contour plots indicate the percentage of IL-10$^+$ CD4$^+$ T cells within total CD4$^+$ T cells. **B** Frequency of IL-10$^+$ CD4$^+$ T cells in lung, PBMC, TBLN and tonsils of infected animals (red dots) and control animals (blue dots) during acute and chronic phase. Numbers next to colored dots indicate numbers of individual animals. Median percent values are indicated by black bars. Medium-corrected percent values are presented (% of IL-10$^+$ CD4$^+$ T cells within total CD4$^+$ T cells for APP-CCE stimulation minus % of IL-10$^+$ CD4$^+$ T cells within total CD4$^+$ T cells for medium incubation).

reactive IL-17A producing CD4$^+$ T cells were nearly completely absent in lymphocytes isolated from control pigs, indicating that APP-naive CD4$^+$ T cells did not respond to in vitro stimulation with APP-CCE.

Human [46] and porcine [17] CD4$^+$ T cells have the capacity to co-produce IL-17A and TNF-α following PMA/Ionomycin stimulation. Furthermore, a synergistic effect between IL-17 and TNF-α has been reported, enhancing

neutrophil migration [47]. Also, TNF-α is known to play a major role in the immune-pathogenesis of APP infection [35, 48]. Following APP-CCE stimulation, we found that the majority of $CD4^+$ T cells that produced IL-17A did not co-produce TNF-α. This suggests that $CD4^+$ T cells are not a main source of TNF-α during APP infection.

Interestingly, a small subset of $CD4^-$ TCR-$\gamma\delta^-$ cells showed production of IL-17A upon APP-CCE stimulation but was also identified in control animals. Innate sources of IL-17 are described [49] such us iNKT cells [50], NK cells [51] and innate lymphoid cells type 3 (ILC3) [52]. To affirm that the population revealed in our study is actually belonging to one of the subsets mentioned above, further investigations would be needed.

For several persistent pathogens like *Mycobacterium tuberculosis* [21], *Leishmania* spp. [23] and *Toxoplasma gondii* [22], IL-10 has been reported to impair their clearance by influencing the delicate balance between suppression and activation of host immune responses. In this study we therefore evaluated the production of IL-10 by $CD4^+$ T cells in different organs but a specific induction upon APP-CCE stimulation was found only in few animals and frequencies of IL-10^+ $CD4^+$ T cells were rather low. In a previous study, IL-10 mRNA was predominantly found within lung lesions of APP-infected pigs but was only minimal in non-affected areas. [53]. Of note, lung tissue samples in our study were derived from a defined anatomic area (dorsal portion of the left caudal lobe) and only in a single animal (#11) sequestra were included in that area. The frequency of IL-10-producing $CD4^+$ T cells derived from this animal was high in both APP-CCE-(0.17%) and medium-(0.17%) stimulated cultures, resulting in a medium-corrected value of zero (Figure 6B, lung). Thus, we cannot exclude a potential role of IL-10 in the immune

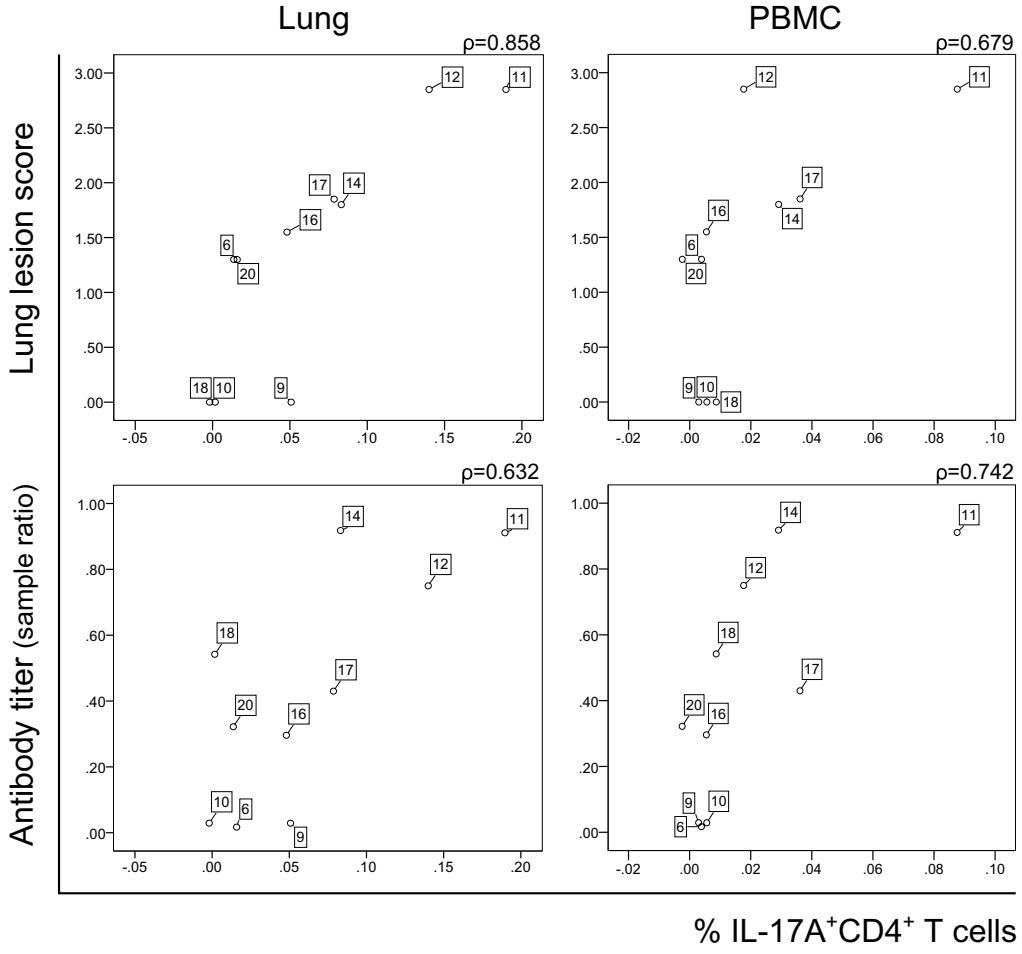

Figure 7 Correlation of the frequency of IL-17A$^+$ CD4$^+$ T cells with lung lesion score and antibody titers during the chronic phase. Scatterplots show correlation of the frequency of IL-17A$^+$ CD4$^+$ T cells isolated from lung and blood with lung lesion score (top panel) and antibody titer (bottom panel) in chronically infected animals. Antibody titer is expressed as a ratio between optical density of the sample (ODs) and the mean of the optical density of the positive control (MODp). Spearman's Rank Correlation coefficients (ρ) are displayed above each scatterplot.

pathogenesis of APP infection. Further studies on affected lung lesions should be carried out in future studies to decipher the exact role of IL-10 in APP infections.

Finally, we observed that the frequency of Th17 cells in lung and PBMCs from chronically infected animals correlated positively with the lung lesion score and APP-specific antibody titers. Such a correlation was not found in the animals during the acute infection phase. This could be related to the enormous variety of lung lesions (diffuse/local necrotic and hemorrhagic areas, fibrosis, formation of sequestra, absence of lesions) observed at the necropsy during the acute phase, as described above. Moreover, no positive correlation between Th17 cells and the histological score of lung tissue samples from which lymphocytes had been isolated was found in the chronic phase of infection. Together with the positive correlation between frequency of Th17 cells in lung tissue as well as blood and the lung lesion score, this may indicate that these APP-specific Th17 cells have a general capacity for lung homing and also recirculate via the bloodstream. This would correspond with functional attributes ascribed to effector memory T cells [54]. However, the precise functional role of these Th17 cells in APP pathology and persistence remains speculative. It is well established that cytokine production by Th17 cells can have protective but also pathologic roles in lung immunity [19]. An excessive recruitment of neutrophils due to IL-17 production by $CD4^+$ T cells could lead to progressive inflammation, which might explain the positive correlation between lung lesion and IL-17 production. Additionally, APP chronic lung lesions are usually characterized by fibroplasia [1] and IL-17 was shown to be involved in the occurrence and the development of pulmonary fibrosis in rats [55]. Nevertheless, our in vitro stimulation system does not allow a distinction between actively IL-17A-producing $CD4^+$ T cells in vivo (at the time of isolation) and the re-stimulation of quiescent APP-specific Th17 memory cells upon a second exposure to the antigen. Therefore, the precise role of the putative APP-specific Th17 cells in APP immunity, identified in our study, remains to be elucidated.

In conclusion, our results support previous findings that T cells are involved in the immune response to APP infection. We could show for the first time that APP-specific T cells with functional attributes of Th17 cells are induced in most APP-infected animals, which during the chronic phase of infection seem to positively correlate with lung lesion formation. Thus, our findings highlight the relevance of detailed immunological studies addressing T-cell differentiation for a better understanding of host-pathogen interactions in APP. Moreover, our infection model provides a solid basis for such studies in a controlled setting. This will contribute to a better understanding of APP pathogenesis and persistence.

Additional files

Additional file 1. Clinical score protocol. Clinical examinations were performed daily throughout the experiment. Alterations in behavior, gait, presence of respiratory symptoms (cough and dyspnea), and body temperature were assessed and scored on a scale from 0 to 4 based on the listed symptoms or traits.

Additional file 2. FCM gating hierarchy. Representative example of the FCM gating strategy used in this study. Data is derived from lung of animal #12 (APP-infected). (**A**) Lymphocytes were gated according to their light scatter properties. (**B**) A FSC-W/H gate coupled with a SSC-W/H gate was applied in order to exclude potential doublet cells. (**C**) Near-IR stain was used for Live/Dead discrimination. Only Near-IR negative cells (live cells) were included in the following analyses. (**D**) Co-expression of CD4 and IL-17A for identification of IL-17A$^+$ CD4$^+$ T cells. (**E**) Cells were further distinguished in either CD4$^+$ or CD4$^-$ T cells. (**F**) Within the CD4$^+$ subpopulation, the production of IL-17A and TNF-α was investigated. (**G**) Within the CD4$^-$ subpopulation, the expression of IL-17A and TCR-γδ was investigated.

Additional file 3. Pathological findings in the lung of acutely and chronically infected animals. Lungs from representative animals, one for the acute and one for the chronic phase, are shown. (**A**) Bilateral diffuse hemorrhagic pneumonia and fibrinous pleurisy in an acutely infected animal (#3). (**B**) Necrotic foci surrounded by scar tissue (sequestra) and adhesive pleurisy with evidence of firm adhesions between visceral and parietal pleura in a chronically infected animal (#11).

Additional file 4. Histological evaluation of lung tissue from infected animals. Lung tissue of the dorsal portion of left caudal lung lobe (adjacent to samples used for lymphocyte isolation) was taken from acutely and chronically infected animals. This tissue was paraffin embedded, stained with hematoxylin and eosin, and examined for presence and quantity of parameters A–H (see legend). The quantity and presence of each parameter were assessed by using a score from 0 to 3 (0 = not present, 1 = low grade, 2 = moderate grade, 3 = high grade). No sample in this study presented lesions of grade 3; therefore this grade is not shown in the legend.

Additional file 5. APP-specific induction of IL-17A$^+$ CD4$^+$ T cells in peripheral blood. PBMCs were incubated overnight with APP crude capsular extract (APP-CCE), medium or PMA/Ionomycin. Living lymphocytes were gated (not shown; see Additional file 1) and further analyzed for the expression of IL-17A and CD4. Data from representative animals from different groups are displayed: #5 and #4 for the acute phase, designated as "high responder" and "low responder" respectively; #11 and #17 for the chronic phase designated as "high responder" and "low responder" respectively; #6, designated as non-responder and control pig #23. Approximately 7×10^5 (APP and medium) and 2×10^5 (PMA/Ionomycin) cells are shown in the contour plots respectively. Numbers displayed within the contour plots indicate the percentage of IL-17A$^+$CD4$^+$ T cells within total CD4$^+$ T cells.

Additional file 6. Expression of CD8α by IL-17A$^+$ CD4$^+$ T cells in peripheral blood. PBMCs were incubated overnight with APP crude capsular extract (APP-CCE), medium or PMA/Ionomycin. Living lymphocytes were gated (not shown; see Additional file 1) and further analyzed for the expression of CD8α and IL-17A. Data from the same animals as in Additional file 2 is shown. Approximately 3×10^5 (APP and medium) and 5×10^4 (PMA/Ionomycin) cells are shown in the contour plots.

Additional file 7. Co-production of TNF-α and IL-17A by CD4$^+$ T cells in peripheral blood. Phenotyping and intracellular cytokine staining were performed on PBMC following overnight in vitro stimulation (APP-CCE, medium, PMA/Ionomycin). (**A**) Living CD4$^+$ T cells were gated (not shown; see Additional file 1) and further analyzed for production of TNF-α and IL-17A. Data from the same animals as in Additional file 2 are shown. Approximately 3×10^5 (APP and medium) and 5×10^4 (PMA/Ionomycin) cells are shown in the contour plots. (**B**) Frequency of IL-17A/TNF-α co-producing CD4$^+$ T cells in PBMC of infected animals (red dots) and control animals (blue dots) during acute and chronic phase. Numbers

next to colored dots indicate numbers of individual animals. Median percent values are indicated by black bars. Medium-corrected percentage values are presented (% of IL-17A$^+$ TNF-α$^+$ cells within total CD4$^+$ T cells for APP-CCE stimulation minus % of IL-17A$^+$ TNF-α$^+$ cells within total CD4$^+$ T cells for medium incubation). Arrow heads are introduced in the main text.

Additional file 8. Production of IL-17A by non-CD4$^+$ cells and γδ T cells in the peripheral blood. PBMC were incubated overnight with APP-CCE, medium or PMA/Ionomycin and subsequently analyzed for CD4, TCR-γδ and IL-17A expression by FCM. Living lymphocytes excluding CD4$^+$ T cells (not shown; see Additional file 1) were gated and further analyzed for expression of IL-17A and TCR-γδ. Data from the same animals as in Additional file 2 are shown. Approximately 7 × 10^5 (APP and medium) and 2 × 10^5 (PMA/Ionomycin) cells are shown in the contour plots. Arrow heads are introduced in the main text.

Additional file 9. APP-CCE-specific IL-10-producing CD4$^+$ T cells in peripheral blood. PBMC were incubated overnight with APP-CCE, medium or PMA/Ionomycin and subsequently analyzed by FCM. Living cells were gated (not shown; see Additional file 1) and further analyzed for expression of IL-10 and CD4. Data from representative animals from different groups are displayed: #15 for the acute phase and #11 for the chronic phase, both designated as "responders"; #6, designated as "non-responder" and control pig #23. Approximately 8 × 10^5 (APP and medium) and 1.5 × 10^5 (PMA/Ionomycin) cells are shown in the contour plots. Numbers displayed within the contour plots indicate the percentage of IL-10$^+$ CD4$^+$ T cells within total CD4$^+$ T cells.

Additional file 10. Correlation of the frequency of IL-17A$^+$ CD4$^+$ T cells with lung lesion score during the acute phase. Scatterplots show correlation of the frequency of IL-17A$^+$ CD4$^+$ T cells isolated from lung and blood with lung lesion score in acutely infected animals. Spearman's Rank Correlation Coefficients (ρ) are displayed above each scatterplot.

Additional file 11. Correlation of the frequency of IL-17A$^+$ CD4$^+$ T cells with histological score of lung tissue during the chronic phase. Scatterplots show correlation of the frequency of IL-17A$^+$ CD4$^+$ T cells isolated from lung and blood during the chronic phase with the histological score of the lung tissue sampled adjacent to tissue used for lymphocyte isolation. Histological scores for each sample were calculated by summing up the grading of all parameters shown in Additional file 4. Spearman's Rank Correlation Coefficients (ρ) are displayed above each scatterplot.

Competing interests
The authors declare that they have no competing interests.

Authors' contributions
ES, WG, AL, IHP: conceived and designed the experiments; JF and JS: prepared the inoculum and carried out microbiological analysis; MS: helped to set up the in vitro assay, isolated the lymphocytes from the organs and applied the stimulus; ES and HS: performed the infection, clinical examination and collected samples; CK, HS, AL, RG: performed the necropsies and harvested samples; BR: performed histopathological analyses; ES: produced the stimulus. ES and ST performed the intracellular cytokine staining and FCM measurements; ST: established the protocol for the intracellular cytokine staining; ES and WG: analyzed and interpreted the results; AL, IHP and MES: contributed to the organization of the experiments and edited the manuscript; ES and WG: wrote the manuscript. All authors read and approved the final manuscript.

Acknowledgements
The authors thank Michaela Koch and Lisa Reiter for their excellent work in the lab and Hanna Koinig for her precious help with the organization of the animal experiment. Elena L. Sassu, Stephanie C. Talker and Janna Frömbling were supported by the Graduate School for Pig and Poultry Medicine of the University of Veterinary Medicine Vienna.

Author details
[1] University Clinic for Swine, Department of Farm Animals and Veterinary Public Health, University of Veterinary Medicine, Vienna, Austria. [2] Institute of Immunology, Department of Pathobiology, University of Veterinary Medicine Vienna, Vienna, Austria. [3] Functional Microbiology, Institute of Microbiology, Department of Pathobiology, University of Veterinary Medicine Vienna, Vienna, Austria. [4] Institute of Pathology and Forensic Veterinary Medicine, Department of Pathobiology, University of Veterinary Medicine Vienna, Vienna, Austria. [5] Division of Swine Medicine, Department of Farm Animals, University of Zurich, Vetsuisse Faculty, Zurich, Switzerland.

Received: 14 September 2016 Accepted: 3 January 2017
Published online: 06 February 2017

References
1. Gottschalk M (2012) Actinobacillosis. In: Zimmerman JJ, Karriker LA, Ramirez A, Schwartz KJ, Stevenson GW (eds) Diseases of Swine. Wiley, New York
2. Angen O, Andreasen M, Nielsen EO, Stockmarr A, Baekbo P (2008) Effect of tulathromycin on the carrier status of *Actinobacillus pleuropneumoniae* serotype 2 in the tonsils of pigs. Vet Rec 163:445–447
3. Chiers K, De Waele T, Pasmans F, Ducatelle R, Haesebrouck F (2010) Virulence factors of *Actinobacillus pleuropneumoniae* involved in colonization, persistence and induction of lesions in its porcine host. Vet Res 41:65
4. Devenish J, Rosendal S, Bosse JT (1990) Humoral antibody response and protective immunity in swine following immunization with the 104-kilodalton hemolysin of *Actinobacillus pleuropneumoniae*. Infect Immun 58:3829–3832
5. Krejci J, Nechvatalova K, Kudlackova H, Faldyna M, Kucerova Z, Toman M (2005) Systemic and local antibody responses after experimental infection with *Actinobacillus pleuropneumoniae* in piglets with passive or active immunity. J Vet Med B Infect Dis Vet Public Health 52:190–196
6. Costa G, Oliveira S, Torrison J, Dee S (2011) Evaluation of *Actinobacillus pleuropneumoniae* diagnostic tests using samples derived from experimentally infected pigs. Vet Microbiol 148:246–251
7. Cruijsen T, van Leengoed LA, Kamp EM, Bartelse A, Korevaar A, Verheijden JH (1995) Susceptibility to *Actinobacillus pleuropneumoniae* infection in pigs from an endemically infected herd is related to the presence of toxin-neutralizing antibodies. Vet Microbiol 47:219–228
8. Li L, Zhu J, Yang K, Xu Z, Liu Z, Zhou R (2014) Changes in gene expression of *Actinobacillus pleuropneumoniae* in response to anaerobic stress reveal induction of central metabolism and biofilm formation. J Microbiol 52:473–481
9. Wherry EJ, Kurachi M (2015) Molecular and cellular insights into T cell exhaustion. Nat Rev Immunol 15:486–499
10. Boer MC, Joosten SA, Ottenhoff TH (2015) Regulatory T-cells at the interface between human host and pathogens in infectious diseases and vaccination. Front Immunol 6:217
11. Furesz SE, Mallard BA, Bosse JT, Rosendal S, Wilkie BN, MacInnes JI (1997) Antibody- and cell-mediated immune responses of *Actinobacillus pleuropneumoniae*-infected and bacterin-vaccinated pigs. Infect Immun 65:358–365
12. Appleyard GD, Furesz SE, Wilkie BN (2002) Blood lymphocyte subsets in pigs vaccinated and challenged with *Actinobacillus pleuropneumoniae*. Vet Immunol Immunopathol 86:221–228
13. Faldyna M, Nechvatalova K, Sinkora J, Knotigova P, Leva L, Krejci J, Toman M (2005) Experimental *Actinobacillus pleuropneumoniae* infection in piglets with different types and levels of specific protection: immunophenotypic analysis of lymphocyte subsets in the circulation and respiratory mucosal lymphoid tissue. Vet Immunol Immunopathol 107:143–152
14. Brogaard L, Klitgaard K, Heegaard PM, Hansen MS, Jensen TK, Skovgaard K (2015) Concurrent host-pathogen gene expression in the lungs of pigs challenged with *Actinobacillus pleuropneumoniae*. BMC Genomics 16:417
15. Stepanova H, Mensikova M, Chlebova K, Faldyna M (2012) CD4$^+$ and γδTCR$^+$ T lymphocytes are sources of interleukin-17 in swine. Cytokine 58:152–157

16. Sedlak C, Patzl M, Saalmüller A, Gerner W (2014) CD2 and CD8α define porcine γδ T cells with distinct cytokine production profiles. Dev Comp Immunol 45:97–106
17. Gerner W, Talker SC, Koinig HC, Sedlak C, Mair KH, Saalmüller A (2015) Phenotypic and functional differentiation of porcine αβ T cells: current knowledge and available tools. Mol Immunol 66:3–13
18. McGeachy MJ (2013) Th17 memory cells: live long and proliferate. J Leukoc Biol 94:921–926
19. Way EE, Chen K, Kolls JK (2013) Dysregulation in lung immunity—the protective and pathologic Th17 response in infection. Eur J Immunol 43:3116–3124
20. McGill JL, Rusk RA, Guerra-Maupome M, Briggs RE, Sacco RE (2016) Bovine gamma delta T cells contribute to exacerbated IL-17 production in response to co-infection with bovine RSV and *Mannheimia haemolytica*. PLoS One 11:e0151083
21. Redford PS, Murray PJ, O'Garra A (2011) The role of IL-10 in immune regulation during *M. tuberculosis* infection. Mucosal Immunol 4:261–270
22. Neyer LE, Grunig G, Fort M, Remington JS, Rennick D, Hunter CA (1997) Role of interleukin-10 in regulation of T-cell-dependent and T-cell-independent mechanisms of resistance to *Toxoplasma gondii*. Infect Immun 65:1675–1682
23. Belkaid Y, Hoffmann KF, Mendez S, Kamhawi S, Udey MC, Wynn TA, Sacks DL (2001) The role of interleukin (IL)-10 in the persistence of Leishmania major in the skin after healing and the therapeutic potential of anti-IL-10 receptor antibody for sterile cure. J Exp Med 194:1497–1506
24. Hennig-Pauka I, Baltes N, Jacobsen I, Stratmann-Selke J, Gerlach GF, Selbitz HJ, Waldmann KH (2008) Study of the virulence of *Actinobacillus pleuropneumoniae* in finishing pigs as a basis for vaccination development. Berl Munch Tierarztl Wochenschr 121:189–197 (in German)
25. Hannan PC, Bhogal BS, Fish JP (1982) Tylosin tartrate and tiamutilin effects on experimental piglet pneumonia induced with pneumonic pig lung homogenate containing mycoplasmas, bacteria and viruses. Res Vet Sci 33:76–88
26. Merialdi G, Dottori M, Bonilauri P, Luppi A, Gozio S, Pozzi P, Spaggiari B, Martelli P (2012) Survey of pleuritis and pulmonary lesions in pigs at abattoir with a focus on the extent of the condition and herd risk factors. Vet J 193:234–239
27. Hussy D, Schlatter Y, Miserez R, Inzana T, Frey J (2004) PCR-based identification of serotype 2 isolates of *Actinobacillus pleuropneumoniae* biovars I and II. Vet Microbiol 99:307–310
28. Schaller A, Djordjevic SP, Eamens GJ, Forbes WA, Kuhn R, Kuhnert P, Gottschalk M, Nicolet J, Frey J (2001) Identification and detection of *Actinobacillus pleuropneumoniae* by PCR based on the gene apxIVA. Vet Microbiol 79:47–62
29. Wittkowski M, Mittelstadt J, Brandau S, Reiling N, Lindner B, Torrelles J, Brennan PJ, Holst O (2007) Capsular arabinomannans from *Mycobacterium avium* with morphotype-specific structural differences but identical biological activity. J Biol Chem 282:19103–19112
30. Reutner K, Leitner J, Essler SE, Witter K, Patzl M, Steinberger P, Saalmüller A, Gerner W (2012) Porcine CD27: identification, expression and functional aspects in lymphocyte subsets in swine. Dev Comp Immunol 38:321–331
31. Saalmüller A, Reddehase MJ, Buhring HJ, Jonjic S, Koszinowski UH (1987) Simultaneous expression of CD4 and CD8 antigens by a substantial proportion of resting porcine T lymphocytes. Eur J Immunol 17:1297–1301
32. Rodriguez-Gomez IM, Talker SC, Kaser T, Stadler M, Hammer SE, Saalmüller A, Gerner W (2016) Expression of T-bet, Eomesodermin and GATA-3 in porcine αβ T cells. Dev Comp Immunol 60:115–126
33. Frank RK, Chengappa MM, Oberst RD, Hennessy KJ, Henry SC, Fenwick B (1992) Pleuropneumonia caused by *Actinobacillus pleuropneumoniae* biotype 2 in growing and finishing pigs. J Vet Diagn Investig 4:270–278
34. Saalmüller A, Werner T, Fachinger V (2002) T-helper cells from naive to committed. Vet Immunol Immunopathol 87:137–145
35. Baarsch MJ, Scamurra RW, Burger K, Foss DL, Maheswaran SK, Murtaugh MP (1995) Inflammatory cytokine expression in swine experimentally infected with *Actinobacillus pleuropneumoniae*. Infect Immun 63:3587–3594
36. Heegaard PM, Klausen J, Nielsen JP, Gonzalez-Ramon N, Pineiro M, Lampreave F, Alava MA (1998) The porcine acute phase response to infection with *Actinobacillus pleuropneumoniae*. Haptoglobin, C-reactive protein, major acute phase protein and serum amyloid A protein are sensitive indicators of infection. Comp Biochem Physiol B Biochem Mol Biol 119:365–373
37. Skovgaard K, Mortensen S, Boye M, Poulsen KT, Campbell FM, Eckersall PD, Heegaard PM (2009) Rapid and widely disseminated acute phase protein response after experimental bacterial infection of pigs. Vet Res 40:23
38. Rosendal S, Mittal KR (1985) Serological cross-reactivity between a porcine *Actinobacillus* strain and *Haemophilus pleuropneumoniae*. Can J Comp Med 49:164–170
39. Baarsch MJ, Foss DL, Murtaugh MP (2000) Pathophysiologic correlates of acute porcine pleuropneumonia. Am J Vet Res 61:684–690
40. Talker SC, Stadler M, Koinig HC, Mair KH, Rodriguez-Gomez IM, Graage R, Zell R, Durrwald R, Starick E, Harder T, Weissenbock H, Lamp B, Hammer SE, Ladinig A, Saalmüller A, Gerner W (2016) Influenza A virus infection in pigs attracts multifunctional and cross-reactive T cells to the lung. J Virol 90:9364–9382
41. Vigre H, Angen O, Barfod K, Lavritsen DT, Sorensen V (2002) Transmission of *Actinobacillus pleuropneumoniae* in pigs under field-like conditions: emphasis on tonsillar colonisation and passively acquired colostral antibodies. Vet Microbiol 89:151–159
42. Tabarkiewicz J, Pogoda K, Karczmarczyk A, Pozarowski P, Giannopoulos K (2015) The role of IL-17 and Th17 lymphocytes in autoimmune diseases. Arch Immunol Ther Exp 63:435–449
43. Rathore JS, Wang Y (2016) Protective role of Th17 cells in pulmonary infection. Vaccine 34:1504–1514
44. Mensikova M, Stepanova H, Faldyna M (2013) Interleukin-17 in veterinary animal species and its role in various diseases: a review. Cytokine 64:11–17
45. Zuckermann FA, Husmann RJ (1996) Functional and phenotypic analysis of porcine peripheral blood CD4/CD8 double-positive T cells. Immunology 87:500–512
46. Kim CJ, McKinnon LR, Kovacs C, Kandel G, Huibner S, Chege D, Shahabi K, Benko E, Loutfy M, Ostrowski M, Kaul R (2013) Mucosal Th17 cell function is altered during HIV infection and is an independent predictor of systemic immune activation. J Immunol 191:2164–2173
47. Griffin GK, Newton G, Tarrio ML, Bu DX, Maganto-Garcia E, Azcutia V, Alcaide P, Grabie N, Luscinskas FW, Croce KJ, Lichtman AH (2012) IL-17 and TNF-alpha sustain neutrophil recruitment during inflammation through synergistic effects on endothelial activation. J Immunol 188:6287–6299
48. Choi C, Kwon D, Min K, Chae C (1999) In-situ hybridization for the detection of inflammatory cytokines (IL-1, TNF-α and IL-6) in pigs naturally infected with *Actinobacillus pleuropneumoniae*. J Comp Pathol 121:349–356
49. Cua DJ, Tato CM (2010) Innate IL-17-producing cells: the sentinels of the immune system. Nat Rev Immunol 10:479–489
50. Michel ML, Keller AC, Paget C, Fujio M, Trottein F, Savage PB, Wong CH, Schneider E, Dy M, Leite-de-Moraes MC (2007) Identification of an IL-17-producing NK1.1(neg) iNKT cell population involved in airway neutrophilia. J Exp Med 204:995–1001
51. Passos ST, Silver JS, O'Hara AC, Sehy D, Stumhofer JS, Hunter CA (2010) IL-6 promotes NK cell production of IL-17 during toxoplasmosis. J Immunol 184:1776–1783
52. Spits H, Artis D, Colonna M, Diefenbach A, Di Santo JP, Eberl G, Koyasu S, Locksley RM, McKenzie AN, Mebius RE, Powrie F, Vivier E (2013) Innate lymphoid cells—a proposal for uniform nomenclature. Nat Rev Immunol 13:145–149
53. Cho WS, Jung K, Kim J, Ha Y, Chae C (2005) Expression of mRNA encoding interleukin (IL)-10, IL-12p35 and IL-12p40 in lungs from pigs experimentally infected with *Actinobacillus pleuropneumoniae*. Vet Res Commun 29:111–122
54. Masopust D, Picker LJ (2012) Hidden memories: frontline memory T cells and early pathogen interception. J Immunol 188:5811–5817
55. Ding W, Zhang XY, Pan M, Zhao B, Chen C, Niu ZH, Huang CL, Li YY, Fan XM, Ma YM, Zhang M, Zhang WJ (2015) Interleukin-17A promotes the formation of inflammation in the lung tissues of rats with pulmonary fibrosis. Exp Ther Med 10:491–497

Additional file 1

Behavior	Gait	Cough	Dyspnea	Temperature	Score
Physiologic	Physiologic	Absent	Absent	38.5-39.5	0
Lethargic	Laying down			39.6-40	1
Apathetic	Sitting-dog position	Present	More costal or abdominal	40.1-41	2
Stupors	Swinging			>41	3
Comatose	Unable to stand		Only costal or abdominal	<38.5	4

Additional file 2

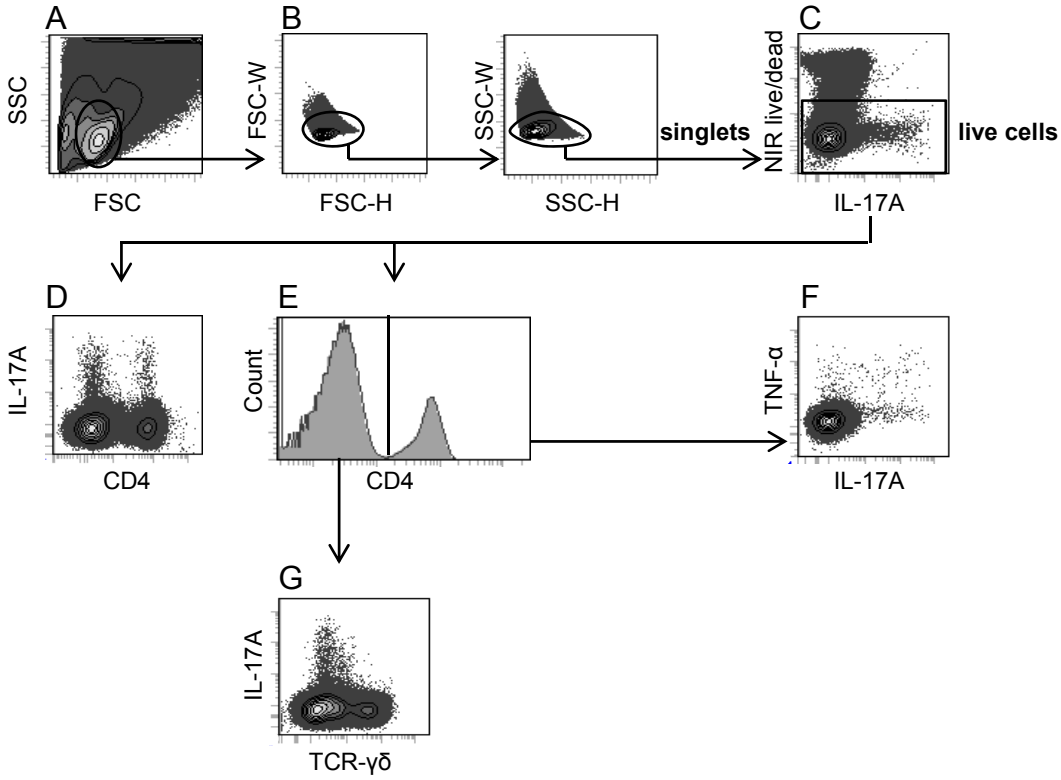

Additional file 3

Acute

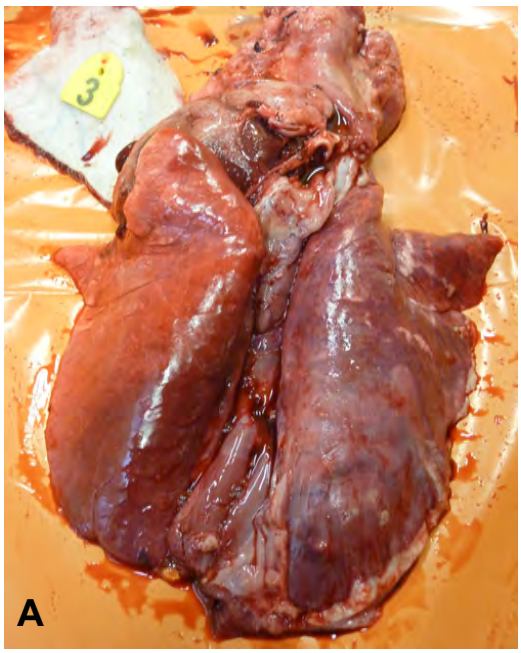

Chronic

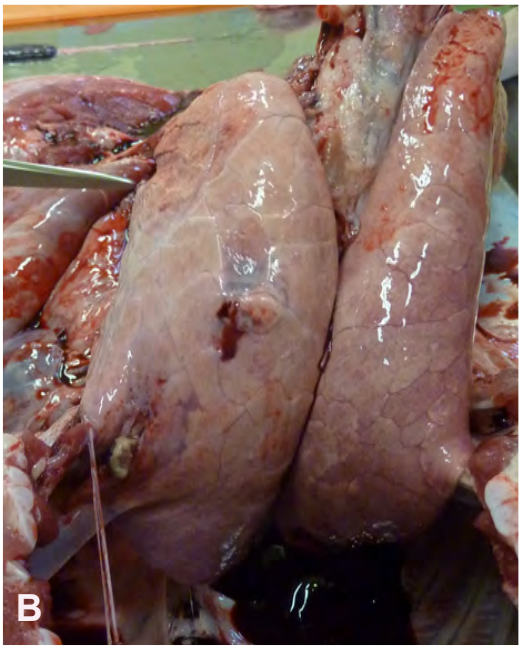

Additional file 4

Acute

#	A	B	C	D	E	F	G	H
1	0	0	1	0	0	0	0	0
2	0	0	0	0	0	0	0	0
3	0	0	0	1	0	0	0	0
4	0	1	0	1	1	1	1	0
5	0	0	0	0	0	1	1	0
19	0	2	2	2	2	2	2	0
7	0	1	1	0	0	0	1	0
8	0	0	0	0	0	0	1	0
13	0	1	0	1	0	0	0	0
15	0	2	1	1	1	1	1	0

A Necrosis of lung tissue
B Neutrophilic and histiocytic infiltration of lung parenchyma
C Lymphocellular infiltration of lung parenchyma
D Vascular leakage in alveolar lumen
E Neutrophilic and histiocytic infiltration of lung septa and pleura
F Lymphocellular infiltration of lung septa and pleura
G Vascular leakage in lung septa and pleura
H Fibroplasia

Chronic

#	A	B	C	D	E	F	G	H
6	0	1	1	1	0	1	1	0
9	0	1	0	1	0	1	0	0
10	0	2	2	2	0	1	1	0
11	1	2	2	0	1	2	1	2
12	0	1	1	0	0	0	0	0
14	0	1	1	1	0	1	1	0
16	0	1	1	2	0	1	1	0
17	0	2	1	1	0	0	0	0
18	0	1	0	0	0	0	0	0
20	0	0	0	0	0	1	0	0

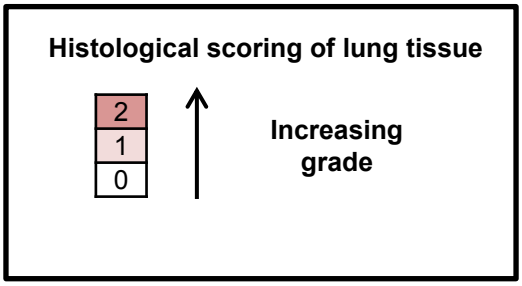

Additional file 5

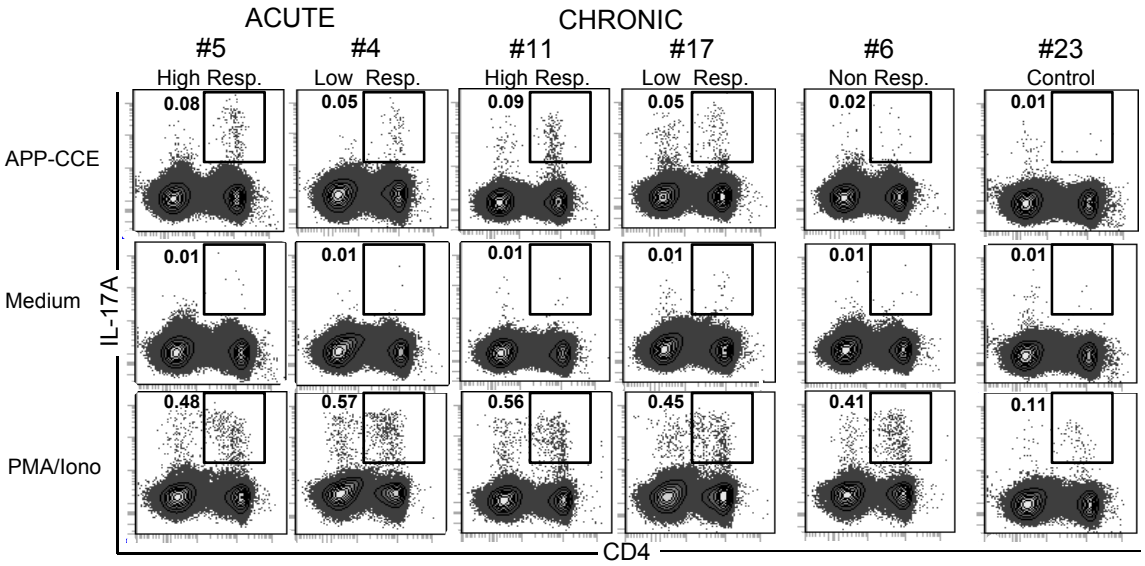

Additional file 6

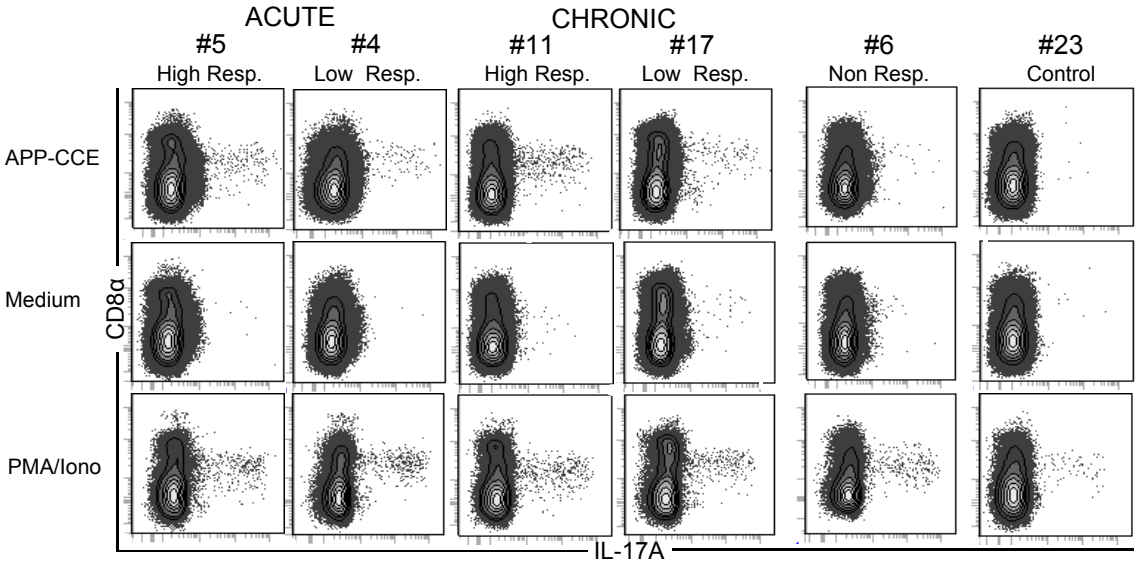

Additional file 7

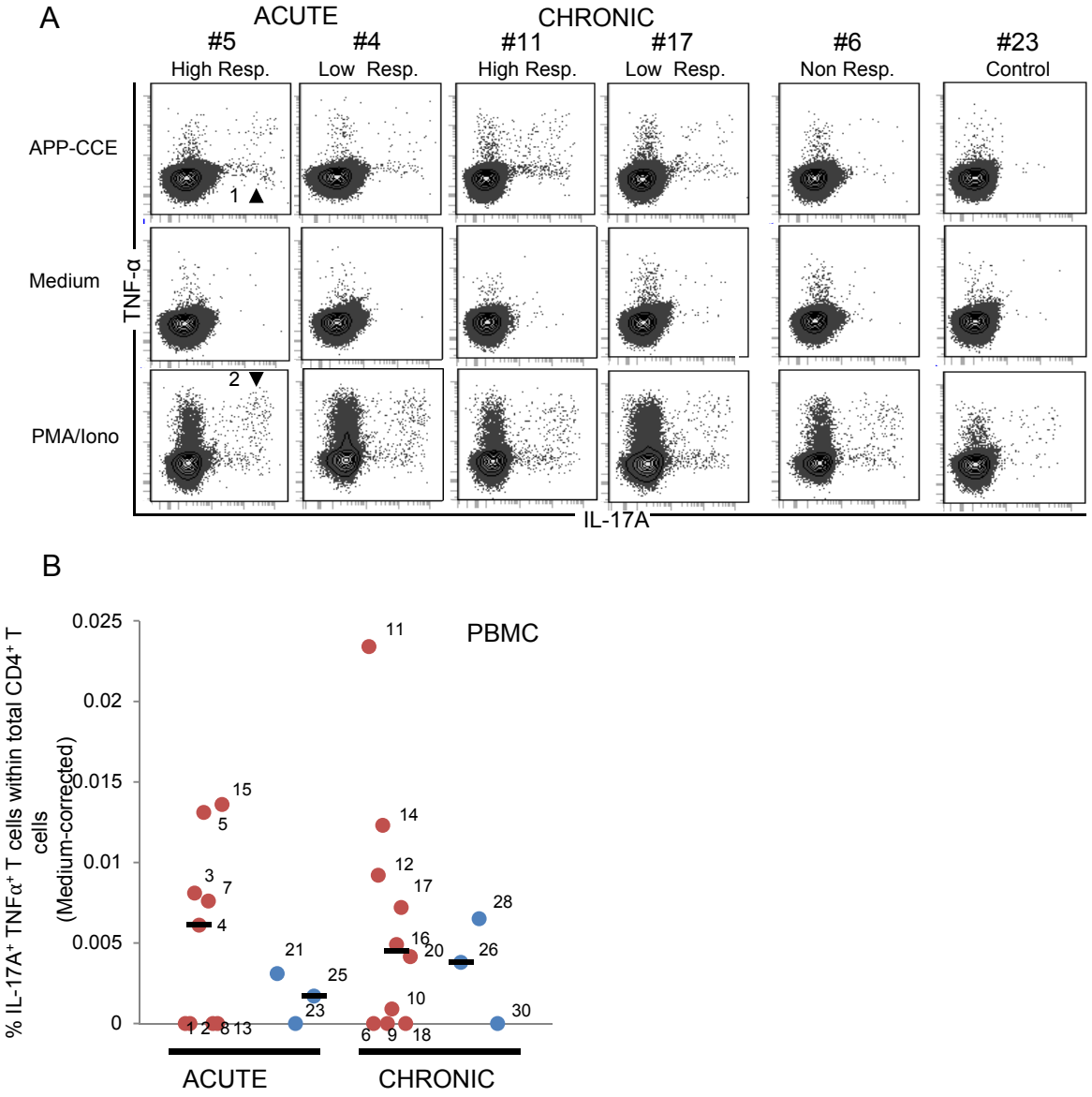

Additional file 8

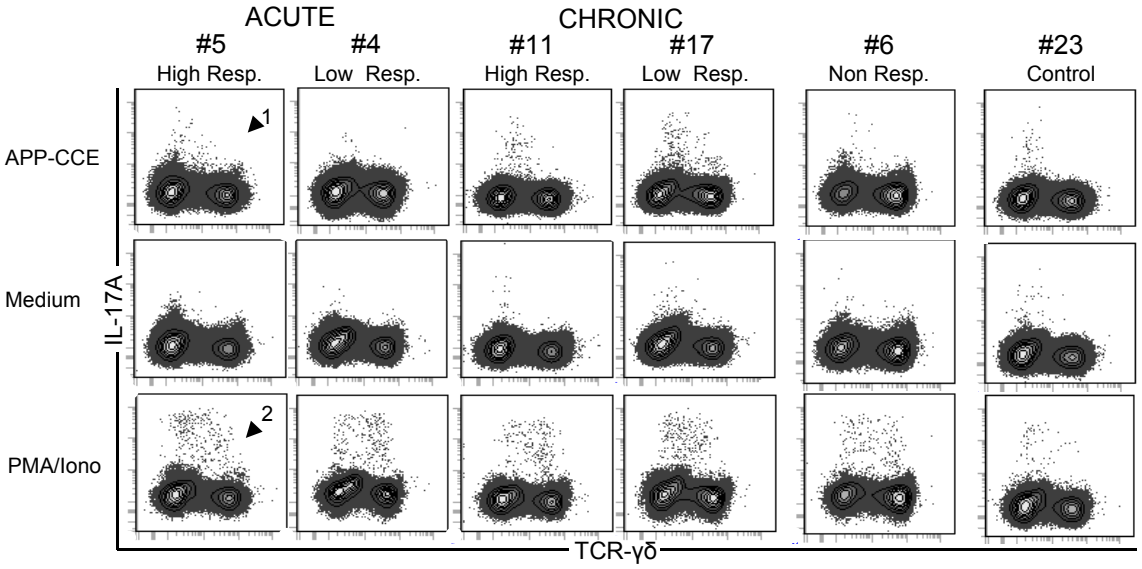

Additional file 9

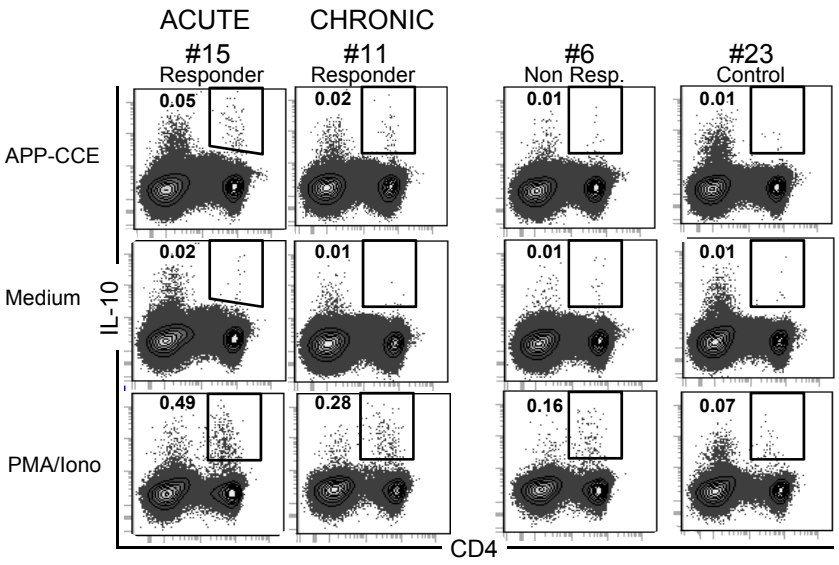

Additional file 10

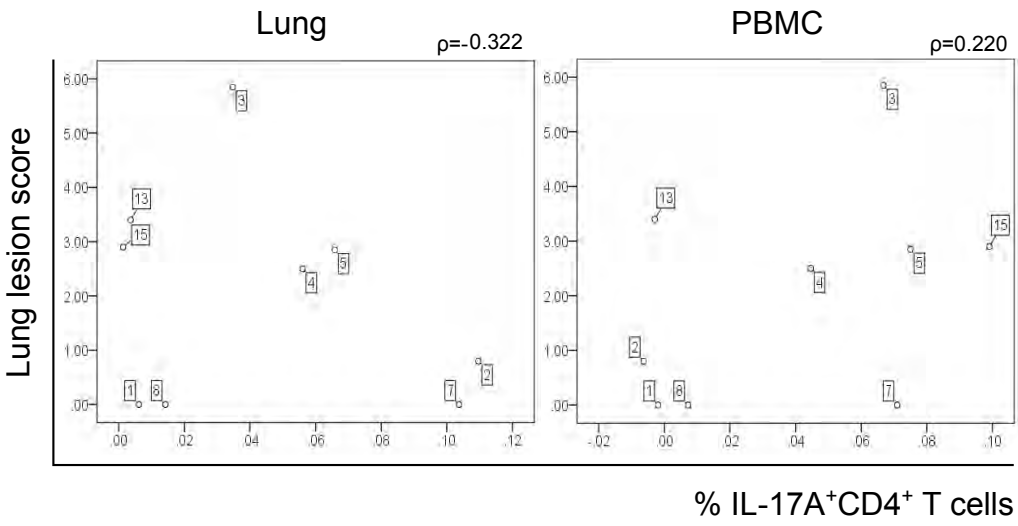

Additional file 11

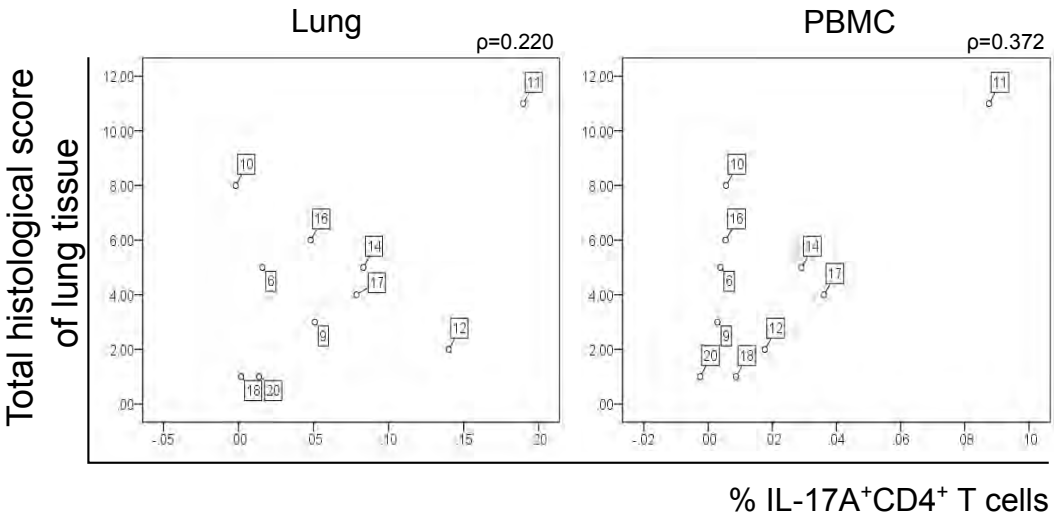

8. DISCUSSION

8.1. Selecting a suitable infection model

To assess porcine immune responses against App at different stages of infection, we performed two animal infection experiments under standardized conditions.

App infection can result in per-acute, acute or chronic disease (Gottschalk, 2012). In experimental infection, the outcome of the disease varies depending on route of infection, dose and virulence of the strain (Rosendal et al., 1985). In both studies, an App biotype 1-serotype 2 strain [(no. C3656/0271/11, isolated from a fattening pig with respiratory symptoms during an acute outbreak of porcine pleuropneumonia in northern Germany and stored at the Institute of Microbiology, University of Veterinary Medicine, Hanover, Germany] was used. This strain has been well characterised by dose-response studies and infection experiments (Hennig-Pauka et al. 2008) and for this reason was chosen for our studies.

In the first experiment intratracheal infection with a relatively high dose (approximately $1.6x10^6$ CFU) of App serotype 2 was performed in order to induce porcine pleuropneumonia in its per-acute/acute stage. Since diffuse bilateral pneumonia can be induced by this model, intratracheal infection is recommended for cytokine expression studies using a small number of animals (Baarsch et al., 2000). In our first study six animals were infected and their organs were analysed for cytokine and acute phase protein expression in comparison to control animals. In parallel, the influence of the host environment on variations in the metabolic fingerprint of App isolated from either the upper and the lower respiratory tract was assessed by Fourier-Transform Infrared (FTIR-) spectroscopy.

In the second experiment, the purpose was to mimic a natural infection and to induce a subclinical disease. For this reason an intranasal administration of the inoculum by a

vaporizer was chosen. Spraying the bacterial solution directly into the nostrils may increase the chance of these small pathogen-containing droplets to reach the lung alveoli (Nicolet et al., 1969). This application method might reduce the amount of infectious solution that is usually lost by swallowing, but could also increase the virulence by allowing the bacteria to reach deep part of the lung. For this reason, the challenge dose was kept to low levels ($2x10^4$ CFU). The infection group consisted of 20 animals that were further divided into 2 groups: one with an endpoint at 6-10 days post infection (dpi) and the other with an endpoint at 27-31 dpi. These endpoints were chosen to enable the investigation of T cells in the early effector phase in the course of a primary immune response whereas the late time point was postulated to allow the analysis of T cells during chronic/subclinical infection.

8.2. Early immune response

8.2.1. Cytokine and acute phase protein expression in tissues and body fluids

Acute phase proteins are known to be primarily synthetized in the liver in response to inflammation (Murata et al., 2004). In addition, non-hepatic production of acute phase proteins has been reported in inflammatory diseases of various species; but little is known for pigs, especially during App infection. Skovgaard et al. looked for cytokine and acute phase protein expression in extra hepatic sites and found that the acute phase response against App is not restricted to the liver, but rather disseminated to other organs (Skovgaard et al., 2009). To determine how much and which organs are actually responsive at this stage of infection, pigs were euthanized eight hours after infection, and samples from liver, lung salivary gland and tonsils were analysed for gene expression.

A wide spectrum of molecules was investigated, such as inflammatory cytokines (IFN-γ, IL-6, IL-1 and TNF-α), T-cell growth factor IL-2, chemokine IL-8 (CXCL8), anti-inflammatory cytokines (IL-4 and IL-10), products of respiratory stress (iNOS and HO1), and acute phase proteins (SAA, CRP and Hp). These molecules were analysed both at a transcriptional and

protein level at different host sites, and the obtained results will be discussed in the following chapter.

Since IFN-γ, IL-2, IL-4, iNOS and HO1 gene expression was below the detection limit, these molecules were not included into further analyses. In the liver, only IL-6 and SAA expression was found to be significantly up-regulated in infected animals compared to controls. Surprisingly, an increase in Hp and CRP expression in liver, which was reported in previous studies (Skovgaard et al., 2009, Hedegaard et al., 2007), was not detected. Additionally, the hepatic production of IL-1 and IL-8, described in another study (Skovgaard et al., 2010), was not observed in our experiment. The greatest cytokine response was detected in the lung, the organ of primary infection. All the investigated pro-inflammatory cytokines were significantly increased in infected animals. In contrast to previous findings using cDNA microarrays (Hedegaard et al., 2007) and in situ hybridization (Cho et al., 2005), where an increase of IL-10 mRNA expression in inflamed areas of the lung was reported, the expression of IL-10 did not differ between the groups in any organ. Within the acute phase proteins, only SAA appeared to be up-regulated in the lung. The high expression of the neutrophilic chemo-attractant IL-8 in the lung, already observed in the past by northern blotting (Baarsch et al., 1995) and in situ hybridization (Myers et al., 2002), probably contributes to the neutrophilic infiltration that characterizes App lung lesions. Moreover, the observed drop in segmented neutrophils combined with a rise in band cells in the blood stream of infected animals might be the result of massive migration of mature neutrophils to the lung. The salivary gland was the only organ that showed a significant up-regulation of all the investigated acute phase proteins, and additionally an increase in IL-6 and IL-1 mRNA expression. Interestingly, tonsils and salivary glands showed opposite immunological reactions. In tonsils no difference in mRNA expression of cytokines or acute phase proteins was found between the groups, even though App was detected at this site. These findings are in accordance with those of

Skovgaard et al., who described tonsils as the least responsive tissue, with only a moderate increase in IL-6 mRNA expression (Skovgaard et al., 2009). Accordingly, in our study only a slight tendency of increased IL-6 expression was observed.

We analysed the acute phase response also on the protein level in host body fluids. In serum, no significant changes in IL-6, IL-1 and TNF-α were detectable. This might be due to the early end-point of our study with 8 hpi. Indeed, the earliest detectable cytokine was shown to be IL-6 which reaches its serum concentration peak at 10 hpi (Wyns et al., 2015). Interestingly CRP serum concentration increased significantly in infected animals, while Hp did not differ between groups. This confirms the assertion that CRP reacts faster than Hp in pigs infected with App (Heegaard et al., 1998, Skovgaard et al., 2009).

In BALF, IL-6 and IL-1 were not significantly increased. The concentration of TNF-α in BALF was opposite to the other cytokines, dropping from in-range concentrations in controls to non-detectable levels in infected animals. This was an unexpected finding, because on the transcriptional level TNF-α was found to be up-regulated in lungs of infected animals. Thus it´s tempting to speculate that App infection could trigger a pathway or a molecule, which either inhibits the translation of TNF-α mRNA or influences detectability of the TNF-α protein further downstream. In saliva, in contrast to serum, a significant increase in Hp was detected, while the increase in CRP concentration was not significant. Further discussion on the role of saliva and the salivary gland during early infection will be given in section 8.2.3.

Overall, the significant increase of SAA gene expression in all organs but tonsils, qualifies this acute phase protein to become a reliable biomarker to evaluate health status in swine. The limitation of our study relies on the fact that we didn´t quantify SAA on the protein level in body fluids. Nevertheless, previous studies provided insight that the measurement of SAA in saliva can be used to differentiate between healthy and diseased animals (Soler et al., 2011).

Thus, it would be worthy to investigate its feasibility as a biomarker in pigs affected by porcine contagious pleuropneumonia.

8.2.2. Host immune response mirrors bacterial adaptation at primary sites of infection

In parallel to host immune response, the metabolic fingerprint of App isolates from the upper and the lower respiratory tract of infected pigs was analysed using FTIR. This technique has been used in the past decades not only for diagnostics but also for studying the influence of external variables, as host genotypes or stress, on the metabolic fingerprints of bacteria (Grunert et al., 2014, Alvarez-Ordonez et al., 2011).

Before undergoing FTIR analysis, App isolates from nostrils, tonsils and lung were subjected to serotype 2 specific PCR (APPcps2), and their M13-PCR profiles were compared to the inoculation strain to confirm their genotypic identity to the App strain used for the infection. Even though all isolates expressed the same profiles on the genotype level; FTIR spectral analysis revealed differences in their phenotype. The fact that the isolates from the lung clustered together with the inoculation strain but apart from the isolates from the upper respiratory tract, might be an indication for a rapid adaptation of App to different host body compartments. Additionally, within these two distinct clusters, the isolates from the lung showed similar phenotypes, while the isolates from the upper respiratory tract were highly diverse. This variation within the latter isolates could reflect the variation in the onset of clinical symptoms in individual animals. With a high probability, coughing facilitated the movement of bacteria from the lung to colonization sites in the upper respiratory tract, and consequently had an influence on the onset of colonization of the tonsils. From the moment of tonsil colonization until the moment of cultivation, the bacteria could have had more or less time to adapt to the newly colonised site depending on appearance of symptoms in each animal.

Considering that tonsils and nostrils are known as niches of bacterial persistence (Sidibe et al., 1993, Vigre et al., 2002), this observed phenotypic metabolic adaptation might be an expression of a switch to the persistent form of App. Since the most pronounced differences in the phenotype were located in the polysaccharide region, App crude capsular extracts (CCEs), which are characterised by high content of polysaccharides, were subjected to FTIR analyses. Comparison of FTIR spectra of CCEs extracted from App isolated from the lower and upper respiratory tract revealed differences in the protein and carbohydrate composition. To identify the molecules that undergo these modifications, further studies are needed.

Regulation of the capsule expression is often a strategy used by bacteria to initiate persistence. *S. aureus*, for example, can maintain chronic infections by losing its capsule (Tuchscherr et al., 2010). Thus, given the importance of the capsule as virulence factor, we hypothesise that an App capsular extract could be a promising candidate to stimulate lymphocytes in a specific manner and characterize App-specific T-cell immune responses. For this reason, we decided to use it as a stimulus in the second experimental study.

Interestingly, the innate immune response of the host and the metabolic bacterial modification follow the same clustering. While, on the host side, the lung showed a strong acute phase reaction and the tonsils had no detectable response, on the bacterial side, App isolates from the lung formed a unique cluster with the inoculation strain and App isolates from the tonsils underwent diverse phenotypic modifications. Thus, it is tempting to speculate that the massive response in the lung might have induced App to migrate to a more comfortable niche where, by switching to a less virulent form, it can evade the immune response.

8.2.3. Salivary gland and its importance in early oral immunity

In our study the highest acute phase response was observed in the salivary gland, namely *glandula mandibularis*. To our knowledge, there are only few studies that investigated the porcine acute phase response in this body compartment. Muneta et al. described IL-18 as a

suitable biomarker for stress response in porcine salivary glands (Muneta et al., 2011) and local production of Hp at this site was detected by immune-histochemical analysis (Gutierrez et al., 2012). Past literature mainly focused on the detection of biomarkers in saliva, such as SAA (Soler et al., 2011), Hp and CRP (Gutierrez et al., 2013, Soler et al., 2013). In our study SAA, Hp and CRP were significantly up-regulated in salivary gland and Hp and CRP were increased in saliva of infected animals already 8 hpi. This finding indicates a major role of the salivary gland in regard to early oral immunity, and promotes further evaluation of this organ for new diagnostic approaches.

8.3. T-cell immune responses to App

8.3.1. $CD4^+$ but not TCR-$\gamma\delta^+$ T cells are the major source of IL-17A after in vitro stimulation

To characterize the T-cell immune responses to App infection, we established an in vitro stimulation assay using a crude capsular extract of App (App-CCE). This method was applied to test the ability of lymphocytes to produce IL-17A, IL-10 and TNF-α in response to a specific stimulus. Lymphocytes were isolated from different host compartments to investigate both systemic (blood) and local (lung, tracheobronchial lymph nodes and tonsils) responses. The most prominent result was the identification of App-specific IL17A-producing $CD4^+$ T cells in the lung and in the blood of the majority of App infected pigs. IL-17A-producing T helper (Th17) cells are involved in the development of autoimmune diseases such as multiple sclerosis (Gold and Luhder, 2008), systemic lupus erythematous (Li et al., 2015) and rheumatoid arthritis (Gaffen, 2009). In the context of combating infections, IL-17A is known to recruit neutrophils as well as to trigger the production of antimicriobial peptides (Iwakura et al., 2008). Its role in various animal diseases (Mensikova et al., 2013) including pulmonary infection (Blanco et al., 2011) has been described. Recently, a high expression of IL-17A mRNA in lung lesions caused by App has also been reported (Brogaard et al., 2015). Our results are thus in line with previous literature and confirm our assumption that these IL-17A producing $CD4^+$ T cells, which are specifically reacting after App-CCE stimulation, are indeed App-specific Th17. Additionally, these putative Th17 cells showed low to intermediate expression of the activation-related molecule CD8α (Saalmuller et al., 2002) . Thus it is tempting to speculate that the stimulation induced in our in vitro assay might be the result of an *in vitro* recall response which is further supported by the observation that these IL-17A producing $CD4^+$ T cells were only identified in App-infected animals but not in control animals.

We investigated in parallel the ability of these cells to co-produce TNF-α together with IL-17A. Co-production of these two cytokines by $CD4^+$ T cells is a known phenomenon in humans (Kim et al., 2013) and pigs (Gerner et al., 2015). Nevertheless, despite the described synergistic effect of IL-17A and TNF-α in enhancing neutrophil migration (Griffin et al., 2012), and the known importance of TNF-α in the response to App infection (Huang et al., 1999, Baarsch et al., 1995, Choi et al., 1999); we observed that most of $CD4^+$ T cells did not co-produce IL-17-A and TNF-α. Following our findings, $CD4^+$ T cells do not seem to play a major role in TNF-α production during App infection.

Even though it is known from literature that next to $CD4^+$ T cells also γδ T cells are source of IL-17 in humans A (Peng et al., 2008), cattle (McGill et al., 2016) and pigs (Stepanova et al., 2012), we could not detect IL-17A production by TCR-γδ T cells upon App-specific stimulation. Nevertheless the ability of this lymphocyte subset of producing IL-17A was confirmed upon stimulation with PMA/Ionomycin. A possible explanation for this finding might be the incapability of our in vitro stimulation system to induce an adequate antigen presentation and related recognition by the TCR-γδ. Recognition of pathogen-associated molecular patterns by TCR-γδ T cells, unlike $CD4^+$ T cells, doesn´t depend on MHC class II-associated molecules. Antigen presenting pathways used by these "unconventional" cells are so far poorly defined (Liuzzi et al., 2015). Taken together, our data indicate that $CD4^+$ T cells are involved in the T-cell response to App by producing IL-17A, i.e. the classical effector molecule of Th17 cells. Thereby, as described for other bacterial infections, a type-3 immune response seems to occur in App infected pigs.

8.3.2. IL-10 and its potential role in App persistence

App is able to persist in the upper respiratory tract of subclinically infected animals, and the proportion of pigs carrying App in their tonsils increases between 4 and 12 weeks of age, when maternal antibodies decline (Vigre et al., 2002). There are several known strategies that

pathogens can use to establish a persistence status in a host (Monack et al., 2004), and exploiting host immune-regulatory mechanisms is one of them (Young et al., 2002). It is known for intracellular microorganisms like *Mycobacterium tuberculosis* (Redford et al., 2011), *Leishmania* spp. (Belkaid et al., 2001) and *Toxoplasma gondii* (Neyer et al., 1997) that IL-10 can suppress inflammatory immune reactions, so that eventually creates a host environment that favours bacterial persistence.

We thus evaluated the production of IL-10 by lymphocytes isolated from tonsils, lung, tracheobronchial lymph node and blood upon App-CCE stimulation. Only few animals responded to App-CCE stimulation with a production of IL-10 and the frequency of these IL-10 producing $CD4^+$ T cells was quite low. In detail, the highest frequencies of these cells were found in lung, tracheobronchial lymph node and PBMC of acutely infected animals, while in tonsils an outlier belonging to the chronic group was detectable.

Hitherto, IL-10 production during App infection has been reported only on mRNA level in affected areas of the lung of acutely diseased animals (Hedegaard et al., 2007, Cho et al., 2005). Since we decided to sample the dorsal part of the left caudal lung lobe independently of the presence of lung lesion, our results could have been biased by the fact that cytokine expression is usually higher in the lesions than in unaltered lung tissue.

Additionally, in parallel to flow cytometry analysis, lung, tracheobronchial lymph node, tonsil and salivary gland were subjected to qRT-PCR. These results have not been published yet. Results of these expression studies indicate a moderate increase of IL-10 mRNA in the lungs of acutely infected animals and a significant up-regulation in tonsils of chronically infected animals (data not shown). Briefly, summing up all results, we can neither confirm nor reject our hypothesis of a role of IL-10 production in App persistence. To better address the role of IL-10 in App infection, both phenotypic and functional analysis of regulatory T cells in tonsils and lung lesions are recommended. Moreover, a correlation analysis between metabolic

bacterial modifications of isolates from tonsils and IL-10 expression at the same site could be beneficial.

8.3.3. Uncharacterized subset of lymphocytes producing IL-17A

Interestingly, a lymphocyte population of $CD4^-$ cells showed the ability to produce IL-17A in parallel to $CD4^+$ after App-CCE stimulation. Since another source of IL-17A in swine is represented by γδ T cells (Stepanova et al., 2012, Sedlak et al., 2014), we gated these IL-17A-producing $CD4^-$ cells for expression of TCR-γδ, but we found that they were TCR-$\gamma\delta^-$. This small subset of $CD4^-$ TCR-$\gamma\delta^-$ cells produced IL-17A after App-CCE stimulation not only in infected animals but also, albeit at a lower frequency, in control animals. This might suggest that these cells do not necessary need previous in vivo priming by App and they could rather belong to the innate immune system. Different source of innate IL-17A have been identified in the past years (Cua and Tato, 2010). Hitherto, only one report described the production of IL-17A by NK cells isolated from mice infected with *Toxoplasma gondii* (Passos et al., 2010). Also in mice, a subset of IL-17A-producing iNKT cells, which are cells of the innate immune system that secrete immune-regulatory cytokines after activation by self or foreign glycolipids, have been identified in the thymus (Michel et al., 2007). Moreover, ILC3s are characterized by their ability to produce IL-17A and/or IL-22 in response to extracellular bacterial or fungal infections (Spits et al., 2013). Unlike ILC1s and ILC2s, ILC3s constitutively express RORγt and include lymphoid‑tissue inducer (LTi) and LTi- like cells which are further subdivided in several subsets (Sutton et al., 2012, Takatori et al., 2009).

Thus, further investigations, targeting additional cell markers, would be needed to exclude or confirm that these $CD4^-$ TCR-$\gamma\delta^-$ cells belong to one of the populations mentioned above.

8.3.4. Frequency of Th17 cells correlates positively with disease parameters in chronically infected animals

In our study, we found that the frequency of Th17 cells in lung and the blood of chronically infected pigs positively correlated with the presence of lung lesions and App-specific antibody titres. This correlation was not observed in acutely infected animals. This could be related to the high variation in lung lesions shown by animals which were euthanized at the early stage. Additionally, we looked for correlation between frequency of Th17 cells and histological score assigned to the parts of lung, which were used to isolate the lymphocytes. In this latter case, we could not find a positive correlation. The fact that the frequency of Th17 cells in lung and blood of chronically infected animals correlates with the overall scoring of the lung, and not with the scoring of the circumscribed lung sample taken for lymphocyte isolation, might be an indication that these Th17 cells are capable of lung homing and can recirculate through the blood stream. Consequently, because of their ability to migrate, these cells could actually be defined as effector memory T cells (Masopust and Picker, 2012). Nevertheless, it is not yet clear which role should be ascribed to these Th17 cells in the immune pathogenesis of App infection. Th17 cells were described both as auxiliaries of protection (Rathore and Wang, 2016) and pathology during lung infection (Way et al., 2013). The massive infiltration of neutrophils that characterizes App lung lesions might be the consequence of an exacerbated Th17 response, thus pending for a pathologic role. This would be in line with the positive correlation between lung lesions and the frequency of IL-17A producing $CD4^+$ T cells.

Nevertheless, another positive correlation was observed in this study: the one between frequency of Th17 cells in lung and blood and App-specific antibody titres.

IL-17A production has been reported to induce humoral immune response (Iwakura et al., 2008). Indeed, antigen-specific antibody production is significantly reduced in IL-$17^{-/-}$ mice

(Nakae et al., 2002) and IL-17A is known to stimulate the formation of autoreactive germinal centres in lymph nodes of autoimmune mice (Hsu et al., 2008). Knowing this involvement of IL-17A in enhancing antibody production, we cannot rule out the possibility that Th17 cells might have a protective role in App infection. To assess whether Th17 cells can actually facilitate the induction of humoral immune response in App infection, further experiments would be needed. In summary, our data could not define if Th17 cells have a protective or pathologic role in pigs affected by App.

In conclusion, this PhD thesis represents an analysis of various aspects of porcine immune responses against App infection at different disease stages. By investigating the host-pathogen interplay both at the lower and upper respiratory tract, we could show that App isolates from the tonsils undertake distinct metabolic adaptations to this niche already eight hours after intratracheal infection. This phenotypic change of App could be interpreted as a switch to a persistent life form. Our in-depth cytokine expression study could identify the salivary gland as a major source of acute phase proteins in acutely infected pigs. This implies a predominant role of this organ in early oral immunity against App and suggested additional research on the use of saliva for monitoring the health status of infected pigs. Additionally, herein we present the first attempt to characterize an App-specific T cell immune response not only at a phenotypic but also at a functional level. Our findings suggest a potential role of Th17 in the immune pathogenesis of App infection. Immunological studies that investigate T-cell immune responses against App can be of high relevance for prevention. A better understanding of the role of these cells in protection and pathology would be beneficial for developing novel prophylactic approaches.

9. REFERENCES

Alvarez-Ordonez, A., D. J. Mouwen, M. Lopez and M. Prieto, 2011: Fourier transform infrared spectroscopy as a tool to characterize molecular composition and stress response in foodborne pathogenic bacteria. *Journal of microbiological methods,* **84**, 369-378.

Andreasen, M., J. Mousing and L. K. Thomsen, 2001: No overall relationship between average daily weight gain and the serological response to Mycoplasma hyopneumoniae and Actinobacillus pleuropneumoniae in eight chronically infected Danish swine herds. *Preventive veterinary medicine,* **49**, 19-28.

Annunziato, F., C. Romagnani and S. Romagnani, 2015: The 3 major types of innate and adaptive cell-mediated effector immunity. *The Journal of allergy and clinical immunology,* **135**, 626-635.

Appleyard, G. D., S. E. Furesz and B. N. Wilkie, 2002: Blood lymphocyte subsets in pigs vaccinated and challenged with Actinobacillus pleuropneumoniae. *Veterinary immunology and immunopathology,* **86**, 221-228.

Archambault, M., J. Harel, J. Goure, Y. D. Tremblay and M. Jacques, 2012: Antimicrobial susceptibilities and resistance genes of Canadian isolates of Actinobacillus pleuropneumoniae. *Microbial drug resistance,* **18**, 198-206.

Baarsch, M. J., D. L. Foss and M. P. Murtaugh, 2000: Pathophysiologic correlates of acute porcine pleuropneumonia. *American journal of veterinary research,* **61**, 684-690.

Baarsch, M. J., R. W. Scamurra, K. Burger, D. L. Foss, S. K. Maheswaran and M. P. Murtaugh, 1995: Inflammatory cytokine expression in swine experimentally infected with Actinobacillus pleuropneumoniae. *Infection and immunity,* **63**, 3587-3594.

Belkaid, Y., K. F. Hoffmann, S. Mendez, S. Kamhawi, M. C. Udey, T. A. Wynn and D. L. Sacks, 2001: The role of interleukin (IL)-10 in the persistence of Leishmania major in the skin after healing and the therapeutic potential of anti-IL-10 receptor antibody for sterile cure. *The Journal of experimental medicine,* **194**, 1497-1506.

Blanco, F. C., M. V. Bianco, V. Meikle, S. Garbaccio, L. Vagnoni, M. Forrellad, L. I. Klepp, A. A. Cataldi and F. Bigi, 2011: Increased IL-17 expression is associated with pathology in a bovine model of tuberculosis. *Tuberculosis,* **91**, 57-63.

Boer, M. C., S. A. Joosten and T. H. Ottenhoff, 2015: Regulatory T-Cells at the Interface between Human Host and Pathogens in Infectious Diseases and Vaccination. *Frontiers in immunology,* **6**, 217.

Brogaard, L., K. Klitgaard, P. M. Heegaard, M. S. Hansen, T. K. Jensen and K. Skovgaard, 2015: Concurrent host-pathogen gene expression in the lungs of pigs challenged with Actinobacillus pleuropneumoniae. *BMC genomics,* **16**, 417.

Chiers, K., E. Donne, I. Van Overbeke, R. Ducatelle and F. Haesebrouck, 2002: Actinobacillus pleuropneumoniae infections in closed swine herds: infection patterns and serological profiles. *Veterinary microbiology,* **85**, 343-352.

Cho, W. S., K. Jung, J. Kim, Y. Ha and C. Chae, 2005: Expression of mRNA encoding interleukin (IL)-10, IL-12p35 and IL-12p40 in lungs from pigs experimentally infected with Actinobacillus pleuropneumoniae. *Veterinary research communications,* **29**, 111-122.

Choi, C., D. Kwon, K. Min and C. Chae, 1999: In-situ hybridization for the detection of inflammatory cytokines (IL-1, TNF-alpha and IL-6) in pigs naturally infected with Actinobacillus pleuropneumoniae. *Journal of comparative pathology,* **121**, 349-356.

Cruijsen, T., L. A. Van Leengoed, E. M. Kamp, A. Bartelse, A. Korevaar and J. H. Verheijden, 1995: Susceptibility to Actinobacillus pleuropneumoniae infection in pigs from an endemically infected herd is related to the presence of toxin-neutralizing antibodies. *Veterinary microbiology,* **47**, 219-228.

Cruijsen, T. L., L. A. Van Leengoed, T. C. Dekker-Nooren, E. J. Schoevers and J. H. Verheijden, 1992: Phagocytosis and killing of Actinobacillus pleuropneumoniae by alveolar macrophages and polymorphonuclear leukocytes isolated from pigs. *Infection and immunity,* **60**, 4867-4871.

Cua, D. J. and C. M. Tato, 2010: Innate IL-17-producing cells: the sentinels of the immune system. *Nature reviews. Immunology,* **10**, 479-489.

Devenish, J., S. Rosendal and J. T. Bosse, 1990: Humoral antibody response and protective immunity in swine following immunization with the 104-kilodalton hemolysin of Actinobacillus pleuropneumoniae. *Infection and immunity,* **58**, 3829-3832.

Dom, P., F. Haesebrouck, E. M. Kamp and M. A. Smits, 1992: Influence of Actinobacillus pleuropneumoniae serotype 2 and its cytolysins on porcine neutrophil chemiluminescence. *Infection and immunity,* **60**, 4328-4334.

Dreyfus, A., A. Schaller, S. Nivollet, R. P. Segers, M. Kobisch, L. Mieli, V. Soerensen, D. Hussy, R. Miserez, W. Zimmermann, F. Inderbitzin and J. Frey, 2004: Use of recombinant ApxIV in serodiagnosis of Actinobacillus pleuropneumoniae infections, development and prevalidation of the ApxIV ELISA. *Veterinary microbiology,* **99**, 227-238.

Faldyna, M., K. Nechvatalova, J. Sinkora, P. Knotigova, L. Leva, J. Krejci and M. Toman, 2005: Experimental Actinobacillus pleuropneumoniae infection in piglets with different types and levels of specific protection: immunophenotypic analysis of lymphocyte subsets in the circulation and respiratory mucosal lymphoid tissue. *Veterinary immunology and immunopathology,* **107**, 143-152.

Fenwick, B. and S. Henry, 1994: Porcine pleuropneumonia. *Journal of the American Veterinary Medical Association,* **204**, 1334-1340.

Fossum, C., E. Wattrang, L. Fuxler, K. T. Jensen and P. Wallgren, 1998: Evaluation of various cytokines (IL-6, IFN-alpha, IFN-gamma, TNF-alpha) as markers for acute bacterial infection in swine--a possible role for serum interleukin-6. *Veterinary immunology and immunopathology,* **64**, 161-172.

Frey, J., 1995: Virulence in Actinobacillus pleuropneumoniae and RTX toxins. *Trends in microbiology,* **3**, 257-261.

Furesz, S. E., B. A. Mallard, J. T. Bosse, S. Rosendal, B. N. Wilkie and J. I. Macinnes, 1997: Antibody- and cell-mediated immune responses of Actinobacillus pleuropneumoniae-infected and bacterin-vaccinated pigs. *Infection and immunity,* **65**, 358-365.

Gaffen, S. L., 2009: The role of interleukin-17 in the pathogenesis of rheumatoid arthritis. *Current rheumatology reports,* **11**, 365-370.

Gerner, W., S. C. Talker, H. C. Koinig, C. Sedlak, K. H. Mair and A. Saalmuller, 2015: Phenotypic and functional differentiation of porcine alphabeta T cells: current knowledge and available tools. *Molecular immunology,* **66**, 3-13.

Gold, R. and F. Luhder, 2008: Interleukin-17--extended features of a key player in multiple sclerosis. *The American journal of pathology,* **172**, 8-10.

Gomez-Laguna, J., A. Gutierrez, F. J. Pallares, F. J. Salguero, J. J. Ceron and L. Carrasco, 2010: Haptoglobin and C-reactive protein as biomarkers in the serum, saliva and meat juice of pigs experimentally infected with porcine reproductive and respiratory syndrome virus. *Veterinary journal,* **185**, 83-87.

Gomez-Laguna, J., A. Islas, D. Munoz, A. Ruiz, A. Villamil, L. Carrasco and M. Quezada, 2014: Infection dynamics and acute phase response of an Actinobacillus pleuropneumoniae field isolate of moderate virulence in pigs. *Veterinary microbiology,* **173**, 332-339.

Gottschalk, M., 2012: Actinobacillosis. In: L. A. K. Jeffrey J. Zimmerman, Alejandro Ramirez, Kent J. Schwartz, Gregory W. Stevenson (ed), *Diseases of Swine*, 10th edn. John Wiley & Sons, New York.

Gottschalk, M., 2015: The challenge of detecting herds sub-clinically infected with Actinobacillus pleuropneumoniae. *Veterinary journal,* **206**, 30-38.

Griffin, G. K., G. Newton, M. L. Tarrio, D. X. Bu, E. Maganto-Garcia, V. Azcutia, P. Alcaide, N. Grabie, F. W. Luscinskas, K. J. Croce and A. H. Lichtman, 2012: IL-17 and TNF-alpha sustain neutrophil recruitment during inflammation through synergistic effects on endothelial activation. *Journal of immunology,* **188**, 6287-6299.

Grunert, T., A. Monahan, C. Lassnig, C. Vogl, M. Muller and M. Ehling-Schulz, 2014: Deciphering host genotype-specific impacts on the metabolic fingerprint of Listeria monocytogenes by FTIR spectroscopy. *PloS one,* **9**, e115959.

Gutierrez-Martin, C. B., N. G. Del Blanco, M. Blanco, J. Navas and E. F. Rodriguez-Ferri, 2006: Changes in antimicrobial susceptibility of Actinobacillus pleuropneumoniae isolated from pigs in Spain during the last decade. *Veterinary microbiology,* **115**, 218-222.

Gutierrez, A. M., K. Nobauer, L. Soler, E. Razzazi-Fazeli, M. Gemeiner, J. J. Ceron and I. Miller, 2013: Detection of potential markers for systemic disease in saliva of pigs by proteomics: a pilot study. *Veterinary immunology and immunopathology,* **151**, 73-82.

Gutierrez, A. M., J. Yelamos, F. J. Pallares, J. Gomez-Laguna and J. J. Ceron, 2012: Local identification of porcine haptoglobin in salivary gland and diaphragmatic muscle tissues. *Histology and histopathology,* **27**, 187-196.

Hedegaard, J., K. Skovgaard, S. Mortensen, P. Sorensen, T. K. Jensen, H. Hornshoj, C. Bendixen and P. M. Heegaard, 2007: Molecular characterisation of the early response in pigs to experimental infection with Actinobacillus pleuropneumoniae using cDNA microarrays. *Acta veterinaria Scandinavica,* **49**, 11.

Heegaard, P. M., J. Klausen, J. P. Nielsen, N. Gonzalez-Ramon, M. Pineiro, F. Lampreave and M. A. Alava, 1998: The porcine acute phase response to infection with Actinobacillus pleuropneumoniae. Haptoglobin, C-reactive protein, major acute phase protein and serum amyloid A protein are sensitive indicators of infection. *Comparative biochemistry and physiology. Part B, Biochemistry & molecular biology,* **119**, 365-373.

Heegaard, P. M., A. Stockmarr, M. Pineiro, R. Carpintero, F. Lampreave, F. M. Campbell, P. D. Eckersall, M. J. Toussaint, E. Gruys and N. S. Sorensen, 2011: Optimal combinations of acute phase proteins for detecting infectious disease in pigs. *Veterinary research,* **42**, 50.

Hoeltig, D., I. Hennig-Pauka, K. Thies, T. Rehm, M. Beyerbach, K. Strutzberg-Minder, G. F. Gerlach, K. H. Waldmann and F. U.-C. Iras, 2009: A novel Respiratory Health Score (RHS) supports a role of acute lung damage and pig breed in the course of an Actinobacillus pleuropneumoniae infection. *BMC veterinary research,* **5**, 14.

Hsu, H. C., P. Yang, J. Wang, Q. Wu, R. Myers, J. Chen, J. Yi, T. Guentert, A. Tousson, A. L. Stanus, T. V. Le, R. G. Lorenz, H. Xu, J. K. Kolls, R. H. Carter, D. D. Chaplin, R. W. Williams and J. D. Mountz, 2008: Interleukin 17-producing T helper cells and interleukin 17 orchestrate autoreactive germinal center development in autoimmune BXD2 mice. *Nature immunology,* **9**, 166-175.

Huang, H., A. A. Potter, M. Campos, F. A. Leighton, P. J. Willson, D. M. Haines and W. D. Yates, 1999: Pathogenesis of porcine Actinobacillus pleuropneumonia, part II: roles of proinflammatory cytokines. *Canadian journal of veterinary research = Revue canadienne de recherche veterinaire,* **63**, 69-78.

Iwakura, Y., S. Nakae, S. Saijo and H. Ishigame, 2008: The roles of IL-17A in inflammatory immune responses and host defense against pathogens. *Immunological reviews,* **226**, 57-79.

Johansson, E., C. Fossum, L. Fuxler and P. Wallgren, 2001: Effects of an experimental infection with Actinobacillus pleuropneumoniae on the interferon-alpha and

interleukin-6 producing capacity of porcine peripheral blood mononuclear cells stimulated with bacteria, virus or plasmid DNA. *Veterinary microbiology,* **79**, 171-182.

Kim, C. J., L. R. Mckinnon, C. Kovacs, G. Kandel, S. Huibner, D. Chege, K. Shahabi, E. Benko, M. Loutfy, M. Ostrowski and R. Kaul, 2013: Mucosal Th17 cell function is altered during HIV infection and is an independent predictor of systemic immune activation. *Journal of immunology,* **191**, 2164-2173.

Lauritzen, B., J. Lykkesfeldt, M. T. Skaanild, O. Angen, J. P. Nielsen and C. Friis, 2003: Putative biomarkers for evaluating antibiotic treatment: an experimental model of porcine Actinobacillus pleuropneumoniae infection. *Research in veterinary science,* **74**, 261-270.

Li, D., B. Guo, H. Wu, L. Tan, C. Chang and Q. Lu, 2015: Interleukin-17 in systemic lupus erythematosus: A comprehensive review. *Autoimmunity,* **48**, 353-361.

Liuzzi, A. R., J. E. Mclaren, D. A. Price and M. Eberl, 2015: Early innate responses to pathogens: pattern recognition by unconventional human T-cells. *Current opinion in immunology,* **36**, 31-37.

Maes, D., K. Chiers, F. Haesebrouck, H. Laevens, M. Verdonck and A. De Kruif, 2001: Herd factors associated with the seroprevalences of Actinobacillus pleuropneumoniae serovars 2, 3 and 9 in slaughter pigs from farrow-to-finish pig herds. *Veterinary research,* **32**, 409-419.

Marois, C., M. Gottschalk, H. Morvan, C. Fablet, F. Madec and M. Kobisch, 2009: Experimental infection of SPF pigs with Actinobacillus pleuropneumoniae serotype 9 alone or in association with Mycoplasma hyopneumoniae. *Veterinary microbiology,* **135**, 283-291.

Masopust, D. and L. J. Picker, 2012: Hidden memories: frontline memory T cells and early pathogen interception. *Journal of immunology,* **188**, 5811-5817.

Mcgeachy, M. J., 2013: Th17 memory cells: live long and proliferate. *Journal of leukocyte biology,* **94**, 921-926.

Mcgill, J. L., R. A. Rusk, M. Guerra-Maupome, R. E. Briggs and R. E. Sacco, 2016: Bovine Gamma Delta T Cells Contribute to Exacerbated IL-17 Production in Response to Co-Infection with Bovine RSV and Mannheimia haemolytica. *PloS one,* **11**, e0151083.

Mensikova, M., H. Stepanova and M. Faldyna, 2013: Interleukin-17 in veterinary animal species and its role in various diseases: a review. *Cytokine,* **64**, 11-17.

Michel, M. L., A. C. Keller, C. Paget, M. Fujio, F. Trottein, P. B. Savage, C. H. Wong, E. Schneider, M. Dy and M. C. Leite-De-Moraes, 2007: Identification of an IL-17-producing NK1.1(neg) iNKT cell population involved in airway neutrophilia. *The Journal of experimental medicine,* **204**, 995-1001.

Monack, D. M., A. Mueller and S. Falkow, 2004: Persistent bacterial infections: the interface of the pathogen and the host immune system. *Nature reviews. Microbiology,* **2**, 747-765.

Muneta, Y., Y. Minagawa, T. Nakane, T. Shibahara, T. Yoshikawa and Y. Omata, 2011: Interleukin-18 expression in pig salivary glands and salivary content changes during acute immobilization stress. *Stress,* **14**, 549-556.

Murata, H., N. Shimada and M. Yoshioka, 2004: Current research on acute phase proteins in veterinary diagnosis: an overview. *Veterinary journal,* **168**, 28-40.

Myers, M. J., M. J. Baarsch and M. P. Murtaugh, 2002: Effects of pentoxifylline on inflammatory cytokine expression and acute pleuropneumonia in swine. *Immunobiology,* **205**, 17-34.

Nakae, S., Y. Komiyama, A. Nambu, K. Sudo, M. Iwase, I. Homma, K. Sekikawa, M. Asano and Y. Iwakura, 2002: Antigen-specific T cell sensitization is impaired in IL-17-

deficient mice, causing suppression of allergic cellular and humoral responses. *Immunity,* **17**, 375-387.

Neyer, L. E., G. Grunig, M. Fort, J. S. Remington, D. Rennick and C. A. Hunter, 1997: Role of interleukin-10 in regulation of T-cell-dependent and T-cell-independent mechanisms of resistance to Toxoplasma gondii. *Infection and immunity,* **65**, 1675-1682.

Nicolet, J., H. Konig and E. School, 1969: [On haemophilus pleuropneumonia in swine. II. A contagious disease of scientific value]. *Schweizer Archiv fur Tierheilkunde,* **111**, 166-174.

Pallares, F. J., S. Martinez-Subiela, J. Seva, G. Ramis, P. Fuentes, A. Bernabe, A. Munoz and J. J. Ceron, 2008: Relationship between serum acute phase protein concentrations and lesions in finishing pigs. *Veterinary journal,* **177**, 369-373.

Park, J., K. W. Seo, S. H. Kim, H. Y. Lee, B. Kim, C. W. Lim, J. H. Kim, H. S. Yoo and Y. S. Jang, 2015: Nasal immunization with M cell-targeting ligand-conjugated ApxIIA toxin fragment induces protective immunity against Actinobacillus pleuropneumoniae infection in a murine model. *Veterinary microbiology,* **177**, 142-153.

Passos, S. T., J. S. Silver, A. C. O'hara, D. Sehy, J. S. Stumhofer and C. A. Hunter, 2010: IL-6 promotes NK cell production of IL-17 during toxoplasmosis. *Journal of immunology,* **184**, 1776-1783.

Peng, M. Y., Z. H. Wang, C. Y. Yao, L. N. Jiang, Q. L. Jin, J. Wang and B. Q. Li, 2008: Interleukin 17-producing gamma delta T cells increased in patients with active pulmonary tuberculosis. *Cellular & molecular immunology,* **5**, 203-208.

Petersen, H. H., J. P. Nielsen and P. M. Heegaard, 2004: Application of acute phase protein measurements in veterinary clinical chemistry. *Veterinary research,* **35**, 163-187.

Ramjeet, M., V. Deslandes, J. Goure and M. Jacques, 2008: Actinobacillus pleuropneumoniae vaccines: from bacterins to new insights into vaccination strategies. *Animal health research reviews,* **9**, 25-45.

Rathore, J. S. and Y. Wang, 2016: Protective role of Th17 cells in pulmonary infection. *Vaccine,* **34**, 1504-1514.

Redford, P. S., P. J. Murray and A. O'garra, 2011: The role of IL-10 in immune regulation during M. tuberculosis infection. *Mucosal immunology,* **4**, 261-270.

Rosendal, S., D. A. Boyd and K. A. Gilbride, 1985: Comparative virulence of porcine Haemophilus bacteria. *Canadian journal of comparative medicine : Revue canadienne de medecine comparee,* **49**, 68-74.

Saalmuller, A., T. Werner and V. Fachinger, 2002: T-helper cells from naive to committed. *Veterinary immunology and immunopathology,* **87**, 137-145.

Sarkozi, R., L. Makrai and L. Fodor, 2015: Identification of a proposed new serovar of Actinobacillus Pleuropneumoniae: Serovar 16. *Acta veterinaria Hungarica,* **63**, 444-450.

Schaller, A., P. Kuhnert, V. A. De La Puente-Redondo, J. Nicolet and J. Frey, 2000: Apx toxins in Pasteurellaceae species from animals. *Veterinary microbiology,* **74**, 365-376.

Sedlak, C., M. Patzl, A. Saalmuller and W. Gerner, 2014: CD2 and CD8alpha define porcine gammadelta T cells with distinct cytokine production profiles. *Developmental and comparative immunology,* **45**, 97-106.

Shin, M. K., M. L. Kang, M. H. Jung, S. B. Cha, W. J. Lee, J. M. Kim, D. H. Kim and H. S. Yoo, 2013: Induction of protective immune responses against challenge of Actinobacillus pleuropneumoniae by oral administration with Saccharomyces cerevisiae expressing Apx toxins in pigs. *Veterinary immunology and immunopathology,* **151**, 132-139.

Sidibe, M., S. Messier, S. Lariviere, M. Gottschalk and K. R. Mittal, 1993: Detection of Actinobacillus pleuropneumoniae in the porcine upper respiratory tract as a

complement to serological tests. *Canadian journal of veterinary research = Revue canadienne de recherche veterinaire,* **57**, 204-208.

Sjolund, M. and P. Wallgren, 2010: Field experience with two different vaccination strategies aiming to control infections with Actinobacillus pleuropneumoniae in a fattening pig herd. *Acta veterinaria Scandinavica,* **52**, 23.

Skovgaard, K., S. Mortensen, M. Boye, J. Hedegaard and P. M. Heegaard, 2010: Hepatic gene expression changes in pigs experimentally infected with the lung pathogen Actinobacillus pleuropneumoniae as analysed with an innate immunity focused microarray. *Innate immunity,* **16**, 343-353.

Skovgaard, K., S. Mortensen, M. Boye, K. T. Poulsen, F. M. Campbell, P. D. Eckersall and P. M. Heegaard, 2009: Rapid and widely disseminated acute phase protein response after experimental bacterial infection of pigs. *Veterinary research,* **40**, 23.

Soler, L., A. Gutierrez, S. Martinez-Subiela and J. J. Ceron, 2011: Fast measurement of serum amyloid A in different specimens from swine by using a new one-step time-resolved fluorescent immunoassay. *Journal of veterinary diagnostic investigation : official publication of the American Association of Veterinary Laboratory Diagnosticians, Inc,* **23**, 902-908.

Soler, L., A. Gutierrez, A. Mullebner, J. J. Ceron and J. C. Duvigneau, 2013: Towards a better understanding of salivary and meat juice acute phase proteins determination in pigs: an expression study. *Veterinary immunology and immunopathology,* **156**, 91-98.

Spits, H., D. Artis, M. Colonna, A. Diefenbach, J. P. Di Santo, G. Eberl, S. Koyasu, R. M. Locksley, A. N. Mckenzie, R. E. Mebius, F. Powrie and E. Vivier, 2013: Innate lymphoid cells--a proposal for uniform nomenclature. *Nature reviews. Immunology,* **13**, 145-149.

Stepanova, H., M. Mensikova, K. Chlebova and M. Faldyna, 2012: CD4+ and gammadeltaTCR+ T lymphocytes are sources of interleukin-17 in swine. *Cytokine,* **58**, 152-157.

Straw, B. E., V. K. Tuovinen and M. Bigras-Poulin, 1989: Estimation of the cost of pneumonia in swine herds. *Journal of the American Veterinary Medical Association,* **195**, 1702-1706.

Sutton, C. E., L. A. Mielke and K. H. Mills, 2012: IL-17-producing gammadelta T cells and innate lymphoid cells. *European journal of immunology,* **42**, 2221-2231.

Takatori, H., Y. Kanno, W. T. Watford, C. M. Tato, G. Weiss, Ivanov, Ii, D. R. Littman and J. J. O'shea, 2009: Lymphoid tissue inducer-like cells are an innate source of IL-17 and IL-22. *The Journal of experimental medicine,* **206**, 35-41.

Tuchscherr, L., B. Loffler, F. R. Buzzola and D. O. Sordelli, 2010: Staphylococcus aureus adaptation to the host and persistence: role of loss of capsular polysaccharide expression. *Future microbiology,* **5**, 1823-1832.

Van Dixhoorn, I. D., I. Reimert, J. Middelkoop, J. E. Bolhuis, H. J. Wisselink, P. W. Groot Koerkamp, B. Kemp and N. Stockhofe-Zurwieden, 2016: Enriched Housing Reduces Disease Susceptibility to Co-Infection with Porcine Reproductive and Respiratory Virus (PRRSV) and Actinobacillus pleuropneumoniae (A. pleuropneumoniae) in Young Pigs. *PloS one,* **11**, e0161832.

Vanni, M., M. Merenda, G. Barigazzi, C. Garbarino, A. Luppi, R. Tognetti and L. Intorre, 2012: Antimicrobial resistance of Actinobacillus pleuropneumoniae isolated from swine. *Veterinary microbiology,* **156**, 172-177.

Vigre, H., O. Angen, K. Barfod, D. T. Lavritsen and V. Sorensen, 2002: Transmission of Actinobacillus pleuropneumoniae in pigs under field-like conditions: emphasis on tonsillar colonisation and passively acquired colostral antibodies. *Veterinary microbiology,* **89**, 151-159.

Wang, L., W. Qin, J. Zhang, C. Bao, H. Zhang, Y. Che, C. Sun, J. Gu, X. Feng, C. Du, W. Han, P. L. Richard and L. Lei, 2016: Adh enhances Actinobacillus pleuropneumoniae pathogenicity by binding to OR5M11 and activating p38 which induces apoptosis of PAMs and IL-8 release. *Scientific reports,* **6**, 24058.

Way, E. E., K. Chen and J. K. Kolls, 2013: Dysregulation in lung immunity - the protective and pathologic Th17 response in infection. *European journal of immunology,* **43**, 3116-3124.

Wyns, H., S. Croubels, M. Vandekerckhove, K. Demeyere, P. De Backer, B. M. Goddeeris and E. Meyer, 2015: Multiplex analysis of pro-inflammatory cytokines in serum of Actinobacillus pleuropneumoniae-infected pigs. *Research in veterinary science,* **102**, 45-48.

Yoo, A. N., S. B. Cha, M. K. Shin, H. K. Won, E. H. Kim, H. W. Choi and H. S. Yoo, 2014: Serotypes and antimicrobial resistance patterns of the recent Korean Actinobacillus pleuropneumoniae isolates. *The Veterinary record,* **174**, 223.

Young, D., T. Hussell and G. Dougan, 2002: Chronic bacterial infections: living with unwanted guests. *Nature immunology,* **3**, 1026-1032.